POLITECNICO
MILANO 1863

SCUOLA DI INGEGNERIA INDUSTRIALE
E DELL'INFORMAZIONE

Bistriazolyl-phenanthroline ligand for sustainable Am(III) separation from simulated spent nuclear fuel solutions

Tesi di Laurea Magistrale in
Nuclear Engineering - Ingegneria Nucleare

Author: **Giulia De Amicis**

Student ID: 244671
Advisor: Elena Macerata
Co-advisor: Andreas Wilden
Academic Year: 2025-26

Abstract

Following the recovery of U and Pu from used nuclear fuel, Am becomes the primary contributor to the long-term radiotoxicity and heat load of the remaining high level waste. The AmSel (Americium Selective) process has been developed for the selective stripping of Am from PUREX (Plutonium Uranium Reduction Extraction) raffinate. It is based on the combined use of two ligands with opposite selectivity and solubility, which work in a push-pull system, allowing a satisfactory separation of Am from Cm and all the lanthanides (Ln). Ethoxyethanol-bis-triazolyl-phenanthroline (EBTzPhen) was investigated as an alternative made only by C, H, O and N to the reference sulphonated hydrophilic ligand. A CHON-compliant molecule can be incinerated without the formation of secondary solid waste, improving the sustainability of the process. The aim of the study was to assess the extraction performance of the EBTzPhen and its selectivity towards Am, in presence of Cm and all the Ln. The behaviour of the system was investigated with batch experiments as a function of different parameters, relevant for the process: initial ligand and nitric acid concentration, temperature and mixing time. Distribution ratios and separation factors were evaluated for all the ions by gamma and alpha spectrometry and ICP-MS measurements. To better understand the complexation mechanism, a UV-VIS metal titration was carried out with Eu nitrate. Heavy Ln were extracted almost completely into the organic phase, while light Ln tended to remain in the aqueous phase, with La being the most retained. Am separation was obtained with 0.1 M ligand and 0.3 M nitric acid concentrations: Cm and La were extracted in the organic phase, while Am was retained in the aqueous phase, yielding separation factors around 2-2.5 for both Cm/Am and La/Am, ensuring no co-extraction. The molecule exhibited fast kinetics, but the system proved to be affected by temperature. Finally, complexation appeared to be affected both by protonation and by the molecule's structure itself. The results obtained in this work demonstrate the potential of EBTzPhen as a promising CHON-compliant alternative for the AmSel process and provide critical insights to further refine the molecular design.

Keywords: AmSel, Hydrophilic ligands, Phenanthroline derivatives, Lanthanides, Partitioning

Abstract in lingua italiana

In seguito al recupero di U e Pu dal combustibile nucleare esaurito, l'Am diventa il principale responsabile di radiotossicità e carico termico a lungo termine dei rimanenti rifiuti ad alta attività. Il processo AmSel (*Americium Selective*) è stato sviluppato per lo *stripping* selettivo dell'Am dal raffinato PUREX (*Plutonium Uranium Reduction Extraction*). Si basa sull'uso combinato di due leganti con selettività e solubilità opposte, che operano in un sistema *push-pull*, consentendo la separazione dell'Am dal Cm e dai lantanidi (Ln). L'etossietanolo-bis-triazolil-fenantrolina (EBTzPhen) è stata studiata come alternativa, costituita unicamente da C, H, O e N, al legante idrofilo solfonato di riferimento. Una molecola conforme al principio CHON può essere incenerita senza la formazione di rifiuti solidi secondari, migliorando la sostenibilità del processo. Lo scopo dello studio è stato quello di valutare le prestazioni di estrazione dell'EBTzPhen e la sua selettività per l'Am, in presenza del Cm e di tutti i lantanidi. Il comportamento del sistema è stato studiato con esperimenti in *batch* in funzione di diversi parametri rilevanti per il processo: concentrazione iniziale di legante e acido nitrico, temperatura e tempo di contatto. I rapporti di distribuzione e i fattori di separazione sono valutati per tutti gli ioni tramite spettrometria gamma e alfa e misurazioni ICP-MS. Per comprendere meglio il meccanismo di complessazione, è stata eseguita una titolazione UV-VIS con nitrato di Eu. I Ln pesanti sono stati estratti quasi completamente nella fase organica, mentre i Ln leggeri hanno mostrato la tendenza a rimanere nella fase acquosa, soprattutto il La. La separazione dell'Am è stata ottenuta con concentrazioni di legante pari a 0.1 M e di acido nitrico pari a 0.3 M: il Cm e il La sono stati estratti nella fase organica, mentre l'Am è stato trattenuto nella fase acquosa, fornendo fattori di separazione intorno a 2-2.5 sia per Cm/Am che per La/Am, garantendo l'assenza di co-estrazione. La molecola ha mostrato una cinetica rapida, ma il sistema si è rivelato influenzato dalla temperatura. Infine, sia la protonazione che la struttura stessa della molecola sembrano avere un impatto significativo sulla complessazione. I risultati ottenuti dimostrano il potenziale dell'EBTzPhen come alternativa CHON per il processo AmSel e forniscono spunti per perfezionare il design molecolare.

Parole chiave: AmSel, Leganti idrofili, Derivati della fenantrolina, Lantanidi, Partitioning

Contents

Introduction

Nuclear energy is a low-carbon and reliable energy source, but the production of long-lived, high level waste introduces severe long term radiotoxicity and decay heat management constraints on the final disposal. The most advanced strategy to mitigate these radiological challenges is the recycling of uranium, plutonium and minor actinides. This approach allows for a significant reduction in the required isolation lifetime of the geological repository: from hundreds of thousands to a few hundreds of years.

While the PUREX (Plutonium Uranium Reduction Extraction) process for U and Pu recycling is well-established and industrially mature, in the context of minor actinides recycling, partitioning of Am still represents a major challenge. The AmSel (Americium Selective Extraction) process was developed for the selective stripping of Am from the PUREX raffinate. It is a hydrometallurgical process based on two ligands with opposite selectivity and solubility, which enable the separation of Am from Cm and all the lanthanides.

However, the reference hydrophilic ligand of the AmSel process is not fully composed by carbon, hydrogen, oxygen and nitrogen (CHON-compliant), but it contains sulphur, which generates solid waste upon incineration. This work investigates a new CHON-compliant hydrophilic ligand as a candidate replacement for the sulphonated molecule. The ligand was extensively tested through solvent extraction experiments and complexation studies, carried out by UV-VIS spectrophotometry, and its performance was compared with alternative molecules proposed in the literature. In the following, a general overview on the nuclear fuel cycle and partitioning processes is given. Then, the requirements of the new hydrophilic ligand for the AmSel process are listed, and a review of the proposed molecules is reported. Finally, the novel ligand investigated in this work is presented, and the obtained results are reported and discussed.

1 | Used nuclear fuel reprocessing

In the present society, energy needs are rapidly increasing due to population growth and development of emerging countries, while the environmental footprint of energy production has to be reduced to mitigate climate change and pollution. Moreover, energy security and independence are a pressing matter. Among the possible energy sources, nuclear is low-carbon, reliable and continuous. Since it is characterized by high capacity factor, which means it is mostly operated in full power with rare interruptions for maintenance and refuelling, it represents the baseload source in the energy mix [1]. Finally, while for fossils the electricity cost is strictly bound to fuel price, for nuclear energy the electricity price is only marginally affected by uranium, because it is mostly affected by capital costs, which leads to price stability [1]. Nevertheless, waste management, safety and high upfront and decommissioning costs represent important concerns, which lead to a lack of public trust.

Improving the sustainability of the nuclear fuel cycle is an important step towards a less impacting energy production. Regarding greenhouse gases (GHG) emissions, nuclear is competitive with renewable sources, but other environmental impact indicators have to be considered as well. The front-end, in particular mining, is the cycle step that mostly affects many of them, such as water pollution, land use, human and ecotoxicity. Instead, fuel utilization is the cycle step that is primarily responsible for water consumption. Finally, the back-end strategy (recycling or direct disposal) appears to have a relatively low impact on such indicators. Nevertheless, even though it is fundamental to act on the front-end, recycling used nuclear fuel can reduce mining and uranium enrichment throughput, lowering their environmental impact [1, 2]. Moreover, the used nuclear fuel, besides a significant quantity of uranium and plutonium, that can be directly recycled, contains a wide range of elements which can be of great importance both in nuclear and general industrial applications, and are not largely available in nature. Many belong to the list of critical raw materials, such as rare earth elements or platinum group metals, whose production is mostly managed by a few countries [3]. Finally, one of the main concerns is the long term hazard of the used nuclear fuel, but back-end strategies that recycle and transmute long-lived radionuclides can significantly reduce the burden on

future generations.

1.1. Nuclear fuel cycle

The nuclear fuel cycle includes all the activities from raw materials sourcing to disposal. It can be divided in three main steps: front-end, fuel utilization and back-end.

1.1.1. Front-end

The front end of the fuel cycle consists in the processes related to fuel supply: exploration, mining and milling, conversion, enrichment and fuel fabrication [4]. Nuclear fuel is mostly based on uranium: natural uranium is mainly composed by U-238 (99.28%), with only a small fraction of U-235 (0.71%) and traces of U-234 (0.01%) [5]. It is widespread across the earth's crust, with an average concentration of 1.7 ppm, and can also be found in seawater (3.3 ppb). It can be present in minerals in low concentrations as a substituent, or in higher concentrations as a major constituent; the metal can be leached by geologic fluids and concentrated in deposits [6]. Australia, Kazakhstan and Canada host around half of the world's natural uranium resources.

There are several mining techniques used to recover uranium ore, determined by costs, deposit features, but also by characteristics and hydrogeology of the surrounding rocks. The conventional techniques are open-pit and underground mining, but uranium can also be recovered by in situ leaching (ISL), or as a by-product or co-product [7]. The product of the mining is purified through solvent-extraction or ion-exchange [8]. Uranium trapped on the resin/polymer after purification extraction is stripped, producing a pregnant solution, which is then precipitated in a solid product called yellowcake. After additional purification, the resulting solid contains almost entirely U_3O_8 [9]. Yellowcake is dissolved again converted to UF_6. At this point, uranium has the natural abundance of the fissile isotope U-235, but for most thermal reactors, which are the prevailing technology, it is necessary to increase its content up to 3-5%. UF_6 is a volatile compound, that allows enrichment through gas centrifugation, which is the most used technique. However, due to the small mass difference between the two molecules, several stages are required. Finally, enriched UF_6 can be converted to UO_2 powder through several reactions. The powder is then pressed into pellets and sintered at 1700°C in a dry hydrogen atmosphere [4], which then are assembled into fuel rods.

There are also secondary uranium sources: civil stockpiles held by governments, military warheads (weapon-grade uranium is converted to fuel), recycled uranium and plutonium

from spent fuel. Additionally, a significant secondary supply is represented by the practice of underfeeding at enrichment plants: the tails assay is lower than the contracted, therefore some natural uranium can be set aside. Finally, depleted uranium that comes from enrichment activities can also be re-enriched and used [10]. Recurring more to secondary uranium sources, among which recycled fissile materials, would reduce the impact of the mining step.

1.1.2. Fuel utilization

After fabrication, nuclear fuel is loaded and burnt in nuclear reactors for a certain amount of time (4 to 6 years on average). The objective when running a power reactor is to run it at nominal power for the majority of its useful life: nevertheless, the fuel is consumed while inside the reactor. This phenomenon is called burnup: it can be defined as the energy extracted from the fuel per unit mass (a common unit of measure is MWd/kgU), and it is used to describe the exploitation of the nuclear fuel. While maximizing the burnup would be ideal from an economic point of view, because it means improving the fuel exploitation, on the other hand the fuel would be more deteriorated, therefore it would require stricter design limits to reach such conditions. The average discharge burnup limit (rod average) depends on the country, but generally lies around 50-70 MWd/kgU [11]. Specifically, it has to be lower than the maximum burnup dictated by material limitations, otherwise the fuel integrity is compromised.

The maximum burnup constraint reduces largely the fraction of fissile material burnt during fuel utilization. Nevertheless, this is partially related to the reactor technology employed. At the present day, most reactors are based on thermal neutrons, which can burn only fissile nuclides, such as U-233, U-235, Pu-239, Pu-241. However, the nuclear fuel contains many fissionable nuclides, such mostly U-238 but also Pu-240, Pu-242, which can only be burnt in a fast spectrum. By integrating the reactor fleet with fast reactors, fuel utilization could be enhanced.

1.1.3. Back-end

Once the fuel has reached the desired burnup, it is discharged from the nuclear reactor. Since burnt fuel assemblies continue to produce heat after discharge, due to radioactive decay, they are stored for some years in spent fuel pools (on-site deep water pools), which allow them to cool down, but also have a shielding purpose [12]. Spent nuclear fuel composition depends on a variety of factors: initial enrichment, irradiation time (burnup) and cooling time, neutron spectrum and flux, but also reactor type. On average, the fuel

discharged from a thermal reactor contains [3]:

- 95.6% uranium, mostly ^{238}U (0.5-1% ^{235}U, and very small amounts of other uranium isotopes);
- 2.9% stable fission products;
- 0.9% plutonium;
- 0.3% caesium and strontium (fission products);
- 0.1% iodine and technetium (fission products);
- 0.1% other long-lived fission products;
- 0.1% minor actinides (americium, curium, neptunium).

In particular, plutonium builds up in the reactor by neutron absorption on U-238 and subsequent $\beta-$ decays:

$$^{238}\mathrm{U}(\mathrm{n},\gamma)^{239}\mathrm{U} \xrightarrow{\beta-} {}^{239}\mathrm{Np} \xrightarrow{\beta-} {}^{239}\mathrm{Pu} \tag{1.1}$$

Other plutonium isotopes and minor actinides (americium, curium, neptunium) are formed by successive neutron captures and $\beta-$ decays on Pu-239 or uranium isotopes [9].

The spent nuclear fuel is characterized by some features, as radiotoxicity or heat load, that represent a challenge for the waste management. Radiotoxicity is measured in terms of dose, normalized by the mass of heavy metal present in the fuel [$\mathrm{Sv/t_{HM}}$], and it varies with time; it is related to both the radiological and chemical hazards, because there are several emitters with different physical and biological half lives that are also heavy metals, toxic if inhaled or ingested.

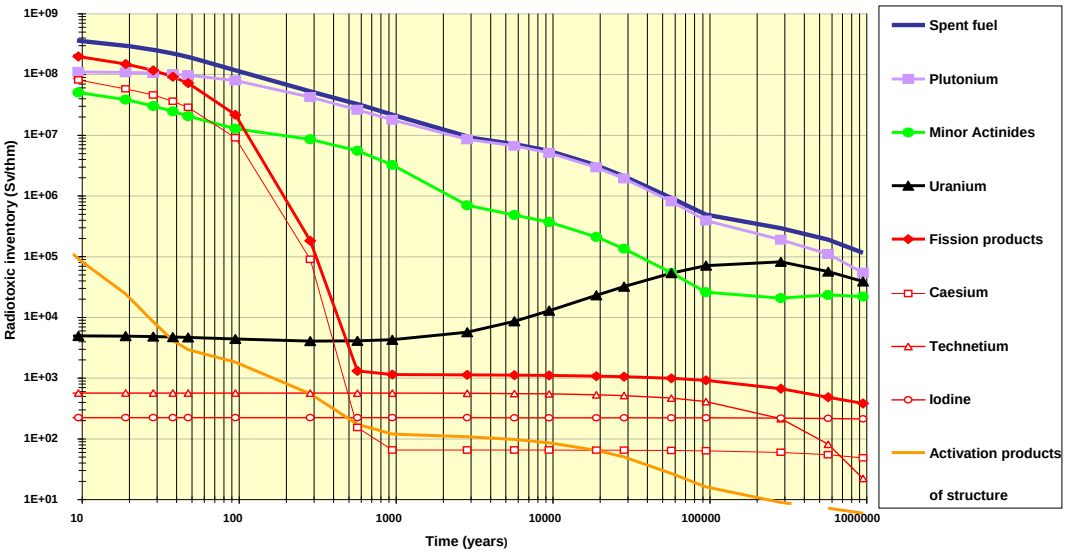

Figure 1.1: Radiotoxic inventory of uranium oxide spent fuel in Sv/t_{HM} [13]

For the first 200 years after discharge, as it can be observed from figure 1.1 the main contribution to radiotoxicity is given by fission products Cs-137 and Sr-90, but also plutonium, while for the medium-long term by plutonium and minor actinides (americium represents the largest contribution). Some long lived fission products like iodine give also a small contribution to the long term radiotoxicity. Heat load is another feature of the spent nuclear fuel that is a concern, especially regarding long term storage; the behaviour of the heat load with respect to time follows the radiotoxicity one (figure 1.2). Finally, spent fuel has also an important neutron emission, to which the main contributor is Cm-244 [13].

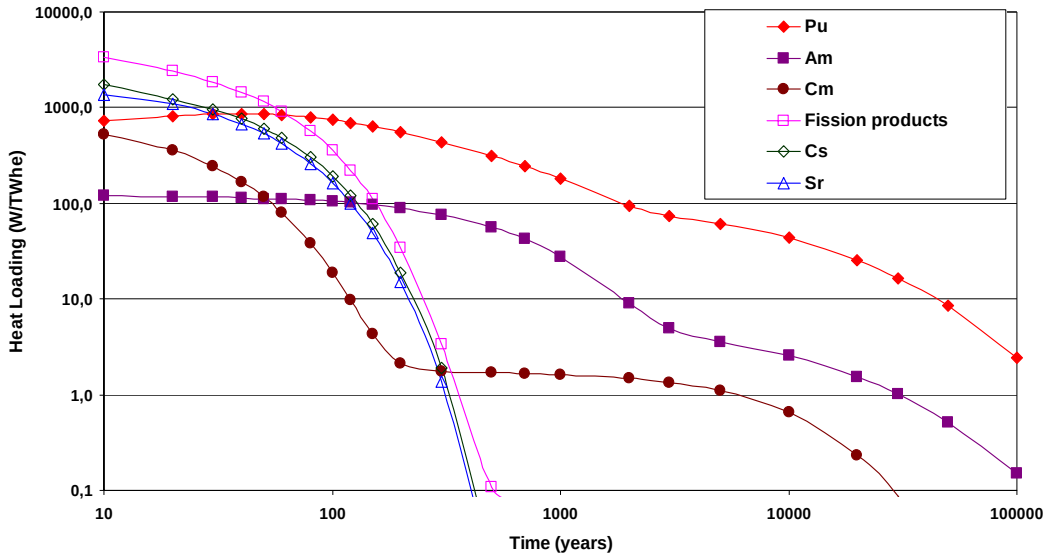

Figure 1.2: Heat load of uranium oxide spent fuel in W/TWhe in function of time [13]

The next step after cooling depends on the country's fuel cycle. In particular, several fuel cycle strategies are possible, which are mainly characterized by different management of the spent nuclear fuel. However, some countries adopt the so-called 'wait and see'; a specific strategy for the spent nuclear fuel has yet to be determined, and interim storage facilities are adopted as a temporary solution. They can be either the wet pool type (Czech Republic, Finland, Germany, Japan, Sweden, United Kingdom) or the dry vault type (France, Germany, United Kingdom) [4]. After the interim storage, the spent fuel can be reprocessed or sent to final disposal.

1.2. Back-end strategies

1.2.1. Open cycle strategy

In the open cycle, or once-through cycle (OTC), spent nuclear fuel is stored for some years in an interim storage facility, then conditioned and located in a long-term geological repository.

In the IAEA waste classification, SNF is considered High Level Waste (HLW): it contains a large quantity of both short and long lived nuclides, and generates a significant amount of heat. For this reason, a high degree of containment and isolation is required for a very long period of time, in addition to a heat dissipation system [14]. The best option for long term disposal of the SNF is a Deep Geological Repository (DGR), which is an

underground facility built hundreds of meters deep within a stable geological formation, and it features a system of tunnels and vaults in which conditioned SNF is stored in canisters, surrounded by backfill material (typically bentonite), to create a multi-barrier system. There are two main design options for a DGR: mined repositories and deep boreholes. Mined repositories are tunnels built in low permeability rock formations; since this option requires a significant land use, it is adopted by countries who have sites availability but also a large amount of radioactive waste. The second design consists into an array of vertical boreholes excavated in the rock up to 5 km deep, in which waste canisters are placed in the lower part while the upper section is filled with backfill material; deep boreholes are designed for small waste forms, hence suitable for countries with small nuclear programs. Several rock formations are studied as feasible solutions to host a DGR; the desired features are low permeability, stability, mechanical resistance. Crystalline rocks and salt formations have both low permeability, but the former has a robust mechanical strength, while the latter has the advantage of creeping under induced stress, gradually sealing fractures and encapsulating waste. Other suitable rock formations are volcanic tuff and clay [15].

A DGR is the preferred strategy for nuclear waste in many countries, among which US, UK, Switzerland, Sweden, Finland, France, Canada, Belgium, Australia [16]. It has to be noted that many of these countries are also actively reprocessing their SNF, like France, or are involved in research regarding the SNF recycling: even in a reprocessing scenario, HLW is produced and has to be stored in a safe site. However, there are also many countries which adopted the once-through cycle as their strategy: among others Finland, Sweden, US, Canada [17].

The advantages of the OTC are that, among the back-end strategies, it presents less technical challenges, as traditional nuclear reactors are employed, and a lower short-term cost. In addition, it is considered to have a lower proliferation risk, as there are no separate streams of metals and the waste is vitrified. Nevertheless, since the volume, heat load and radio-toxicity of the conditioned waste represent constraints for the final disposal, a suitable geology and space have to be selected for the DGR. Moreover, this option involves a low exploitation of the resources, and requires a continuous supply of raw material. This represents an obstacle for energy independence, especially for countries that do not have exploitable uranium resources on national territory [12].

1.2.2. Pu mono-recycling strategy

When the spent nuclear fuel is recycled, it is more correct to talk about Used Nuclear Fuel (UNF). This cycle option is called twice-through fuel cycle (TTC), or Pu mono-recycling: after cooling, UNF is sent to a reprocessing plant where uranium and plutonium are recovered separately as oxides.

UNF reprocessing has been performed for a long time. Initially, it was for military purposes: the aim was to recover plutonium for weapons. In this historical context, during the Manhattan Project, the PUREX (Plutonium Uranium Reduction Extraction) process was developed [18], and it is still used today in civil reprocessing plants. It is a hydrometallurgical process, during which the used fuel is dissolved in nitric acid, and separation occurs by means of a solvent containing tributyl phosphate (TBP), an extracting agent. The uranium-plutonium separation is achieved by modifying their oxidation state, rendering them more or less affine to TBP. This strategy is adopted in several countries, among which many European countries, Russia, China and Japan [19]. Specifically, France has two reprocessing plants in La Hague, and a plant (Melox) for MOX fuel fabrication. La Hague plant not only processes the French reactor's LWR fuel, but also UNF sent from other countries, such as Germany, Japan, Switzerland, Belgium, the Netherlands, and Italy; at the end, the resulting HLW is sent back to the origin country [20]. UK had a reprocessing plant in Sellafield, but ceased operation. Russia also has an active reprocessing plant, and another one not yet operational [19]. Finally, Japan also has a reprocessing plant in Rokkasho, about to become operational.

The recovered plutonium oxide is employed in MOX fuel, while uranium oxide is usually stored [12]. Due to the presence of different uranium isotopes in the UNF, reprocessed uranium (RepU) contains 0.5-1% U-235, 0.4-0.7% U-236, traces of U-234 and U-232, with the remaining being U-238. Although U-232 in the reactor is converted into fissile U-233, its decay produces strong γ-emitting daughters (Tl-208): handling RepU for re-enrichment imposes particular shielding requirements. Additionally, U-236 is a strong neutron absorber, and its quantity increases with the burnup. For this reason, RepU requires about 1.5% more feed material for the enrichment process and more separative work has to be performed. In conclusion, enrichment of RepU presents several concerns, with respect to natural uranium, that could result in increased costs: its value was calculated to be 50-80% the value of natural uranium. RepU is not usually re-enriched (although this possibility has been demonstrated to be feasible), but it is stored and eventually can be used for High-Enriched Uranium (HEU) down-blending. Instead, plutonium oxide isotopic composition depends on the initial fuel composition and irradiation time: besides

Pu-239, with increasing burnup the fraction of higher plutonium isotopes increases (Pu-240, Pu-241, Pu-242). Plutonium isotopes are mainly α-emitters, but during an α-decay usually gamma rays are also emitted. Hence, it is very radio-toxic if inhaled or ingested, but it poses also external radiation concerns, making it difficult to handle. Finally, fissile Pu-241 decays into Am-241, which emits α and penetrating gamma radiation. For this reason, in addition to proliferation concerns, it is preferred to use plutonium directly after reprocessing and avoid its storage: the longer it is stored, the more its fissile worth is depleted [5].

Plutonium oxide is mixed with depleted uranium oxide to fabricate Mixed Oxide (MOX) fuel. Plutonium content in MOX fuel is determined by its fissile percentage, but on average it is around 9.5%. It has to be noted that even Pu isotopes and Am-241 act as neutronic poisons in thermal spectrum, hence their reactivity worth has to be accounted for in neutronic calculations. Nevertheless, MOX is loaded in thermal reactors, usually one-third of the core. Its percentage can be increased up to 50% without changing the operating characteristics of the reactor, even though the plant needs to be slightly adapted, while for a core with more than 50% MOX loading, reactors need to be designed accordingly [21]. Spent MOX fuel is not reprocessed again, but it is conditioned and sent to final disposal. Additionally, since minor actinides and fission products resulting from the U and Pu recovery are also HLW, they are conditioned and sent to final disposal as well [12].

The mono-recycling strategy has many advantages, including better resource exploitation: natural uranium needs are nearly 75% or the quantity needed in the open cycle [12]. Additionally, volume, heat load and radiotoxicity of the HLW are reduced, especially long term, due to plutonium being the main cause; this reduces the space requirements for the DGR, at the same time decreasing the cost of HLW disposal. Moreover, PUREX process and MOX fuel fabrication are industrially mature technologies, and the recycling can be carried out in LWRs. However, there are also some drawbacks; the main concern is an increased proliferation risk, since plutonium is separated in a single stream. For this reason, the COEX process has been developed in France, but not yet employed in industry: it allows to co-extract uranium and plutonium, producing directly a mixed oxide powder. At the same time, in Japan, Rokkasho plant is going to adopt a process in which U and Pu co-extraction takes place [19]. Another disadvantage is the fact that new facilities are required, such as reprocessing plants, MOX fuel fabrication plants, causing an increase in the fixed costs. Additionally, MOX fabrication, due to handling concerns (presence of γ and α-emitters), it is more expensive than UO_2 fuel fabrication. Finally, it is a partial recycling strategy, as spent MOX fuel is not reprocessed; nevertheless, it is

a step towards a circular economy and energy independence.

1.2.3. Pu multi-recycling strategy

In this scenario, fuel is recycled multiple times, continuously recovering U and Pu, while minor actinides are disposed as HLW. In fact, it has been demonstrated in the La Hague plant that MOX fuel can be reprocessed again, even though it is not the current policy. Spent MOX fuel, due to the high plutonium content, contains a large amount of minor actinides and even plutonium isotopes, causing it to be more radioactive than spent UO_2 fuel [21]. Even though this is a handling concern, it does not represent an obstacle for reprocessing. In general, the fissile content in reprocessed MOX fuel would not be sufficient to carry out the recycling in a LWR. Therefore, for the second recycling, a fast reactor would be required (unless additional fresh fissile material is added to the recycled fuel) [12]: in the fast spectrum, fissionable nuclides also contribute to fission chain reaction, while in the thermal there would be an increased build up of minor actinides and even plutonium isotopes, due to capture cross sections being predominant. Moreover, captures by ^{238}U are enhanced in the fast spectrum, hence more fissile material can be bred [22]. This strategy is not implemented yet, but it is investigated in multiple countries. It presents many technical challenges: MOX fuel reprocessing presents stricter handling requirements, and fast reactor fuel necessitates different handling and fabrication techniques. In addition to these new facilities, also a fast reactor fleet is necessary in this back-end strategy. However, this option allows a drastic reduction in heat load and radiotoxicity, decreasing DGR costs. Moreover, it leads to a better exploitation of natural resources, natural uranium needs are reduced by 99% [12] and RepU stockpiles can also be used. This cycle can be self sustainable, and if all the facilities are in national territory, the country adopting it would be totally independent. In this scenario, as opposed to the case of fossil fuels, political instabilities affecting the uranium providing countries would not significantly impact the worldwide energy production. Finally, this strategy increases the proliferation resistance of the cycle by continuously recycling plutonium, avoiding it to remain in stockpiles for a long time.

1.2.4. Pu multi-recycling + MA recycling strategy

In the previous recycling strategies, PUREX raffinate is always disposed as HLW. However, minor actinides (MAs) represent an important contribution to heat load and radiotoxicity of the HLW: for cooling times between 1000 and 10^5 years, they are the main radiotoxicity contributors alongside plutonium, and they also contribute to the heat production of the waste. Therefore, minor actinides removal would reduce the burden on

the repository. The most abundant MAs present in the spent fuel are americium, neptunium and curium, hence they are the main candidates for partitioning and transmutation (P&T): in this strategy, they would be separated from the HLW, and transmuted in a reactor, either by neutron capture (when the daughter is a shorter-lived isotope) or by neutron induced fission. Americium is present mainly as Am-241, with a half life of 432 years, but also other isotopes are found, and it is the most abundant minor actinide in the fuel. It contributes significantly to gamma activity and radiotoxicity, especially after 500 years of cooling time, when fission products contribution is minimal. Am-241 has several gamma lines, among which an intense one at 59 keV, while Am-243 has an intense gamma emission at 75 keV, and its daughter Np-239 has also a very energetic gamma emission. Regarding neutron emissions, they occur mainly by (α,n) reactions on Am-241. Neptunium's predominant isotope is Np-237, which contributes significantly to the long-term radiotoxicity due to the very long half life, but not to the heat load; the gamma emissions are mild (low rate, low energy). Finally, curium is present in smaller quantity with respect to Am and Np mainly as Cm-242 and Cm-244, both with relatively short half lives, compared to the other actinides (163 days and 18.1 years respectively for the two Cm isotopes). It makes an important contribution to gamma activity and radiotoxicity, but most importantly neutron emissions: Cm-244 has a high spontaneous fission branching ratio, in addition to (α,n) reactions [23].

Minor actinides transmutation can occur in both thermal and fast reactors. Thermal reactors are considered a viable option mainly because they represent the majority of existing reactors. However, inserting TRU-loaded fuel in a thermal reactor presents several drawbacks; for instance, in the thermal spectrum neutron captures predominate, hence these nuclides behave as neutron poisons and a significant fuel enrichment is required. In addition, since in thermal spectrum transmutation is achieved mainly by successive captures, a greater number of higher-mass isotopes (Bk, Cf) will be produced. The preferred option for transmutation are fast reactors: since fission to absorption ratio is much higher in the fast spectrum, generation of higher actinides is reduced, and fission rates are also higher. Actinides contribute with fission instead of behaving as neutron poisons, hence no particular enrichment is required, instead fast reactors can also be used as breeders. Finally, fast reactors do not require oxide fuels, but they can employ different kinds of fuel and coolant. ADS (Accelerator Driven Systems) are also a possible option for transmutation [13, 24].

Overall, minor actinides recycling has the important advantage of decreasing volume, heat load and radiotoxicity of the HLW, hence reducing the burden of the DGR and making waste management and disposal easier. However, it presents several technical

challenges: new techniques have to be developed for fuel recycling and fuel fabrication, a fast reactor fleet is required, and finally new reprocessing and fabrication plants are also necessary. When added to a critical core, minor actinides impact largely on reactivity coefficients and parameters affecting the kinetics of the reactor, such as delayed neutron fraction, expansion coefficients, density coefficients [13]. Nevertheless, it should be noted that complete transmutation of actinides is not possible in any reactor system: a residual amount of minor actinides will remain at the end of irradiation. A single recycling scheme has been considered: actinide bearing fuel is sent to the DGR after burning and proper conditioning. However, this fuel cycle option presents very high costs related to the plants and the technology, and single recycling would not be economically feasible, especially since it leads to a very limited reduction of the minor actinides content in the repository. On the other hand, multi recycling means that the actinide bearing fuel is reprocessed as well: this option allows a significant reduction of radiotoxicity and decay heat levels. However, the mass of minor actinides that have to be processed is significant, hence the cost is overall high. Moreover, the large amount of minor actinides in the fuel cycle overall implies an increased risk of release of radionuclides. Finally, a cycle of separation, fabrication, irradiation, cooling and transport might take many years: the number of recycling processes should be kept to a reasonable value [23].

Hydrometallurgical reprocessing

There are two main routes of UNF reprocessing for actinides recycling: pyrochemical and hydrometallurgical. Hydrometallurgical reprocessing exploits liquid-liquid extraction, in which metal ions are separated in two immiscible liquid phases by means of an extractant or ligand, which is able to complex certain metals in solution. On the other hand, pyrochemical reprocessing exploits electrochemical and chemical processes in molten salts, such as electroreduction and electrorefining. Since no extractant is employed, this method overcomes radiolysis concerns that instead represent an important problem for hydrometallurgical processes. Therefore, this route is better suited for high-burnup and high Pu content UNF with a short cooling time, hence highly radioactive, like fast reactors fuel. Pyrochemical reprocessing has several advantages such as high efficiency and simple procedures, no radiolytic degradation concerns, compact equipment. However it presents also many challenges, such as the necessity of corrosion resistant materials, remote maintenance, and radioactive gaseous waste and waste molten salt management [25].

At the European level the effort is directed mainly towards the hydrometallurgical route, which is considered generally safer, due to the lack of gaseous emissions and low temperature procedures. In liquid-liquid extractions, the two immiscible phases are aqueous and

organic, respectively. The aqueous phase is often a nitric acid solution, while the organic phase is usually composed by a diluent (mostly aliphatic/aromatic hydrocarbons), and an extractant or ligand. Together, the mixture of ligand and diluent is called solvent. Hydrometallurgical separation is often carried out as a forward extraction: the aqueous phase contains all the metal ions resulting from UNF dissolution or from the PUREX process, while the ligand is lipophilic, dissolved in the organic phase. At the interface between the two phases, complexation reaction occurs and the complexed metal ions are transferred to the organic phase. Instead, the stripping is carried out by contacting the loaded organic phase with a clean aqueous phase, for the release of the target ions. In certain situations, low acidity is sufficient for the metal's release: this is often the case in which the organic phase contains only the target ions, because it is not a selective process. When some unwanted ions are co-extracted in the organic phase, a hydrophilic ligand is used to selectively strip the ions of interest. Sometimes, both kinds of ligand are employed, and hydrophilic ligands act as masking agents: they complex some ions preventing their extraction. Finally, a scrubbing section aims to selectively remove unwanted from the organic phase. Since the complexation occurs at the interface, the phases are contacted by means of different devices, such as centrifugal contactors, mixer settlers, or pulsed columns. To achieve complete separation, the process is usually continuous, counter-current and multi-stage.

Homogeneous recycling

A first actinides recycling strategy that is investigated is homogenous recycling: uranium and transuranics are contained in a single fuel type and recycled together, hence minor actinides are homogenously distributed and burnt in the core [26]. In this kind of fuel the MA content is limited to a few percent (5%), to minimize their impact on reactor parameters [27]. In this strategy, no pure plutonium stream is generated, increasing proliferation resistance, reactor physics is not affected, and fuel fabrication is more straightforward [26]. Specifically, this strategy is the preferred option for neptunium, because its burn-out rate is similar to plutonium and uranium, and moreover its shielding requirements are not particularly demanding [23]. However, americium and curium, even though present in the fuel in a small fraction, largely impact on the shielding requirements of the fuel fabrication facility. Additionally, all the fuel has to be produced accordingly to such requirements, hence the fuel fabrication cost is increased, and the fuel fabrication plant should have a sufficient capacity to deal with large fuel throughputs [23]. Finally, separation chemistry is complicated with respect to other strategies [26].

In Europe, the GANEX (Grouped ActiNide Extraction) hydrometallurgical process was

developed for the homogeneous recycling of transuranics, and it is organized in two cycles. The first cycle, named GANEX-1, aims at a bulk recovery of uranium from the dissolved used nuclear fuel, by contacting the latter with a solvent made of N,N'di-(ethyl-2-hexyl)isobutyramide (DEHiBA), a ligand selective for U(VI), in an aliphatic diluent. This is performed to obtain high purity uranium product, but mostly to reduce the volume of material to process and simplify the feed for the next cycle. For the second cycle (GANEX-2), different schemes have been developed. The aim is the co-extraction of transuranics, which are present in different oxidation states (III and IV), from a feed that contains lanthanides (III) and other fission products. Therefore, a common feature of the developed schemes is the combined use of different ligands and masking agents, and different scrubbing sections to remove undesired elements. Additionally, transuranics have to be stripped back in a clean aqueous phase [26].

Heterogeneous recycling

Overall, americium and curium are the main contributors to heat load and radiotoxicity of the fuel, hence they are the main candidates for transmutation. Neptunium transmutation, on the other hand, is not particularly impactful: due to its long half-life (Np-237), it has a very low activity [13, 23]. Therefore, the other investigated strategy is heterogeneous recycling: through the PUREX process, uranium and plutonium are recycled into MOX fuel (the main fuel loaded in the reactor) and neptunium can be recovered upon a process modification [28], while americium and possibly curium are separated from the PUREX raffinate and loaded into fuel targets [26]. In the target elements, the MA fraction is kept around 10 - 20% [27]. This is the preferred option for americium and curium: the targets can be positioned in the reactor to optimise the burn-out of the minor actinides, and they can also can be retained in the core for a longer time than the main fuel. In addition, a separated fuel fabrication facility carries out independently the target fuel production with respect to the bulk fuel, hence strict handling requirements would be applied only to a small fuel throughput. Finally, the PUREX process is already industrially mature, making this option the preferred one. However, it is necessary to guarantee compatibility between target and bulk fuel, and a pure plutonium stream is produced [23].

1.3. Heterogeneous recycling processes

PUREX raffinate is a problematic High Level Waste, which contains minor actinides (mostly americium and curium), lanthanides, fission and corrosion products. Various advanced partitioning processes have been developed, first to separate minor actinides from

lanthanides, while later the focus shifted from actinide-lanthanide separation (product: MA(III)) to americium-curium separation (product Am(III)). Some examples of heterogeneous partitioning processes, which were tested in a multi-stage system, can be observed in figure 1.3.

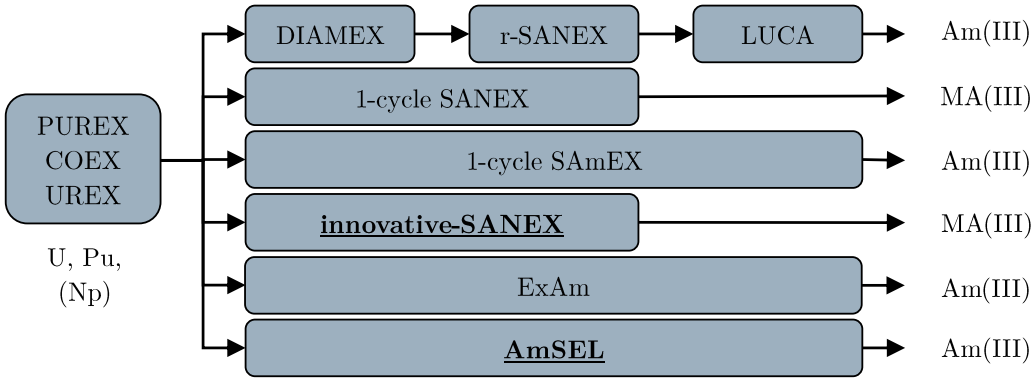

Figure 1.3: Heterogeneous hydrometallurgical process

1.3.1. Actinide-lanthanide separation

The separation of MA(III) from the lanthanides is particularly challenging, due to their similar chemistry and size. Nevertheless, since lanthanides are characterized by important neutron capture cross section [29] and are in much larger concentration [3], this separation is a constraint for the recycling of minor actinides.

DIAMEX+r-SANEX process

The DIAMEX (Diamide Extraction) process takes the PUREX raffinate as feed, and performs a co-extraction of actinides and lanthanides in the organic phase. First, malonamide extractants were used [30], later substituted by diglycolamide extractants (TODGA used together with TBP) [31]. Finally, actinides and lanthanides are stripped.

The second step is the selective extraction of actinides from the product of the DIAMEX process, called r-SANEX (regular - Selective Actinide Extraction). Since oxygen based ligands, such as diglycolamides, do not display any actinide-lanthanide selectivity, nitrogen or sulfur based ligands are adopted for this step, like dithiophosphinic acids or bis-triazinyl pyridines (BTP) [32]. The final flowsheet uses an organic phase containing TODGA and $CyMe_4-BTBP$, a lipophilic bis-triazinyl bipyridine. TODGA is used as a phase transfer agent in low concentration, to improve the slow kinetics of the other extractant. Finally, after a scrubbing section with nitric acid, actinides are stripped from the organic phase

with glycolic acid [33].

1-cycle SANEX

The drawback of the DIAMEX+r-SANEX is that it is a multi-cycle process, with several stripping and re-extraction steps. To simplify the process, the 1-cycle SANEX was developed: actinides are selectively extracted from the PUREX raffinate with a similar organic phase to the one used in the r-SANEX, and after some decontamination steps they are stripped in glycolic acid as in the r-SANEX. The process is simplified, but due to the more complex feed, two scrubbing sections are required, which employ some masking agents to remove unwanted co-extracted ions [34].

i-SANEX

The innovative-SANEX (i-SANEX) process is based on a selective actinide stripping, which significantly simplifies the flowsheet. A TODGA based organic phase co-extracts actinides and lanthanides from the PUREX raffinate. After two scrubbing sections, actinides are selectively stripped in the aqueous phase by means of a hydrophilic ligand. First, a hydrophilic BTP ($SO_3-Ph-BTP$) was used [35], but later a new ligand, PyTri-Diol (PTD) was proposed as an alternative stripping agent [36, 37]. To recycle the organic phase, lanthanides are also stripped.

1.3.2. Am-Cm separation

Americium removal has the largest impact on radiotoxicity and heat load for cooling times around 1000 years, and it can be incorporated in nuclear fuel with no particular concerns, but its gamma emissions impact the reprocessing and fuel fabrication facilities, imposing shielding requirements. Curium isotopes have a very short half-life, hence interim-storage might be the best strategy for these nuclides. In addition, it is difficult to handle, due to its high decay heat and neutron emission caused by an important branching ratio of spontaneous fission. Finally, curium is not well suited to transmutation, because its isotopes have quite low fission and capture cross-sections [23]. Curium irradiation has been considered an option because its separation from americium is quite challenging, since they are both trivalent ions, adjacent in the periodic table, with similar ionic radius (IR): for a coordination number 9, $IR_{Am^{3+}}$=1.157, $IR_{Cm^{3+}}$=1.147 [38].

Several processes for Am-Cm separation were developed. Some exploit a fundamental difference between the two elements: differently from Cm(III), Am(III) can be oxidized to a higher oxidation state. The potential selectivity achieved is high, but there are some

drawbacks: first, higher oxidation states of Am are usually unstable in acid solution; second, in the context of the separation from the PUREX raffinate, it is difficult to avoid unwanted oxidation and extraction of other metal ions, such as Ru, Ce or Zr; finally, formation of precipitates and corrosion due to strong oxidation potential [39]. Other methods are based on liquid-liquid extraction, in which no oxidation is carried out.

LUCA process

The LUCA (Lanthaniden Und Curium Americium Trennung) process takes as a feed the DIAMEX product (actinides and lanthanides) or the r-SANEX product. The solvent is bis-(chlorophenyl)-di-thiophosphinic acid (the extractant) and tri-ethylhexylphosphate (TEHP, a synergist) in t-butylbenzene (TBB) and isooctane. The organic phase is contacted with the feed, then Am is stripped with nitric acid. The system achieved remarkably good separation of Am from Cm and the lanthanides [39, 40].

ExAm

A system able to separate Am directly from the PUREX raffinate was implemented with the french EXAm process. It is based on the combined action of two lipophilic ligands, N,N'-dimethyl-N,N'-dioctyl-hexyloxyethyl-malonamide (DMDOHEMA) and di-2-ethylhexylphosphoric acid (HDEHP), and a hydrophilic diglycolamide (TEDGA). The selective Am extraction is based on the slight preference of DMDOHEMA for Am and the one of TEDGA for Cm. Nevertheless, the process presents some problems: TEDGA tends to distribute across the phases, and Am is co-extracted with light Ln, Mo and Ru, which can be stripped with some buffer solutions [39, 41, 42]. However, the pH range in which separation takes place is limited. Therefore, efforts are made towards a more robust system.

1-cycle SAmEX

Also this process, whose feasibility was demonstrated with batch experiments but no continuous large scale experiment was performed, aims at the selective extraction of Am from PUREX raffinate. It is based on the combination of the lipophilic $CyMe_4-BTPhen$, with a larger affinity for Am, and the hydrophilic TEDGA, which lead to a satisfactory Am-Cm separation. Bimet (a hydrophilic complexant containing sulphur) was used to suppress Pd and Ag co-extraction [39, 43].

AmSel

The AmSel process has been presented for the first time by Wagner et al. [44]: first the co-extraction of trivalent actinides and lanthanides by TODGA takes place, then Am(III) is selectively stripped in the aqueous phase by means of $SO_3-Ph-BTBP$, a sulphonated hydrophilic ligand. The AmSel process exploits the opposite selectivity of TODGA and $SO_3-Ph-BTBP$ to separate Am from Cm.

Subsequently, a flowsheet has been developed for the Am stripping and Cm re-extraction, and tested in the Forschungszentrum Jülich centrifugal contactors battery (figure 1.4 [45]). Previously, extraction and scrubbing steps were already tested in the same facility [35]. An existing model, which simulated the extraction of Am, Cm and lanthanides by TODGA, was modified to account for the Am and Cm complexation by $SO_3-Ph-BTBP$, using all the data gathered from batch experiments. The model was then implemented in the PAREX+ code to develop a possible flowsheet design [46]. It has to be noted that, with the characteristic selectivity of the AmSel system, at least 20 to 30 stages are necessary to achieve an americium recovery rate over 70%. Additionally, it has been observed that the flowsheet performances are highly sensitive to various parameters, such as ligand or nitric acid concentration. For instance, a change of 0.1 M HNO_3 in the stripping solution impacts largely the Am recovery rate [45].

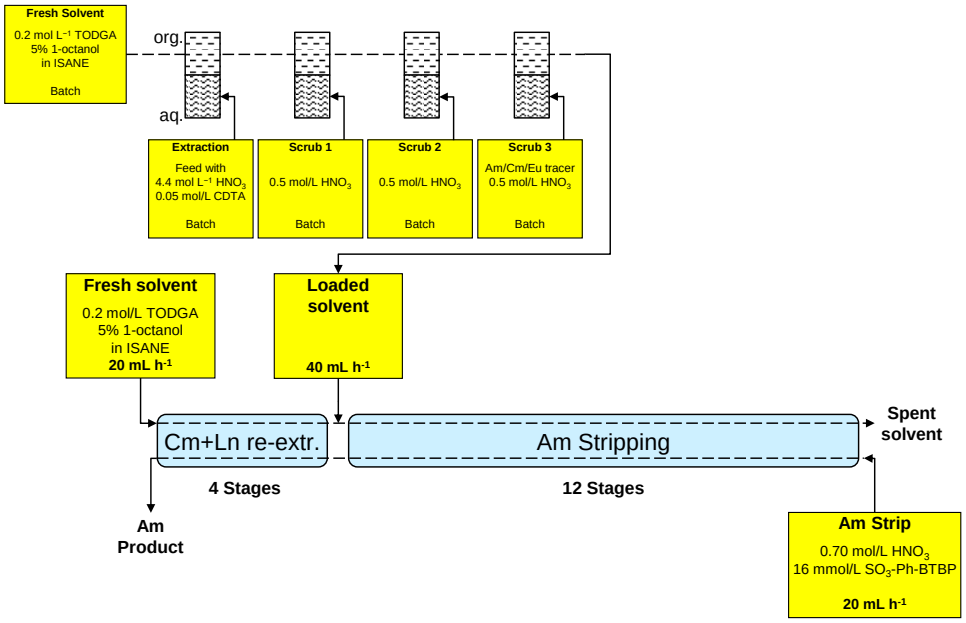

Figure 1.4: Flowsheet for the AmSel process [45]

2 | New hydrophilic ligands for the AmSel process

2.1. Complexation chemistry

A ligand is a molecule able to create complexes with metal ions: the latter are Lewis acids, or electrophiles, while the former contains donor atoms (atoms with a lone pair of electrons, such as O, N, S, P), hence it is a Lewis base. The ligand structure includes a complexing core, which contains the donor atoms, and side groups. The denticity is the number of donor atoms that can coordinate the metal [47]. The complex consists of a central metal ion, coordinated by a certain number of ligand molecules, whose donor atoms bind to the metal through their lone pairs. The complex stoichiometry is determined by the ligand's denticity and the metal's coordination number (CN), which is the number of donor atoms that can coordinate it. Actinides and lanthanides, since they are particularly large atoms, display CN from 8 to 10 [38]. A ligand can form complexes of different stoichiometry with the same metal, which can be simultaneously present in solution, and whose respective concentration is affected by the environment.

The formation of a $M : L$ complex with stoichiometry $1 : n$, in which a metal M is coordinated by n ligand L molecules, occurs as a stepwise complexation described in equation 2.1 [48].

$$ML_{n-1} + L \rightleftharpoons ML_n \tag{2.1}$$

According to the law of mass action, the associated equilibrium constant K_n is related to the concentration of reagents and product by equation 2.2.

$$K_n = \frac{[ML_n]}{[ML_{n-1}][L]} \tag{2.2}$$

The overall complexation reaction (equation 2.3) is described by the stability constant

$\beta_{1:n}$, which is the product of all the constants of the stepwise equilibria (equation 2.4).

$$M + nL \rightleftharpoons ML_n \tag{2.3}$$

$$\beta_{1:n} = K_n \cdot K_{n-1} \cdot ... \cdot K_1 = \frac{[ML_n]}{[M][L]^n} \tag{2.4}$$

The value of the stability constant $\beta_{1:n}$ is an indication of the thermodynamic stability: whether the direction of the reaction is towards the complex ($\beta_{1:n} \gg 1$) or the free species ($\beta_{1:n} \ll 1$). A complex is thermodynamically stable if the equilibrium is shifted to the right. Another definition is that the free energy of the products is lower than the one of the reagents ($\Delta G_0 < 0$, as shown in figure 2.1) [47]. On the other hand, kinetic stability or inertness describes the speed at which the reaction moves towards equilibrium, and it is related to the activation energy E_A that has to be overcome for the reaction to occur [47]. If the energy required to go from the formed complex to the activation state is low, the complex is labile, while in the opposite case it is called inert [47]. It has to be noted that, since complexation occurs in solution, there are competing equilibria: metal ions in water are solvated or, if an acid is present, the ligand donor sites can be occupied by protons. Moreover, other ligands can be present. If the complex is labile, ligand substitution occurs quickly, and the metal might not be retained in the desired phase.

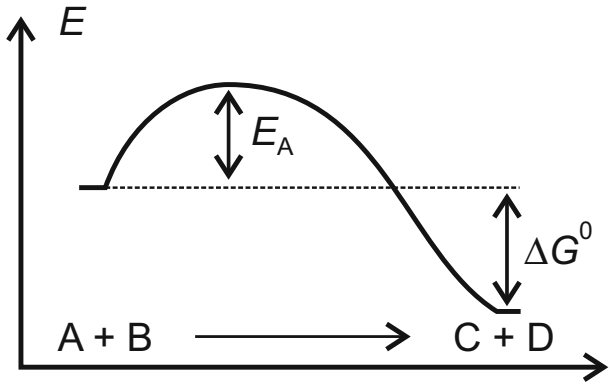

Figure 2.1: Activation energy E_A and difference in free energy ΔG_0 between products and reagents [47].

The ligand's denticity affects the stability of the complex: multi-dentate ligands (chelants) form more stable complexes, both from the thermodynamic and kinetic point of view. The reason for thermodynamic stability is that complexation with a chelant leads to an increase in the number of molecules in solution, which translates into a positive entropic

contribution. Kinetic stability is achieved because when the first donor atom coordinates the metal, all the others come into proximity, hence coordination is faster. On the other hand, since all the bonds must be broken for the ligand to dissociate, decomplexation has an elevated activation energy [47].

2.2. Requirements

To be employed in a large scale process, a ligand must fulfil several requirements, including selectivity towards the target ions, fast kinetics, solubility. Moreover, the whole extraction system employed in the process must exhibit robust resistance to radiolysis and chemical hydrolysis, comply with the CHON principle, and remain stable despite operational fluctuations in process parameters.

2.2.1. Selectivity

The selectivity of the ligand towards the target ions is dictated by the number and kind of donor atoms, but also by the core structure. Hard donors are typically small and highly electronegative atoms, while soft donors are larger with lower electronegativity; for instance, oxygen or nitrogen are hard donors, while phosphorous is a soft donor. According to the HSAB theory (Hard Soft Acid Base), hard acids preferentially bind to hard bases via electrostatic interactions, while soft acids coordinate preferably with soft bases through bonds with a more covalent character [47]. In the context of UNF reprocessing, the ions of interest are actinides and lanthanides; since both are trivalent, they are hard acids. However, actinides have a softer character, due to their lower charge density. An oxygen based ligand is a hard base that will bind with both actinides and lanthanides. It has been observed that nitrogen based ligands are instead more selective towards actinides: even though nitrogen is a hard donor, it is softer than oxygen because it is less electronegative, and binds more favourably to softer acids. To modulate the hardness of the ligand, hence the selectivity, it is possible to employ both hard and soft donor atoms.

On the other hand, the core structure affects the selectivity with respect to the size of the ion. The complexing core can be rigid and preorganized, or present a certain conformational variability. A ligand with conformational variability can adapt its configuration and can be selective towards a larger number of metal ions. This feature is highly desirable for bulk extractions where the simultaneous removal of multiple ions is required. Nevertheless, even broadly selective flexible ligands can express size-selectivity, as certain conformations are more favoured than others. As an example, flexible alkyl-substituted

diglycolamides (DGAs) can complex both trivalent actinides and lanthanides, with no particular selectivity towards one series or the other. However, they systematically display an increasing affinity with decreasing ionic radius [49]. Conversely, in case of a preorganized and sterically rigid core, the selectivity of the ligand will be higher towards ions whose ionic radius fits perfectly in the complexing pocket. However, the ligand has to be designed specifically to fit the target ions, otherwise they will not be complexed [50]. For instance, Am(III) and Cm(III) have nearly the identical hardness and similar ionic radius. Their separation can be achieved employing a ligand whose cavity is tailored for Am(III) better than Cm(III); this can be achieved by means of a highly preorganized ligand.

2.2.2. Solubility

For the separation to take place effectively, the ligand has to be soluble only in a single phase. Donor atoms, due to their lone electron pairs, increase the polarity of the molecule. However, this effect can be offset by a bulky core structure. Therefore, if the ligand is designed to be lipophilic, long aliphatic side chains are often used. In the opposite case, side chains contain polar atoms or ionizable groups to increase hydrophilicity. It should be noted that normally side chains do not directly participate in complexation, but they heavily affect it: they can host electron-withdrawing groups that deplete the electron density of the donor atoms, contain auxiliary donor sites that alter the complex stoichiometry, introduce steric hindrance, or influence the conformation of the molecule.

If the ligand does not express good solubility, it can form a third phase; to prevent this phenomenon, phase modifiers can be used. As an example, TODGA is a widely used oxygen based lipophilic ligand, highly selective for trivalent ions, that has exhibited a third phase in many aliphatic diluents [51]. 1-octanol was found to be the solution: added as a phase modifier, it increased just enough the polarity of the organic phase to avoid completely this phenomenon [52]. Clearly, also the complexes formed by the ligand have to display a good solubility in the correct phase, otherwise the complexed ions remain in the third phase and no effective separation is carried out.

2.2.3. Fast kinetics

The residence time or mixing time is the time during which phases are contacted in the contacting device. It is an important parameter because the mixing between the phases should last a sufficient time for the distribution ratios to reach equilibrium. The residence time inside some contacting devices is inversely proportional to the flowrate,

hence it represents a constraint for the latter [53].A ligand with fast kinetics, which reaches equilibrium within a short time (1–2 minutes), is desirable to reduce the required residence time, thereby allowing for higher flow rates and increasing the overall throughput of the process. However, kinetics is largely affected by the extracting system in which the ligand is used: it depends on mixing efficiency, temperature, viscosity of the two phases. Complexation kinetics is strongly influenced by the ligand's structure. If it is preorganized already in the configuration required for complexation, the molecule does not need to overcome configurational change energy barriers, making the complex formation more efficient and improving the kinetics of the reaction [54]. Kinetics stability is fundamental in this context: while a fast complexation is required for the process, a labile complex is undesired. As an example, in the AmSel process the hydrophilic ligand aims to strip Am(III) in the aqueous phase from a loaded organic phase. For the stripping to occur, the complexes with the hydrophilic ligand should have a more inert character than the ones with the lipophilic ligand.

2.2.4. Resistance to radiolysis and hydrolysis

The ligand, or better the whole extracting system, should be resistant to radiolysis and hydrolysis, because it operates in a particularly hostile environment, highly active and highly acidic. Radiolytic and hydrolytic degradation deplete the active ligand concentration. Furthermore, temperature, which often increases during phase contacting, plays a critical role: beyond altering complexation equilibria, it significantly accelerates degradation kinetics. Moreover, degradation products might affect the process, because they can display a different selectivity with respect to the non-degraded molecule, compromising the separation or co-extracting unwanted ions. Ideally, a ligand should degrade into species that do not interfere with the selectivity of the system. Additionally, degradation products of both the ligand and the diluent can cause third-phase formation or phase entrainment. Degradation products are also an obstacle for organic phase recycling: the more they accumulate, the more fresh phase has to be introduced in the system.

2.2.5. Compliance with the CHON principle

The CHON principle dictates that all newly synthesized ligands (both hydrophilic and lipophilic) and their associated diluents must be composed exclusively of Carbon, Hydrogen, Oxygen, and Nitrogen atoms. This principle aims to improve the sustainability of the process: when a CHON molecule is incinerated for waste disposal, it is degraded in gaseous products (H_2O, CO_2, N_2) without producing secondary waste. Additionally, the use of fully incinerable CHON reagents simplifies the eventual downstream recovery of

the separated target metals from the aqueous phases.

2.3. Evaluation and screening of new ligands

Prior to large-scale experiments, such as multi-stage counter-current demonstration runs in centrifugal contactors, newly synthesized ligands must undergo an extensive screening process to assess the viability of the extracting system. In fact, multi-stage trials require significant quantities of ligand. However, the synthesis process of novel ligands yields an insufficient amount of product for these experiments, typically milligram-scale quantities. Therefore, a scale up of the synthesis process has to be optimized. For this reason, in addition to the significant volume of radioactive waste produced as a result of the high radiotracer activity used, a large-scale test is particularly costly. Moreover, the operational window of the system has to be determined, and complexation and fluid-dynamic data have to be gathered to model the process and optimize the number of stages to employ in the different sections.

2.3.1. Batch experiments

To evaluate its operational window, in which a successful separation is performed, the investigated ligand is tested with batch extraction experiments according to a standardized procedure, in the context of the extracting system in which it is employed. The performance evaluation is carried out by calculating two fundamental parameters for every metal of interest.

- The distribution ratio D: the D_A of metal A is the ratio between its concentration in the organic phase and in the aqueous phase (equation 2.5).

$$D_A = \frac{[A]_{org}}{[A]_{aq}} \tag{2.5}$$

  It is greater than 1 when the metal is mostly present in the organic phase, while it is lower than 1 when the metal is mostly retained in the aqueous phase.

- The separation factor SF: the $SF_{A/B}$ between two metals A and B is a measure of the selectivity of the system. It is the ratio of the distribution ratios of the two metals (equation 2.6).

$$SF_{AB} = \frac{D_A}{D_B} \tag{2.6}$$

  Conventionally, the SF is calculated in order to be greater than 1, thus it is the ratio of the D of the element more retained in the organic phase and the D of the

element more retained in the aqueous phase.

Another important parameter is the extraction efficiency E, which is defined from the distribution ratio D of a metal (equation 2.7). It is the percentage of metal extracted in a single stage [55].

$$E(\%) = \frac{D}{D+1} \cdot 100 \tag{2.7}$$

Commonly investigated variables are nitric acid and ligand concentration, temperature, contacting time. Besides the operational window determination, extraction tests are useful to determine the resistance of the extracting system to process fluctuations, and to highlight the occurrence of phenomena that might compete with complexation.

Slope analysis

Additionally, extraction experiments allow to gather some preliminary information regarding complexation. If the logarithm is applied to equation 2.4, and the terms are re-arranged, equation 2.8 is obtained, in which the logarithm of the concentration ratio is related to the logarithm of the ligand concentration through a coefficient equal to the stoichiometry of the complex.

$$\log \frac{[ML_n]}{[M]} = n \log [L] + \log \beta \tag{2.8}$$

By varying the ligand concentration, and evaluating the slope of $\log D$ vs $\log [L]$, it is possible to determine the stoichiometry of the complexes. However, this evaluation yields an exact value if only one complex is present in solution. Moreover, $[L]$ is the free ligand concentration after complexation. Often, in extraction experiments, only the initial ligand concentration is known. If the metal is largely substoichiometric with respect to the ligand, the approximation holds. However, if other phenomena including protonation or ligand extraction in the organic phase occur, the slope analysis does not produce significative results.

For the specific case of the AmSel process, where two ligands are employed, slope analysis can still be carried out. Considering that the metal is substoichiometric with respect to the ligands, and it is present only in form of complexes, the equilibrium between the two phases can be described by equation 2.9. The equilibrium constant can be evaluated with the law of mass action (equation 2.10).

$$nL_{aq} + M(L_{org})_m \rightleftharpoons mL_{org} + M(L_{aq})_n \tag{2.9}$$

$$K = \frac{[M(L_{aq})_n][L_{org}]^m}{[M(L_{org})_m][L_{aq}]^n} = \frac{[L_{org}]^m}{D[L_{aq}]^n} \tag{2.10}$$

By applying the logarithm on both the terms of the equation, and rearranging the factors, the relationship between the $\log D$ and $\log [L_{aq}]$ is found to be again linear, as observed in equation 2.11.

$$\log D = -\log K + m \log [L_{org}] - n \log [L_{aq}] \tag{2.11}$$

2.3.2. Complexation and molecular structure studies

Complexation studies aim to quantify the equilibrium stability constants ($\beta_{1:n}$), evaluate the complex stoichiometries and the ligand speciation, and determine the influence of competing phenomena.

An example of competing equilibrium is protonation: the ligand's donor sites can bind hydrogen ions present in an acid solution. The determination of the ligand's protonation constants (pK_a) is fundamental to determine the concentration of the free ligand available for complexation at a given pH. The pK_a can be evaluated with a potentiometric titration: the ligand in acid solution is titrated with a strong base, and the change in H^+ concentration is measured [56].

Spectroscopic techniques are a common method to investigate the complexation behaviour of a ligand, by performing a metal titration: a metal solution of fixed concentration is added in small aliquots to the ligand in solution or viceversa. When a ligand complexes a metal, some parameters change with respect to the free species, and the differences can be observed by recording a spectrum after every addition. By observing the spectral changes, it is possible to determine the stoichiometry of the complexes and evaluate their stability constants through proper fitting. The specific titration procedure and fitting methods depend on the investigated parameter and the chosen spectroscopic method. Commonly used spectroscopic techniques are TRLFS and UV-VIS (figure 2.2. In Time-Resolved Laser Fluorescence Spectroscopy (TRLFS), a laser excites the electrons of solvated metal ions in solution, and the fluorescence spectrum is measured. The titration is carried out by adding ligand aliquots to the metal and recording the emission spectrum after every addition. Peaks are related to different electronic transitions, which are sensitive to changes in symmetry or in the inner coordination sphere; when the electronic configuration of the metal changes upon complexation, the peaks display shifts, splitting, intensity changes. Additionally, the fluorescence lifetime can be measured. The emission spectra provide information on stability constants and stoichiometry, while the fluorescence lifetime on the hydration/solvation, since these phenomena have quenching effects and decrease it

[48]. Instead, with UV-VIS spectroscopy, the absorbance spectrum of the ligand in solution is measured. The titration is carried out by stepwise addition of metal aliquots; the absorbance spectrum is recorded after every addition. As in TRLFS, peaks are associated to different electronic transitions, but related to the ligand. When the complex is formed, the electronic configuration changes, causing the peaks to shift, split or change in intensity. By fitting the titration data, stability constants and stoichiometry of the complexes can be evaluated [57].

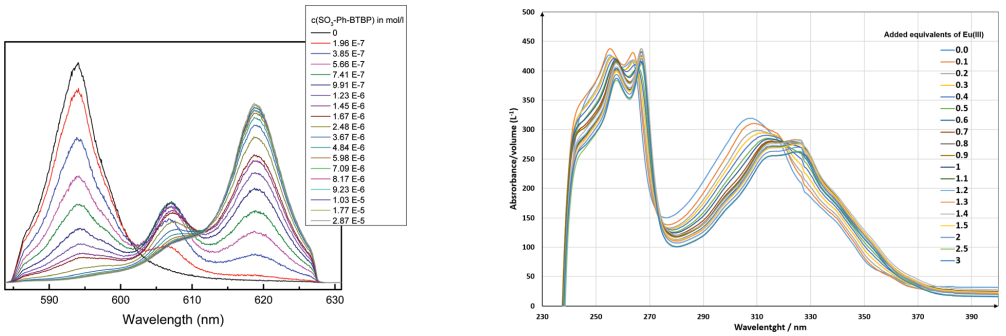

(a) TRLFS titration of Cm(III) with $SO_3-Ph-BTBP$ in 10^{-3} M $HClO_4$ [48].

(b) UV-VIS titration of a sulfonated BTrzPhen with $Eu(NO_3)_3$ in neutral water [58].

Figure 2.2: Examples of spectra obtained by TRLFS and UV-VIS spectroscopy.

Finally, computational and crystallographic studies are fundamental to understand the favoured conformations of the ligand molecule, the bond lengths with the coordinated metal, and interactions with the side chains, if present. Commonly used computational tools are Molecular Mechanics and Density Functional Theory (DFT) calculations, while a common crystallographic investigation technique is single crystal X-ray diffraction (SC-XRD) [59, 60].

2.4. The reference AmSel system

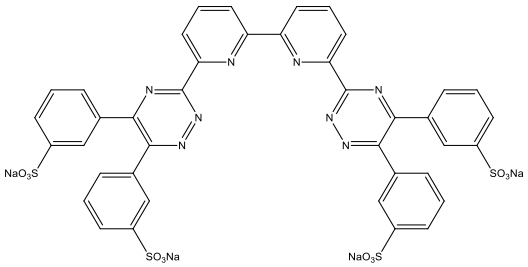

(a) $SO_3-Ph-BTBP$ structure [48].

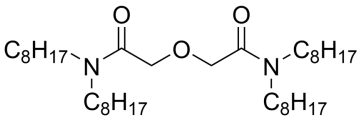

(b) TODGA structure [61].

Figure 2.3: Reference AmSel system [44].

2.4.1. Organic Phase

The lipophilic ligand used in the AmSel process is N,N,N',N'-tetraoctyl diglycolamide (TODGA), displayed in figure 2.3b. It was synthesized by Sasaky et al. [49] among other diglycolamides (DGA), as a promising extractant for trivalent actinides and lanthanides in n-dodecane.

No useful selectivity is exhibited by the molecule for actinide-lanthanide separation. However, a size selectivity emerged: the distribution ratios were found to increase with the inverse of the ionic radius. Moreover, an increase of the D values with nitric acid concentration of the aqueous phase was observed: TODGA creates positively charged 1:3 and 1:4 complexes with the metals, that are neutralized by nitrates [49, 62]. The neutral complex is preferred due to its better stability. An increase in nitrate concentration will move the equilibrium of the complexation reaction to the right, increasing the extraction, as it can be observed for 1:3 complexes in equation 2.12.

$$M^{3+}_{aq} + 3NO^{-}_{3,aq} + 3TODGA_{org} \rightleftharpoons [M(TODGA)_3](NO_3)_{3,org} \tag{2.12}$$

Additionally, TODGA has good radiolytic and hydrolytic stability [62], and it has fast kinetics [63, 64].

In the AmSel process, but also in SANEX-type processes, the organic phase is 0.2 M TODGA in 5% v/v 1-octanol/ISANE IP-175. Nevertheless, the choice of the diluent-phase modifier mixture has changed significantly over the years. The maximum concentration of metal ions that can be loaded in the organic phase without third-phase formation is

called limiting organic concentration (LOC) [62]. Since the concentration of lanthanides in the PUREX raffinate is large, TODGA, as other extractants when contacted with such aqueous phase, is subject to this phenomenon. Therefore, several phase modifiers have been investigated, together with different diluents. The diluents were found to affect both the third-phase formation and the distribution ratios. From n-dodecane or kerosene, the preferred choice for partitioning processes became TPH (hydrogenated tetrapropylene). It is a mixture of C10-C13 alkanes (isoparaffines), adopted to reduce the density and viscosity of the organic phase and improve hydraulic properties [65]. Later, it was substituted by ISANE IP-175, another isoparaffinic diluent (C11-C12). Among the phase modifiers, 1-octanol was found to be the most suitable: it is CHON-compliant, it suppresses successfully third-phase formation and, in a 5% v/v concentration, it presents a limited extraction of HNO_3 [51, 52]. In this organic phase, TODGA forms prevalently 1:3 complexes [48].

2.4.2. $SO_3-Ph-BTBP$

The reference hydrophilic ligand for the AmSel system is sodium 3,3',3",3"'-([2,2'-bipyridine]-6,6'-diylbis(1,2,4-triazine-3,5,6-triyl))tetrabenzenesulfonate, or $SO_3-Ph-BTBP$ (SO_3^- counterion does not make a particular difference in the complexation of Am), synthesized by Lewis et al. [66], whose structure is dispayed in figure 2.3a. It is a nitrogen based ligand, with a BTBP (6,60-bis(1,2,4-triazin-3-yl)-2,20-bipyridine) core (tetradentate), highly selective towards actinides with respect to lanthanides [67]. As mentioned before, since nitrogen based ligands are soft, they will bond preferably with actinides with respect to lanthanides. In fact, the bonds formed will have a more covalent character, hence the complex will be more stable. The bipyridine moiety contains a single carbon-carbon bond, that allows the structure to rotate: the molecule can modify itself spatially. This feature has one drawback: some ions with different dimensions might be complexed, due to the core space mobility [50]. Finally, the triazine rings participate to the complexation, and together with the sulfonated phenyl moieties improve the solubility in the aqueous phase.

From the batch experiments performed by Wagner et al. [44], several important characteristics of $SO_3-Ph-BTBP$ were observed. With ligand concentrations in the order of tens of mM and nitric acid concentrations around 0.5 M, $SF_{Cm/Am}$ ranged in between 2.5 and 3. Moreover, separation from the lanthanides was achieved successfully, ($SF_{Eu/Am} = 600$ at 20 mM $SO_3-Ph-BTBP$, 0.5 M HNO_3). Additionally, the system is characterized by fast kinetics (7 minutes, but D_{Am} is close to its equilibrium value after 2 min), differently from other lipophilic BTBP ligands [54].

Slope analysis for actinides was also performed, which yielded a slope of -1.3, suggesting 1:1 complexes. Subsequently, TRLFS studies were performed, to better investigate the complex stoichiometry. Only 1:3 TODGA complexes were observed in the organic phase. On the other hand, 1:2 $SO_3-Ph-BTBP$ complexes ($[Cm(SO_3-Ph-BTBP)_2]^{5-}$) were the only species found in the aqueous phase. This result has also been confirmed by other TRLFS studies [48]. A later study explained the behaviour of these systems with the formation of heteroleptic complexes [68]: actinides complexes with both TODGA and the hydrophilic ligand molecules can form and be extracted in the organic phase.

By varying the nitric acid concentration, it has been observed that $SF_{Cm/Am}$ decreases with increasing nitric acid concentration, due to the protonation of the ligand: the free ligand concentration decreases. TRLFS studies have highlighted the influence of nitrates, protonation and ionic strength on the complexes [48]. It has been observed that nitrates compete with $SO_3-Ph-BTBP$ in the complexation of Cm. Nevertheless, protonation was found to have the most impact on complexation: in 0.5 M acid, more than 90% of the $SO_3-Ph-BTBP$ is protonated.

Additionally, lanthanides behaviour was investigated by Wagner et al. [44]: the light Ln displayed a linear increase in the distribution ratios with nitric acid concentration, while the heavy Ln (Tb-Lu) displayed a decrease in the distribution ratios after a certain HNO_3 concentration. At 1.5 M HNO_3, the D of Ho-Lu were found to be below 1. A later study by Sauerwein et al. [69] investigated the complexation kinetics of heavy lanthanides, both in stripping and forward extraction conditions. Stripping kinetics experiments showed that the complexation of heavy Ln is stronger with TODGA than with $SO_3-Ph-BTBP$, because they remained in the organic phase after a long contacting time. Instead, forward extraction kinetics experiments highlighted that $SO_3-Ph-BTBP$ kinetically inhibits the metal extraction by TODGA. Since TODGA usually ensures a fast extraction, the inhibition is related to $SO_3-Ph-BTBP$ slow decomplexation. Additionally, the decomplexation seems to be slower at higher concentration of nitric acid.

2.5. Proposed hydrophilic ligands

The main drawbacks of the reference hydrophilic ligand used in the Amsel process are the non compliance to the CHON principle and the limited selectivity between Am and Cm. Many hydrophilic ligands have been proposed for an improved AmSel process, aiming at higher $SF_{Cm/Am}$, but also at a better separation from lanthanides. Other important features are fast kinetics and good solubility. Candidate molecules are still in an initial screening phase, and additional information necessary for scale-up tests has yet to be

acquired.

For the separation of actinides from lanthanides, the preferred choice falls on nitrogen based heteroaromatics: commonly used moieties are pyridine, 2,2'-bipyridine or 1,10-phenanthroline. Nevertheless, tridentate pyridine based ligands like $SO_3-Ph-BTP$ [70] or PyTri (pyridine-2,6-bis(1H-1,2,3-triazol-4-yl)) [36] do not express any Cm/Am selectivity. For selective separation of Am(III) from the PUREX raffinate, tetradentate bipyridine or phenanthroline based ligands have to be adopted. The side rings can be of different nature, such as triazine (as in case of BTBP), pyridine or triazole. The high selectivity towards actinides, and specifically Am(III), is partially size-based. In fact, a study on DDP (2,9-Di(pyrid-2-yl)-1,10-phenanthroline) highlighted a preference of polypyridyl-type ligands for metal ions with M-N bond length close to 2.65 Å, which is close to the one of Sm(III), but Am(III) has a similar M-N bond length. The authors added that this preference possibly occurs also for molecules with triazine as side groups because, besides some small differences in the bond lengths, these structures have a very similar geometry and hence similar properties [59].

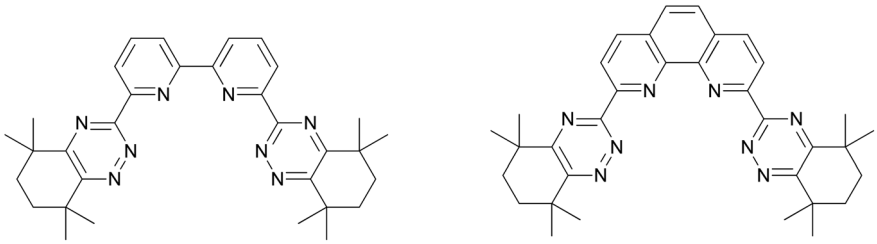

(a) $CyMe_4-BTBP$ structure. (b) $CyMe_4-BTPhen$ structure.

Figure 2.4: comparison of $CyMe_4-BTBP$ and $CyMe_4-BTPhen$ [71].

Phenanthroline based ligands are of great interest for an improved AmSel process, since bipyridine based ligands, even though they have been the reference molecules for actinides and lanthanides separation, have shown a rather slow kinetics. This is attributed to the molecule's conformational change from its trans-conformation to its less favourable cis-conformation before metal complexing. This reorganization is fundamental, as the cis-conformation is required to form a complex. In a study by Lewis et al. [54], the authors proposed to swap the 2,2'-bipyridine core to a cis-locked 1,10-phenanthroline core: the latter is rigid and already in a cis-conformation, leading to a faster and more thermodynamically favoured complexation, since no reorientation is needed. In fact, the more the molecule is preorganized, which means that its free conformation is constrained or close to the one required to complex the target ion [59], the easier the binding pro-

cess. The study was performed on the bis-triazine phenanthroline based lipophilic ligand $CyMe_4$–BTPhen, which was compared to its bipyridine equivalent $CyMe_4$–BTBP (figure 2.4. Solvent extraction studies have shown good selectivity regarding actinides, high extraction efficiency and fast kinetics. The high surface activity, together with its preorganization, are believed to be responsible for the ligand's improved kinetics with respect to $CyMe_4$–BTBP. Molecular modelling was used to study the conformer distribution in a successive study [72]: the types of conformations of the molecule and which ones are the most present in a solution. Regarding $CyMe_4$–BTBP, it is known that the conformations relevant to binding are controlled by the central torsion angle, associated to the single C-C bond of the bipyridine moiety, but they are also influenced by the torsion angles associated to the core-triazine C-C bonds. Instead, the conformations of $CyMe_4$–BTPhen are dominated only by the latter. The ligand has a significantly lower conformational variability with respect to $CyMe_4$–BTBP, and this large preorganization might explain the improved extraction kinetics. In order to reach the binding conformation, both ligands have to overcome a small energy barrier related to the rotation of the triazine rings, but $CyMe_4$–BTBP has to overcome an additional barrier related to the central torsion angle. Furthermore, in a subsequent study, $CyMe_4$–BTBP and $CyMe_4$–BTPhen complexes with Cm(III) and Am(III) have been investigated with TRLFS [71]. The hypothesis that the preorganization of BTPhen improves the complexation properties is confirmed by the results, in which stability constants for $CyMe_4$–BTPhen complexes are systematically higher than in the case of $CyMe_4$–BTBP. Finally, as previously pointed out, preorganization and low conformational variability can result in improved selectivity towards metal ions whose radius fits in the coordination cavity [50].

2.5.1. A recent CHON hydrophilic ligand: PrOH-BPTD

In the work of Weßling et al. [73], the first CHON-compliant ligand for the AmSel process was synthesized and tested: PrOH-BPTD (3,3'-([2,2'-bipyridine]-6,6'-diylbis(1H-1,2,3-triazole-4,1-diyl))bis-(propan-1-ol)). As it can be observed in figure 2.5, the bipyridine moiety was maintained due to its selectivity towards Am, while triazole rings were added to improve solubility. Specifically, the addition of triazole moieties and propanol side chains aimed to obtain the same high solubility of another CHON-compliant ligand for the i-SANEX process (3,3'-(pyridine-2,6-diylbis(1H-1,2,3- triazole-4,1-diyl))bis(propan-1-ol) or PTD) [36].

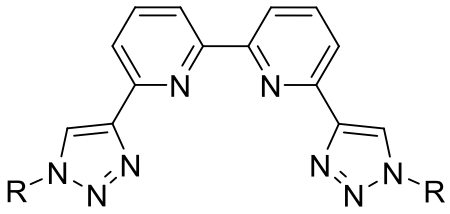

Figure 2.5: BPTD core structure [73]

Extraction experiments showed an effective separation of Am from Cm and all the Ln with a nitric acid concentration in between 0.33 and 0.39 M, with a ligand concentration of 40 mM. Specifically, $SF_{Cm/Am}$ is around 2, and $SF_{La/Am}$ is around 6. Through TRLFS studies, PrOH-BPTD is found to form significantly stronger complexes with Cm than with Eu, by comparing their respective stability constants. However, when compared to $SO_3-Ph-BTBP$, the stability constants are overall lower, and also the difference among Cm and Eu is diminished: selectivity between An and Ln appears to be lower. Regarding complex stoichiometry, the slope analysis yielded a value of -0.88 for Am(III), indicating 1:1 complexes formation. On the other hand, TRLFS results indicated the formation of 1:2 complexes. This behaviour was already observed for $SO_3-Ph-BTBP$, and it was attributed to heteroleptic complexes [68]. Overall, the selectivity is similar to $SO_3-Ph-BTBP$, but slightly lower: the achieved $SF_{Cm/Am}$ is around 2. Moreover, the separation from the lanthanides is satisfactory, but worse with respect to the reference system.

2.5.2. A phenanthroline based sulfonated ligand: TS−BTPhen

Given the remarkable selectivity towards actinides displayed by $CyMe_4-BTPhen$, the hydrophilic equivalent was developed with the addition of sulfonated-phenyl moieties [66], the same used in $SO_3-Ph-BTBP$. TS-BTPhen ($SO_3-Ph-BTPhen$) displayed a high aqueous solubility and suppressed successfully Am extraction by TODGA at nitric acid concentrations lower than 0.5 M, resulting in high $SF_{Eu/Am}$. Further solvent extraction experiments and spectroscopic studies were carried out on TS-BTPhen as a possible hydrophilic ligand for the AmSel process [74]. TS-BTPhen displayed a $SF_{Cm/Am}$ ranging between 2.4 and 4.5 (HNO_3 concentration between 0.01 and 1 M). The conditions of interest for Am separation were found to be around 0.65 M HNO_3, with a ligand concentration of 0.01 M. The achieved $SF_{Cm/Am}$ was around 3.6, while the $SF_{Eu/Am}$ was around 300. Lanthanides were all extracted with satisfactory distribution ratios, with La being the least extracted. The slope analysis yielded a value of -0.8, while TRLFS studies

on Cm(III) showed that only 1:2 complexes were present at high ligand concentrations (HNO_3 concentration of 0.5 M). Also in this case, the slope analysis result was attributed to heteroleptic complexes. However, since their concentration was very low, they were not detected by the TRLFS measurement [68]. Overall, the complexation behaviour is very similar to $SO_3-Ph-BTBP$ [48], but the TS-BTPhen complexation with Cm is slightly stronger than with Eu: this effect was attributed to BTPhen being a more preorganized molecule [71].

2.5.3. The new bis-triazolyl phenanthroline ligands: BTrzPhen

The first CHON-compliant 2,9-bis-triazolyl-1,10-phenanthroline (BTrzPhen) ligands were presented by Edwards et al. [75]. As in the case of PrOH-BPTD [73], this kind of molecules aims to combine the complexing properties of the 1,10-phenanthroline moiety and the hydrophilicity of the triazole rings [36]. The authors synthesized and tested two ligands, one with ethanol side chains and the other with propane-1,2-diol (BTrzPhen-tetraol). Both resulted to be soluble in 0.3-3.0 M nitric acid aqueous solutions, but the second displayed a better solubility (down to 0.01 M HNO_3). With respect to the extraction behaviour, used together with TODGA, at 0.33 M HNO_3, the $SF_{Eu/Am}$ is similar for both molecules. Moreover, BTrzPhen-tetraol yielded a $SF_{Cm/Am}$ around 2.5 at 0.3 M HNO_3. In both cases the selectivity decreases with increasing nitric acid concentration, probably due to protonation. Additionally, stability constants for Eu(III) complexes are evaluated with UV-VIS metal titrations: the first molecule was studied in 0.1 M HNO_3, and exhibited only 1:1 complex formation, while the second showed that 1:2 complexes are the dominating species at 0.01 M HNO_3.

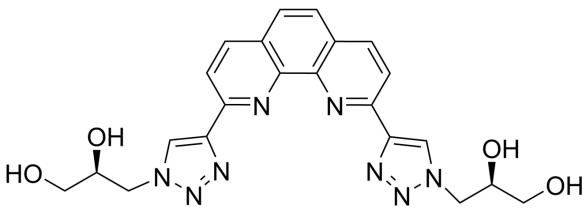

Figure 2.6: BtrzPhen-tetraol [73].

Further stripping studies have been performed on BTrzPhen-tetraol [76] (figure 2.6. Equilibrium was reached after 5 minutes, and separation conditions were achieved at 0.26 M HNO_3 and 30 mM ligand concentration: the $SF_{Cm/Am}$ is around 2.3. Ligand concentration appears to have a small impact: while increasing, it slightly decreases the distribution ratios of Am and Cm, and it has no effect on Eu(III) and the other Ln. Moreover, no

linear trend was observed. The small variation of the D was attributed to protonation, while the non-linearity was attributed to mixed complexes. Finally, it has to be noted that some co-stripping with heavy Ln(III) was observed. The authors concluded that, at such low nitrate concentration, the system does not perform optimally. The two molecules developed by Edwards et al. [75] display better selectivity at low nitric acid concentration, but their solubility was not satisfactory in such conditions. Wan et al. made an effort to develop two more soluble BTrzPhen ligands, employing different hydrophilizing moieties [58]. The authors adopted the well known sulfonated phenyl groups (DS-BTrzPhen) and amino-acidic moieties (DAA-BTrzPhen). While the first exhibited insufficient solubility, and additionally it was not CHON-compliant, the second resulted to be inefficient, displaying a low $SF_{Eu/Am}$ when tested in the same condition of the first ligand. Finally, recent studies reported also hydrophobic BTrzPhen ligands for actinide-lanthanide separation [77, 78].

2.5.4. Novel mixed core CHON phenanthrolines: DAPhen

Instead of triazine or triazole moieties, 1,10-phenanthroline-2,9-dicarboxamides (DAPhen) employ two amide functional groups. They were investigated for Am-Cm separation for the first time in the work of Wan et al. [79]. In this study, two CHON-compliant DAPhen were synthesized with the addition of ethoxy-ethanol (AE-DAPhen) and bis-ethoxy-ethanol (AEE-DAPhen) as side chains (figure 2.7).

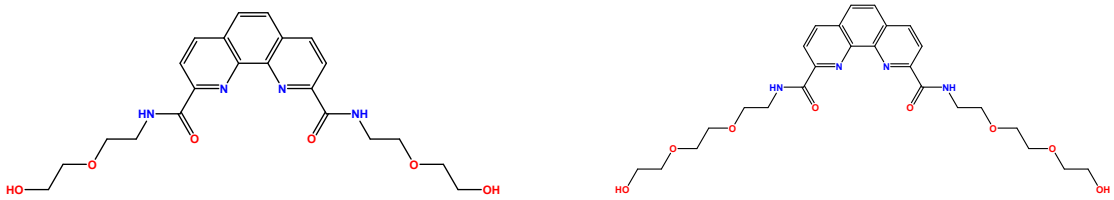

(a) AE-DAPhen structure. (b) AEE−DAPhen structure.

Figure 2.7: comparison of AE-DAPhen and AEE-DAPhen [79].

The ligands were tested both in stripping and in forward extraction conditions, which led to almost identical results. Both the molecules exhibited an increasing $SF_{Eu/Am}$ with nitric acid concentration, likely due to increased TODGA extraction of Eu. However, for concentration values above 0.75 M, $SF_{Eu/Am}$ decreased. This effect was attributed by the authors to ligand protonation. Nevertheless, the optimal acidity range at 10 mM ligand concentration was in between 0.5 and 0.75 M, in which $SF_{Eu/Am}$ was in the order

of 200 for both ligands. Additionally, fast complexation was observed, and exceptionally high $SF_{Cm/Am}$ was obtained, ranging in between 7 and 7.8. Even though this value was probably affected by a significant uncertainty, since it was obtained by liquid scintillation counting from two different experiments, one spiked with Eu and Am, the other with Eu and Cm, it is remarkably high among the proposed molecules. This improved extraction efficiency, confirmed by the high stability constants obtained by UV-VIS titration, and selectivity is probably due to the oxygen donor atoms of the amide group, which increase slightly the hardness of the ligand. Nevertheless, this feature could represent a downside: it could make the molecule more affine to lighter lanthanides, causing a co-stripping. Moreover, the hydrophilizing side chains contain oxygen, which can participate in the complexes. The lower $SF_{Eu/Am}$ and $SF_{Cm/Am}$ obtained by AEE-DAPhen were attributed to an interference of the longer terminal groups.

2.6. Aim of the thesis

In the present work, a novel CHON-compliant hydrophilic ligand synthesized in Politecnico di Milano was investigated. It is a 2,2'-((((1,10-phenanthroline-2,9-diyl)bis(1H-1,2,3-triazole-4,1-diyl))bis(ethane-2,1-diyl))bis(oxy))bis(etha-1-ol) (EBTzPhen): it belongs to the BTrzPhen family, with the addition of highly hydrophilizing ethoxy-ethanol moieties (figure 2.8). Due to the pre-organized phenanthroline core, it is expected to have a fast kinetics, while the triazole rings and ethoxy-ethanol side chains should improve the solubility in the aqueous phase.

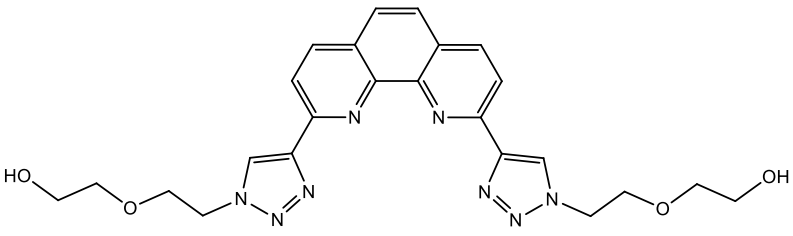

Figure 2.8: EBTzPhen structure [50].

In this work, EBTzPhen selectivity towards Am with respect to Cm and all the lanthanides was tested in multiple conditions through solvent extraction studies. Specifically, process parameters were systematically varied to optimize the extraction efficiency and to assess the robustness of the system against minor operational fluctuations. Since the co-stripping of light lanthanides is often a limiting factor for these systems, particular attention was paid to La, the least extracted lanthanide by TODGA. Additionally a UV-VIS titration was performed to gather preliminary information on the complexation behaviour.

3 | Materials and methods

3.1. Chemicals and stock solutions

- TODGA was purchased from Technocomm LTd. (Edinburgh, UK), batch 009-R (purity: 99%).
- ISANE IP-175, an isoparaffinic diluent, was provided by CEA (Marcoule, France).
- EBTzPhen was synthesized in Politecnico di Milano, Department of Chemistry, Materials and Chemical engineering.
- Radioactive tracer: the tests were spiked with a radioactive tracer containing Am-241, Cm-244, Eu-152, which is obtained by several 1:2 dilutions from a concentrated standard. The activity concentrations of the tracer after the final dilution are 155 kBq/L for Am-241, 151 kBq/L for Cm-244 and 278 kBq/L for Eu-152, while the nitric acid concentration is 0.01 M.
- HNO_3 solution: Nitric acid was purchased from Merck AG. Various HNO_3 solutions were prepared by dilution from a more concentrated solution, while other were already available. Dilutions were performed using ultra-pure water (18.2 MΩ) obtained using a Elga Purelab water purification system.
- HNO_3 10^{-5} M Ln all solution: it is a nitric acid solution containing all the Ln (besides Pm, with the addition of Y) in a 10^{-5} M concentration each (total metal concentration is around 10^{-4} M). Some of these solutions were already available in different HNO_3 concentrations. To prepare a new solution, a dilution with a specific nitric acid concentration was performed from a stock solution containing all the Ln in 10^{-4} M concentration, to obtain at the end a HNO_3 10^{-5} M Ln all solution of the desired HNO_3 concentration.
- HAR (High Activity Raffinate) was used from laboratory stock. It is a simulant solution of the PUREX raffinate, which has HNO_3 concentration of 3.568 M and contains all the lanthanides (from La to Eu, except Pm), fission, activation and corrosion products (Se, Rb, Sr, Y, Zr, Mo, Ru, Rh, Pd, Ag, Cd, Sn, Sb, Te, Cs, Ba,

Na, Cu, Ni, Fe, Al, Cr) in high concentration.

- $Eu(NO_3)_3$ hexahydrate used for UV-VIS titration was purchased by Alfa Aesar (purity: 99.9%).
- All the used solutions were titrated using Titrando 907 from Metrohm GmbH & Co. KG (Filderstadt, Germany).
- the other reagents used were purchased by various suppliers and used without further purification.

3.2. Phase preparation

3.2.1. Organic phase

The organic phase was prepared at the beginning of the tests, in order to use the same for every experiment. TODGA was weighted on a Mettler Toledo scale (5 decimal), then the calculated volume of diluent was added in order to reach the target 0.2 M TODGA concentration. The diluent used was ISANE IP-175, with 5% v/v 1-octanol as phase modifier.

3.2.2. Aqueous phase

The EBTzPhen was weighted with a plastic spatula (to avoid metal contamination) on a Mettler Toledo scale (5-decimal) and dissolved in a HNO_3 10^{-5} M Ln all solution. For the dissolution, both a Heidolph REAX Top shaker (not thermostatically controlled) and a BANDELIN Sonorex Digitec ultrasonic bath were used in an alternating way, until the solution was clear and no significant undissolved particles were present. The ultrasonic bath was set at ambient temperature, however repeated use caused the temperature to increase gradually up to 30°C. The aqueous phases were prepared always on the same day of the experiment to avoid any hydrolysis effects. Different nitric acid (0.25-0.4 M) and ligand concentrations (1-100 mM) were investigated.

3.3. Extraction experiments

3.3.1. Pre-equilibration of the organic phase

The organic phase was pre-contacted with a nitric acid solution of the same concentration as the one used for the actual experiment. The reason is that both TODGA and 1-

octanol extract nitric acid, modifying its concentration in the aqueous phase [52]. This is avoided by pre-loading the organic phase with nitric acid, and using it for the extraction experiment. 700 µL of the organic phase were contacted with 700 µL of nitric acid solution in a mechanical shaker (IKA VIBRAX VXR) at 22°C for 15 minutes, then centrifuged for 5 minutes at 3000 rpm. 500 µL of the loaded organic phase were taken for the extraction test. The process was repeated for each sample on the day of the test to avoid any hydrolysis effects.

3.3.2. Phase contacting and separation

500 µL of aqueous phase were added in a 2 mL glass vial with 500 µL of the pre-contacted organic phase, and 10 µL of the radioactive tracer. The sample was then shaken on a IKA VIBRAX VXR mechanichal shaker at 22°C normally, or the desired temperature (the temperature is maintained by a Julabo F25 thermostat) for 60 minutes (or the desired mixing time) and centrifuged for 10 minutes at 3000 rpm. Some experiments were performed on another mechanical shaker (IKA MATRIX Orbital Delta Plus). Then, for the phase separation, 200 µL were taken from the top phase, and placed in a 1.5 mL glass vial for gamma measurements. Then, 20 µL were taken for the ICP-MS and 10 µL for the alpha spectrometry. The remaining top phase was removed, then the same aliquots were taken from the bottom phase, making sure to avoid cross contamination with the top phase.

3.4. Stripping experiment

3.4.1. Aqueous phase preparation

The HAR contains the metals in a very high concentration: to get metal concentrations similar to the ones used in the other experiments, it was diluted by a factor 400 with a 0.5 M HNO_3 10^{-5} M Ln all solution. The final solution was titrated (HNO_3 concentration of 0.5093 M), and to evaluate the concentrations of all the metals it was measured with the ICP-MS (table A.1 in appendix A).

3.4.2. Organic phase loading

In a 9 mL glass vial, 2.5 mL of aqueous phase previously prepared and 50 µL of radioactive tracer were added to 2.5 mL of organic phase (not pre-equilibrated). The vial was closed, wrapped in parafilm and shaken in a Heidolph REAX Top shaker (speed 2) for 30 minutes, then centrifuged for 5 minutes. The loaded organic phase was saved for 4 extractions (4

x 500 µL). On the other hand, the aqueous phase was titrated to evaluate the nitric acid extraction during loading. For both phases, aliquots for gamma, alpha and ICP-MS measurements were saved.

3.4.3. Stripping

500 µL of loaded organic phase were contacted with 500 µL of a 0.3 M HNO_3, 0.1 M EBTzPhen solution on a mechanical shaker (IKA MATRIX Orbital Delta Plus) at 22°C for different mixing times, then centrifuged for 10 minutes at 3000 rpm. The phases were separated with the procedure described above, and the aqueous phase of each sample was titrated to monitor nitric acid concentration.

3.5. Sample preparation for measurement

3.5.1. Gamma samples

The gamma samples consisted in 1 mL glass vials containing 200 µL of the phase to measure. The gamma lines at 59.5 keV and 121.8 keV were measured, respectively, for Am-241 and Eu-152. An EG&G ORTEC high-purity Germanium detector was used, while spectra were evaluated using GammaVision Software; since the detector was not completely shielded, for very low activity samples peak discrimination was difficult, causing higher uncertainties. Measurements were run either for 24 hours or when the lowest activity nuclide had a net number of integral counts greater than 10000. The evaluated volume was always the same, therefore the efficiency was the same for organic and aqueous phase. An activity balance was evaluated for each sample directly with the count rates: the sum of the count rates in both organic and aqueous phase of a sample should be a constant value throughout all the samples, as the added activity is always the same. The standard deviation of the total activities of the different samples should be low, around 2%.

3.5.2. Alpha samples

In 1.5 mL plastic Eppendorf tubes, 10 µL of the phase to measure were added to 100 µL of Zaponlack solution (1% v/v ZAP/Acetone), which acted as a carrier. The liquid was mixed for three times with a 150 µL pipette and distributed on an metal plate (previously cleaned with acetone and isopropanol). It is essential to take care that the liquid is evenly distributed in a flat surface, and it is kept distant from the plate border (3-4 mm). The alpha plate was placed under a heating lamp to evaporate the Zaponlack solution, then the leftover deposit was burnt with a flame. Therefore, only the nuclides were left on the

plate. Measurements were carried out with an ORTEC/Ametek ALPHA-ENSEMBLE-8 eight chamber alpha spectrometer with PIPS detectors purchased from Ametek GmbH (Meerbusch, Germany), either for 24 hours or when the lowest activity nuclide had a net number of integral counts greater than 10000. The organic and aqueous phases were measured in the same cell, to have the same efficiency. The efficiency of each cell was known, and it was used to convert count rates in activity, to perform at the end an activity balance of the sample. The sum of the activities contained in aqueous and organic phase should be a constant value among the samples, since the added tracer amount is always the same, and the same activity is split into the two phases. For the total activities, standard deviation was evaluated; usually, for alpha samples, values should remain below or around 4%.

3.5.3. ICP-MS samples

In a 10 mL plastic vial, 0.1 mL of concentrated ultrapure nitric acid (65%) were added to 9.9 mL of ultrapure water (to get 1% HNO_3 solution). For the organic samples, 230 µL were removed from the vial; 200 µL of 10% TRITON X-100 (a surfactant used to mix the organic phase in an aqueous solution), 10 µL of In standard (inactive) and 20 µL of organic phase were added. For the aqueous samples, only 30 µL were removed, 10 µL of In standard and 20 µL of aqueous phase were added. The Indium standard was added to every sample in a known amount, to check whether the measurement was carried out correctly, and the instrument was working properly. Since 20 µL of sample were diluted in a 10 mL solution, the final dilution of the sample to measure was 1:500. This dilution factor was used because it enables all the ions measured in aqueous and organic phase to be in a concentration above the LOD and the LOQ of the instrument, starting from an initial concentration of 10^{-5} M. The measurements were carried out using a Perkin Elmer NexION 2000C. For the lanthanides and Y, calibration standards of 0.0001, 0.001, 0.01 and 0.05 mg/L were used: calibration curves were evaluated and cps were converted to concentrations [mg/L]. The concentration in the original sample was obtained by multiplying the dilution factor (500). Also Am and Cm were measured, but standards are not available and neither a mother solution: distribution ratios are obtained using the cps in each phase. Am and Cm measurements are used to check whether gamma and alpha measurements are coherent, but they are not used for calculations. To check the mass balance for the measured elements, a third kind of sample was prepared: 0.1 mL of concentrated nitric acid were added to 9.9 mL of ultrapure water, then 30 µL of solution were removed. Then, 10 µL of In standard and 20 µL of the HNO_3 10^{-5} M Ln all solution used in the corresponding sample were added. This kind of sample resembles

a mother solution, whose concentration of Ln should be the sum of the aqueous and organic phase concentrations. It was prepared for every nitric acid concentration value used in the aqueous phases. If only one value was used, it was produced and measured in a triplicate for statistic purposes. The mass balance of an element in a sample was evaluated considering the sum of the evaluated concentration in organic and aqueous phases, minus the concentration in the mother solution, all divided by the latter. Ideally, this number would be zero, however small variations (4-5%) are typical. Heavy Ln always present large errors in the mass balance (-20 to -30%), due to difficulties in organic phase measurements in the ICP-MS (no third phase is formed in the analysed system).

3.6. Parameters evaluation

The performance evaluation of the investigated ligand was carried out by calculating distribution ratios and separation factors.

- Distribution ratio D: When the metal concentration is evaluated by ICP-MS, the D is the ratio between the concentrations in the two phases. On the other hand, when the measurement is radiometric, if the efficiency is the same for the two phases the D is the ratio of the count rates. For Eu both gamma and ICP-MS measurements are available, but the two do not always overlap. ICP-MS measurements are usually affected by higher uncertainties, and measure the inactive Eu-153. Gamma measurements were used to evaluate the distribution ratio, because of the lower uncertainty. However, due to Eu being often mostly retained in the organic phase, measurement in the aqueous phase is difficult and not always accurate. Additionally, contamination by the organic phase can occur during separation: since it contains traces of the other phase, the aqueous phase displays a higher activity than the real one, yielding a lower D. This is detrimental in the D evaluation of elements like Eu, heavily retained in the organic phase. Instead, for La and all the other lanthanides, ICP-MS measurements were used for the D evaluation. For Cm both alpha and ICP-MS measurements are available, but only alpha ones were used for the calculations. Finally, for Am gamma, alpha and ICP-MS measurements are available, but only alpha were used. Nevertheless, alpha and gamma measurements overlap almost perfectly: since Am in the investigated system is retained in equal order of magnitude in both phases, its gamma measurements do not suffer from eventual organic phase contamination. ICP-MS measurements were used to check whether they correspond with the other two measurements, but they were not used for calculations.

- Separation factor SF: The separation factor was evaluated between Am and Cm, since their separation is the most challenging: normally, their D calculated with alpha spectrometry were used to evaluate $SF_{Cm/Am}$. As a measure of the actinide-lanthanide selectivity, $SF_{Eu/Am}$ is conventionally used, because Eu is considered a good representative of the lanthanides. It was calculated using the gamma measurements of Eu and the alpha measurements of Am. In addition, also $SF_{La/Am}$ was evaluated, because La appears to have the least affinity with TODGA and among the Ln it is the most likely to be retained in the aqueous phase [49]. Am alpha measurements and La ICP-MS measurements are used.

3.7. Uncertainty evaluation

There are several uncertainty sources affecting an extraction experiment. First, there are uncertainties related to the instruments: pipettes have an error related to the volume, both statistical and systematic, the scale has an uncertainty which depends on the mass weighted and the conditions (usually around 0.01 – 0.05 mg), and the thermal regulation of the shaker has an uncertainty of 1°C on the target temperature. These uncertainty sources, together with human error, contribute to the uncertainty of the solutions preparation, the sample preparation, the phase separation and all the other procedures leading to the final results. For instance, titration of the solutions includes all of the uncertainty sources previously mentioned, plus a statistical uncertainty. Moreover, the measurement itself has an uncertainty on the count rate. Gamma and alpha measurements usually have an error (indicated by the instrument) ranging from 0.1 to 0.5%, but it depends on the activity of the sample: when it is particularly high, the error decreases, while for very low activity samples the error reaches higher values, up to 3%. However, the distribution ratio is a ratio of two measurements and its uncertainty is the combination of both errors: a D that has a very high ($D \gg 1$) or very low ($D \ll 1$) value implies a very active phase and a with very low activity one, hence the uncertainty is going to be higher than when the activity is spread equally in the two phases. As said previously, ICP-MS uncertainties are usually higher, ranging in between 1 and 10%. A conservative uncertainty estimation for D values evaluated with radiometric measurement lying between 0.01 and 100 is ±5%, while it is higher for values outside this range. On the other hand, for D values evaluated with ICP-MS lying in the same range, a reasonable estimation is 10%.

For data lying out of trend, the activity balance between aqueous and organic phase can indicate if there has been a pipetting error, or whether phase contamination has occurred. Nevertheless, for elements mostly retained in one of the two phases, the count rate of the

low activity phase does not change significantly upon phase contamination, leaving the activity balance unchanged. On the other hand. the measured D is visibly lower than the actual value. In this instance, the measurement should be performed again.

Heavy Ln have big errors in the mass balance due to difficulties in measuring the organic phase, because of which part of the metal is not detected: in this work they were off by negative 20-30%. Therefore, the specific values obtained for the distribution ratios are not significative, and only the global trend is observed. To improve the heavy Ln measurement, and obtain more precise information about their D, it is possible to do a back extraction in aqueous phase. However, since they are largely retained in the organic phase [62], this lies outside the scope of the present work.

3.8. Plots and tables

Error bars are not displayed because in most cases they are hidden by the marker. The plots in which the distribution ratio of Am, Cm, Eu and La is reported as a function of a process variable show both gamma and ICP-MS measurements of Eu for comparison. In the tables indicating D and SF for these elements, Eu parameters are calculated with gamma measurements. Instead, in the plots reporting the D as a function of the inverse of the ionic radius for actinides and lanthanides, for the former alpha measurements are used, while for the latter, including Eu, ICP-MS measurements are showed. The ionic radii for 9-fold coordination are taken from the work of D'Angelo et al. [80, 81] and Lundberg et al. [38].

3.9. UV-VIS study

For this study, a UV-VIS/NIR spectrophotometer Lambda19 by Perkin Elmer was used, with the software Lambda SPX/P. The measurements were carried out in quartz cuvettes with 1 cm optic length; before the use, the cuvettes were washed with acetone, then distilled water and subsequently with 0.01 M HNO_3. Additionally, the external part was cleaned with acetone, to remove any grease or particles. Since acetone traces produce an absorbance peak around 280 nm, which is in the interest wavelength range, the subsequent washes with water and nitric acid are fundamental, and it is also important to make sure no acetone traces are left on the external part of the cuvettes. For all the measurements, the spectrum baseline (absorbance 0) was recorded by placing both in the reference and in the sample cuvette a 0.01 M HNO_3 solution.

3.9.1. Solutions used

- Solution A: 10^{-4} M EBTzPhen in 0.01 M HNO_3.
- Solution B: $2{\cdot}10^{-5}$ M EBTzPhen in 0.01 M HNO_3, obtained by 1:5 dilution of solution A.
- Metal stock solution: 10^{-3} M $Eu(NO_3)_3$ in 0.01 M HNO_3.
- Solution C: $4{\cdot}10^{-4}$ M $Eu(NO_3)_3$ in 0.01 M HNO_3, obtained by 1:25 dilution of the metal stock solution.
- Solution D: $4{\cdot}10^{-4}$ M $Eu(NO_3)_3$ and $2{\cdot}10^{-5}$ M EBTzPhen in 0.01 M HNO_3, obtained by addition of 200 µL of metal stock solution, 1 mL of solution A and 3.8 mL of 0.01 M HNO_3.

3.9.2. Ligand spectrum determination

The reference cuvette contained 1 mL of 0.01 M HNO_3, while the sample cuvette contained 1 mL of solution B. The spectrum was recorded in 'scan' mode, with a 200-440 nm wavelength range. It is important to choose a EBTzPhen concentration value that leads to an absorbance within 0 and 1, to remain in the linear range of the instrument. For molecules containing a phenanthroline moiety, a concentration in the order of 10^{-5} M is sufficient.

3.9.3. Molar absorbance coefficient calculation

This measurement was carried out in single-use plastic cuvettes, with 1 cm optic length. The measurement was performed in 'conc' mode: it allows to evaluate the unknown concentration of the molecule in a sample. If the molar absorption coefficient at the selected wavelength is unknown, it is possible to evaluate it through a calibration, during which several standards at known concentration are measured. From the ligand's spectrum, 261 nm was the selected wavelength, as it is the centre of the tallest absorbance peak. The standards were obtained through several dilutions of solution A; the selected concentrations of EBTzPhen were such that the absorbance at 261 nm remained in between 0 and 1: 0.5, 1, 1.5, 2 and $2.5{\cdot}10^{-5}$ M. The reference cuvette contained 0.01 M HNO_3. The selected interpolation method was 'linear through zero'.

3.9.4. Titration with $Eu(NO_3)_3$

At the beginning of the titration, 2 mL of 0.01 M HNO_3 were added to the reference cuvette, while 2 mL of solution B were added to the sample cuvette. Then, the spectrum between 240 and 420 nm was recorded. For every step of the titration, 10 µL of solution C were added to the reference cuvette, and 10 µL of solution D to the sample cuvette. A 10 µL addition, given the concentration of EBTzPhen in the cuvette and $Eu(NO_3)_3$ in solution D translates into a 0.1 equivalents added for every titration step. 15 steps were carried out this way (up to 1.5 equivalents added), then the last three steps were performed with a 50 µL aliquot (up to 3 equivalents added). Solution C was added to the reference cuvette to avoid recording any effect due to the increasing amount of nitrates in solution, while solution D contains also the ligand to keep the EBTzPhen concentration unchanged and avoid dilution effects. After every addition, the solution was stirred in both cuvettes. Moreover, 10 minutes were kept between the addition and the measurement to ensure equilibrium was reached. Titration data were modelled with HypSpec2014.

4 | Extraction experiments

To assess the extraction performances and determine the features of EBTzPhen, several extraction experiments were performed. The investigated variables (ligand concentration, nitric acid concentration, temperature and mixing time) were varied to test the extracting system in multiple conditions, and the obtained trends were observed and interpreted. The range investigated for each variable was selected with the aim of a possible industrial implementation, considering the constraints required by the AmSel process. Due to this reason, in addition to the ligand's limited availability, extreme conditions such as very low pH, or extreme temperatures were not tested. Moreover, from preliminary tests carried out in Politecnico di Milano [50], [82], it resulted that the best extraction conditions (D_{Am} <1, D_{Cm} >1 and D_{Eu} >1) are achieved at 0.1 M EBTzPhen in 0.35 M HNO_3. Therefore, ligand and nitric acid concentrations were investigated in a range close to these values. Furthermore, TODGA concentration was not varied and the ratio between the phases was kept 1:1, in order to test the ligand in the same conditions adopted in the AmSel process. It is important to note that EBTzPhen was available in different batches (table 4.1) from the synthesis. Each experiment was performed using a single batch, but to check the differences in extracting behaviour each was tested in the same extraction conditions, and then distribution ratios and separation factors were compared.

The same molecule was reported in a very recent work by Wan et al. [60]. Since it was investigated for a possible application in the i-SANEX process, only the Am-Eu selectivity was studied, in very different conditions from the ones required by the AmSel process: the ligand was used in the concentration of 10 mM, and in presence of 1 M $NaNO_3$ due to the significantly low nitric acid concentration adopted (0.01 M).

4.1. Ligand batches and solubility

The synthesis (figure 4.1) was carried out according to the process described by Edwards et al. and in previous thesis [50, 75, 82], with some modifications.

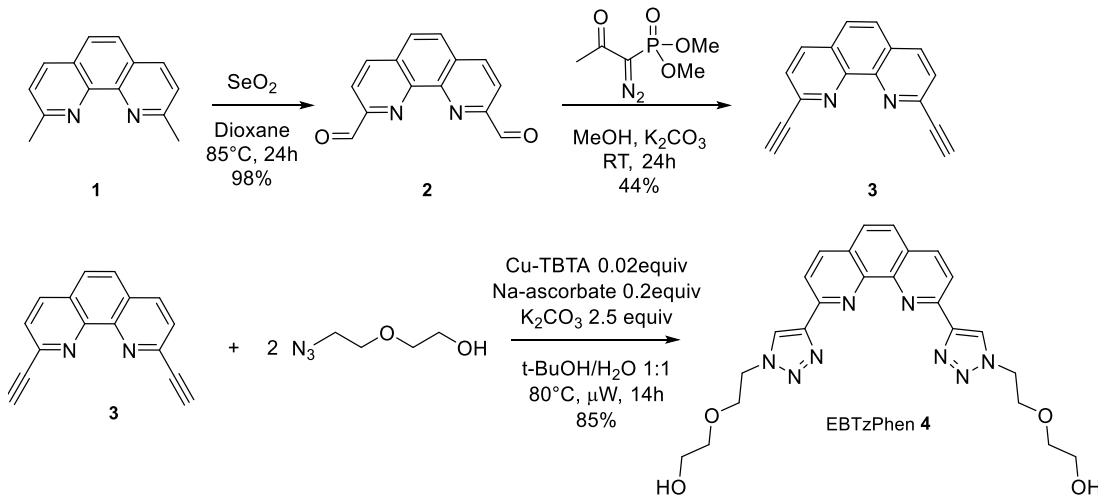

Figure 4.1: Synthetic pathway for the synthesis of EBTzPhen.

The final product was a solid, crystalline powder, usually ochre or reddish, depending on the batch (figure 4.2). Nevertheless, batches were characterized by NMR (Nuclear Magnetic Resonance) and the purity appeared to be the same.

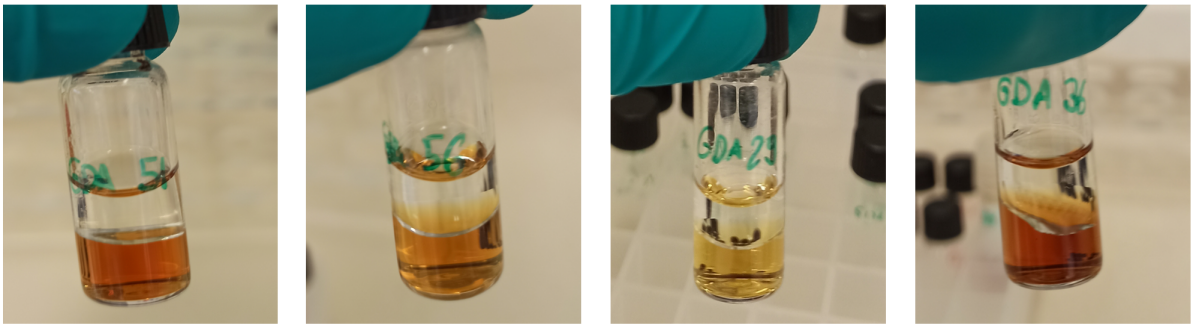

Figure 4.2: Org.: 0.2 M TODGA in 5% v/v 1-octanol/ISANE IP175; Aq.: 0.1 M EBTzPhen in 0.3 M HNO_3; 10^{-5} M Ln(III) (w/o Pm, incl. Y); Am-241, Cm-244, Eu-152; different batches.

The dissolution was not immediate, but alternating agitation of the solution with a vortex shaker and ultrasonic bath for some minutes allowed to reach complete solubilization: after such steps were repeated for a certain amount of times, no turbidity was observed. The harshest conditions tested were 0.1 M ligand, 0.25 M HNO_3, but nitric acid concentration appeared to not affect the solubility in the investigated range. However, among the different batches analysed, in some cases small solid particles remained in suspension, even after several minutes in the ultrasonic bath (table 4.1), while the bulk of the ligand was completely dissolved. It has to be noted that the undissolved amount was very low,

hence the actual concentration of the ligand in solution was assumed to be close to the target value. Nevertheless, small differences in concentrations can lead to a different extraction performance. To account for these differences, identical experimental points were included across the tests performed with different batches.

Table 4.1: Mass and solubility of the batches of EBTzPhen.

Batch ID	Mass [mg]	Undissolved particles
ALFAZIDE	134	Almost none
GMA061	88.4	Almost none
MGH005	66.7	Significant amount
MGH006	82.4	None
GMA066	242	Almost none
GMA068	122	Small amount
GMA069	108	Small amount

4.2. Ligand concentration dependence

It is known from previous experiments that the best extraction conditions were achieved with a 0.1 M EBTzPhen. A first series of extraction tests was performed with values of ligand concentration close to 0.1 M, to determine whether a satisfactory separation could be achieved using a lower amount. Later, a second test was carried out to perform a slope analysis, in which several concentration values were tested.

4.2.1. First extraction series

A first series of experiments was performed in order to understand how ligand concentration affect the extraction efficiency and whether a low ligand concentration enables a satisfactory Am separation. The investigated concentrations were 60, 80 and 100 mM. Since this was a preliminary test, the nitric acid concentration adopted was 0.35 M, the one in which best separation conditions have been achieved in previous works [82].

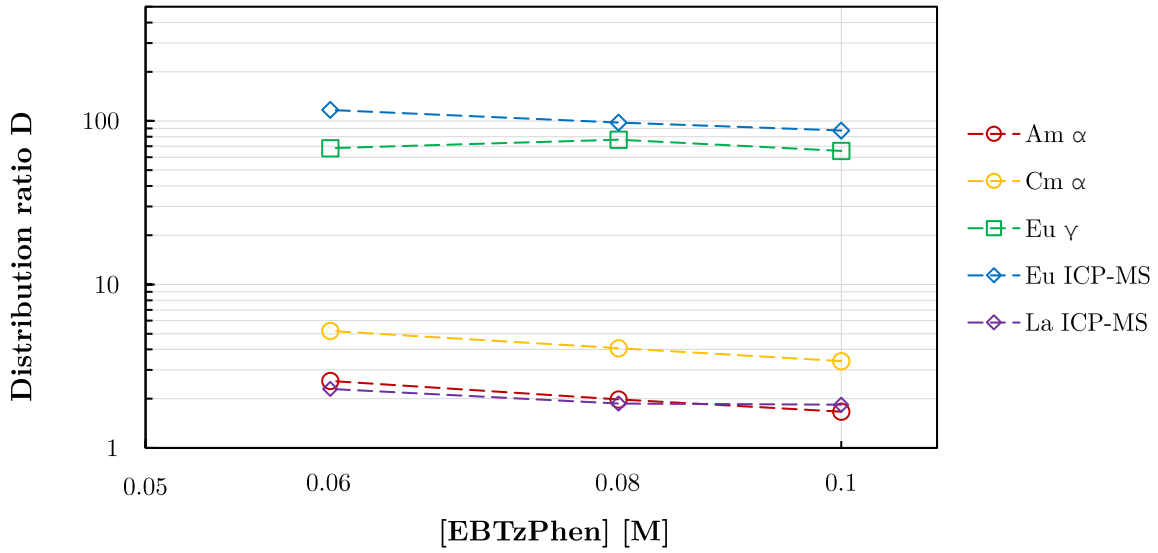

Figure 4.3: Org.: 0.2 M TODGA in 5% v/v 1-octanol/ISANE IP-175; Aq.: EBTzPhen (batch: MGH005) in 0.35 M HNO_3; 10^{-5} M Ln(III) (w/o Pm, incl. Y); Am-241, Cm-244, Eu-152; 60 min; 22°C.

As expected, the D of all the elements decreases with increasing concentration of the ligand (figure 4.3). The $SF_{Cm/Am}$ is approximately constant and close to 2 (table 4.2), but at this nitric acid concentration $D_{Am} > 1$. Moreover, La is retained in the aqueous phase with Am. Therefore, a lower nitric acid concentration has to be adopted to decrease the D of the metals. Nevertheless, it is necessary to point out that this batch presented some issues in solubility, as it can be seen from table 4.1.

Table 4.2: Distribution ratios for Am, Cm, Eu and La and separation factors as a function of ligand concentration. Eu data calculated with gamma measurements.

[EBTzPhen] [M]	D_{Am}	D_{Cm}	D_{Eu}	D_{La}	$SF_{Cm/Am}$	$SF_{Eu/Am}$	$SF_{La/Am}$
0.10	1.67	3.40	65.61	1.84	2.04	39.4	1.10
0.08	1.98	4.07	76.83	1.87	2.06	38.8	0.94
0.06	2.57	5.20	68.24	2.30	2.02	26.6	0.89

The selectivity between Am and Cm, which translates into the distance among the different lines, does not vary with the ligand concentration, and remains around 2. The separation of Eu and Am instead increases alongside with the ligand concentration. By looking at the results, in principle it should be possible to perform the tests even at lower EBTzPhen concentration. However, the lower the ligand amount, the larger the

D of the different ions: since at this nitric acid concentration the D are >1, the ligand concentration is maintained at 0.1 M.

Slope analysis

The slope of log(D) vs log([EBTzPhen]) was evaluated for Am and Cm, even though more experimental points would have been necessary to perform a proper slope analysis. The slope value of Am is -0.85, the one of Cm is -0.83. Such a slope indicates 1:1 complexes, however a slope equal to -2 is expected for this kind of ligand (1:2 complex formation has been demonstrated for phenanthroline-based ligands [71, 73, 74]). A slope closer to -1 when the hydrophilic ligand creates 1:2 complexes has been found for several systems in which both TODGA and another ligand in the aqueous phase (SO_3–Ph–BTBP, TS-BTPhen, PrOH-BPTD) are used [44, 73, 74]; in the case of SO_3–Ph–BTBP, this different slope has been attributed to the presence of heteroleptic complexes, demonstrated by the presence of the hydrophilic ligand in the organic phase [68].

4.2.2. Second extraction series

A second series of extraction tests was performed in a wider range of ligand concentration to derive information from slope analysis. The investigated values were 1, 5, 10, 60, 80 and 100 mM.

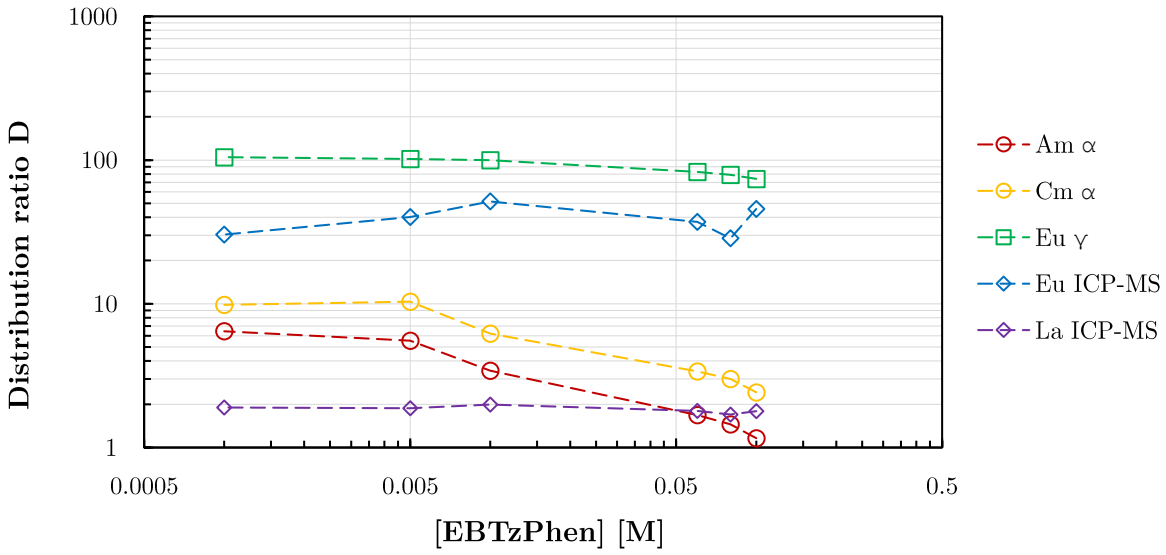

Figure 4.4: Org.: 0.2 M TODGA in 5% v/v 1-octanol/ISANE IP-175; Aq.: EBTzPhen (batch: GMA069) in 0.3 M HNO_3; 10^{-5} M Ln(III) (w/o Pm, incl. Y); Am-241, Cm-244, Eu-152; 60 min; 22°C.

As it can be observed in figure 4.4 and table 4.3, distribution ratios of all the metal ions decrease with increasing EBTzPhen concentration, but for Am and Cm this phenomenon is largely more significant: this indicates a higher affinity of the ligand towards actinides, with respect to lanthanides, which is desirable for the hydrophilic ligand in this process. It should be noted that ICP-MS measurements for Eu are systematically lower than gamma measurements, but this is explained by the mass balance in between the two phases, which is off by -20% for all the data points.

Table 4.3: Distribution ratios for Am, Cm, Eu and La and separation factors as a function of ligand concentration. Eu data calculated with gamma measurements.

[EBTzPhen] [M]	D_{Am}	D_{Cm}	D_{Eu}	D_{La}	$SF_{Cm/Am}$	$SF_{Eu/Am}$	$SF_{La/Am}$
0.100	1.16	2.42	74.0	1.79	2.09	63.7	1.54
0.080	1.45	3.00	78.9	1.70	2.07	54.5	1.17
0.060	1.68	3.39	82.8	1.80	2.02	49.2	1.07
0.010	3.43	6.19	100	1.99	1.81	29.2	0.581
0.005	5.53	10.4	102	1.87	1.87	18.4	0.339
0.001	6.44	9.85	105	1.90	1.53	16.3	0.295

Extraction conditions, in which Am is sufficiently separated from Cm and from La, the least extracted lanthanide by TODGA [49], are achieved only with EBTzPhen concentration close to 100 mM. Compared to other hydrophilic ligands proposed for the AmSel process, with which satisfactory separation is obtained for concentrations in the order of tens of mM at similar nitric acid concentration [44, 73, 74, 76], it is a quite high value, indicating low complexation efficiency. Additionally, by observing figure 4.4 and table 4.3, it appears that there is a change in the ligand behaviour when a low concentration is used: the slope decreases, and the $SF_{Cm/Am}$ also decreases. This non-linearity could be related to protonation, which could have a more important effect at lower ligand concentrations.

In the work of Wan et al. [60], protonation was considered one of the main drawbacks of this molecule. Additionally, complexation studies indicated weak complexes, predominantly 1:1. The authors pointed at the ethoxy-ethanol side chains as possible cause for the lower complexation efficiency. Crystallography studies indicated that the ligand adopts an *anti-anti* conformation, with the side chains towards the complexation pocket of the molecule (figure 4.5a. It was found to be the most stable by computational analysis, in agreement with the XRD studies [82] and DFT calculations [50] performed in previous thesis works. In the *anti-anti* conformation, the side chains are close to the bonding

site. Moreover, a *syn-syn* conformation (figure 4.5b) is required for complexation: this conformational change is thermodynamically costly.

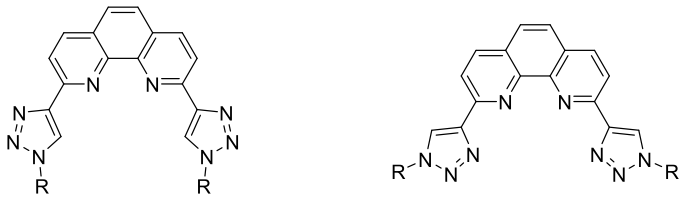

(a) *Anti-anti* conformation. (b) *Syn-syn* conformation.

Figure 4.5: *Anti-anti* and *syn-syn* conformations of EBTzPhen [50].

In conclusion, the high ligand concentration required to achieve separation is likely due to two phenomena. First, the investigated ligand is partially protonated: at high ligand concentrations, the separation is carried out regardless, because the metals are largely substoichiometric. Second, the side chains could contribute causing steric hindrance, but also the *anti-anti* configuration that the ligand adopts in solution could be related to the low complexation efficiency observed. More insights regarding this aspect can be gathered through complexation studies (chapter 5).

Slope analysis

The slope evaluated in a slope analysis is indicative of the stoichiometry of the metal complexes only if calculated on the concentration of free ligand, not involved in complexes. In this experiment, the initial ligand concentration is known, but this value does not necessarily coincide with the free ligand concentration: if part of the ligand is protonated, the free ligand concentration is a smaller value. Even though the experimental points do not appear to have a linear behaviour, the slope analysis was performed for Am and Cm. The values found were respectively -0.39 and -0.32: quite in disagreement with the expected values for a phenanthroline ligand and also with the previous extraction series. Nevertheless, due to non-linearity, the calculated slopes are not meaningful. However, the experimental points at 60, 80 and 100 mM present a $SF_{Cm/Am}$ consistent with previous results (around 2), hence protonation effect is considered to be not impactful. As said previously, separation is carried out regardless due to the low metal concentration. If the slope is evaluated considering only such points, it is significantly closer to the values obtained in the previous slope analysis, around -0.8, indicating 1:1 complexes.

4.3. Nitric acid concentration dependence

At 0.35 M HNO_3, both Am and Cm have a distribution ratio larger than 1, and La is retained in the aqueous phase, as it can be seen in figure 4.3. This could be related to both the nitric acid concentration and the specific batch behaviour. Therefore, at 0.1 M EBTzPhen, different nitric acid concentrations were investigated (0.25, 0.3, 0.35, 0.4 M) using a different ligand batch, to find the conditions in which Am is separated from La and Cm. The investigated range was limited due to different reasons. On the one hand, a very low pH is not feasible in an industrial process. On the other hand, after a certain nitric acid concentration protonation effect may become significant, as it was observed for SO_3−Ph−BTBP [44].

As expected, the distribution ratio for all the elements increases with nitric acid concentration (figure 4.6).

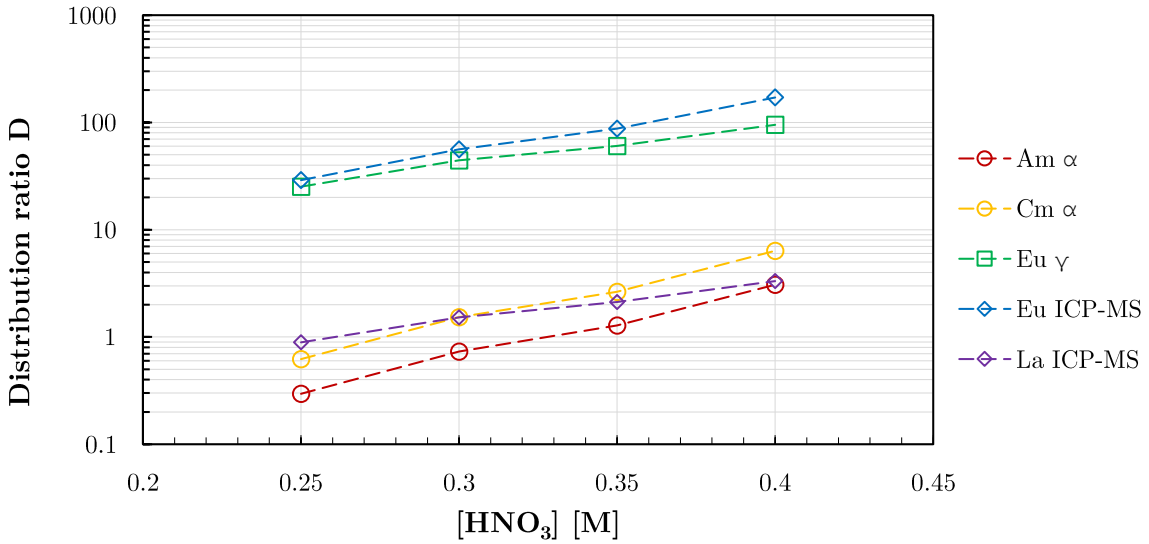

Figure 4.6: Org.: 0.2 M TODGA in 5% v/v 1-octanol/ISANE IP-175; Aq.: 0.1 M EBTzPhen (batch: ALFAZIDE) in HNO_3; 10^{-5} M Ln(III) (w/o Pm, incl. Y); Am-241, Cm-244, Eu-152; 60 min; 22°C.

$SF_{La/Am}$ and $SF_{Eu/Am}$ are decreasing with increasing nitric acid concentration, as it can be seen in table 4.4. Eu is always separated from Am, since it is mostly retained in the organic phase, while La, which tends to remain in the aqueous phase, is effectively separated for nitric acid concentrations lower than 0.3 M. The ideal separation condition, with La and Cm being in the organic phase (D>1) and Am being in the aqueous phase (D<1) is found at 0.3 M HNO_3 ($SF_{Eu/Am}$ = 60.6, $SF_{La/Am}$ = 2.08). It has to be noted

that results at 0.1 M EBTzPhen in 0.3 M HNO_3 are quite different from the ones obtained in the same conditions, in the previous experiment (figure 4.4). This is probably related to the different ligand batch used.

Table 4.4: Distribution ratios for Am, Cm, Eu and La and separation factors as a function of nitric acid concentration. Eu data calculated with gamma measurements.

[HNO_3] [M]	**D_{Am}**	**D_{Cm}**	**D_{Eu}**	**D_{La}**	**$SF_{Cm/Am}$**	**$SF_{Eu/Am}$**	**$SF_{La/Am}$**
0.25	0.296	0.622	25.2	0.892	2.10	85.2	3.02
0.30	0.733	1.53	44.4	1.53	2.09	60.6	2.08
0.35	1.28	2.64	60.5	2.12	2.06	47.2	1.65
0.40	3.07	6.36	95.1	3.32	2.07	30.9	1.08

It is known from the literature [58, 75, 76] that BTrzPhen ligands used in a system with TODGA suffer from protonation effect for nitric acid concentration values larger than 0.5 M: a steep deterioration of the $SF_{Eu/Am}$ occurs. Specifically, certain types of BTrzPhen molecules perform a satisfactory separation between Eu and Am only for HNO_3 concentration lower than 0.1 M [58]. In the work of Wan et al., separation was achieved for HNO_3 concentration lower than 0.01 M; nevertheless, nitrate addition was performed to force TODGA extraction and a significantly lower ligand concentration was used [60]. In this test, since the $SF_{Cm/Am}$ remains quite constant, protonation effect, if present, does not affect significantly the system, probably due to the metal being largely substoichiometric with respect to the ligand. Moreover, given the limited pH range investigated, no significant differences are to be expected.

The slopes found for Am and Cm are respectively 4.6 and 4.56. The slope of Am for a system with only TODGA (0.2 M in 5% 1-octanol/TPH) is approximately 2 [52]. However, it has been shown in a system with TS-BTPhen and TODGA, that the slope of log(D) vs log([HNO_3]) is larger than in a TODGA only system [74]. It is important to notice that lanthanides behaviour with respect to nitric acid concentration seems to be a bit different than actinides: slopes for Eu and La are respectively 2.61 and 2.59. The observed differences in the slopes suggest a variation in the number of nitrates involved in the first coordination sphere. Although TRLFS measurements would be necessary to investigate this aspect, they were not pursued in the present work.

4.4. Optimal extraction conditions

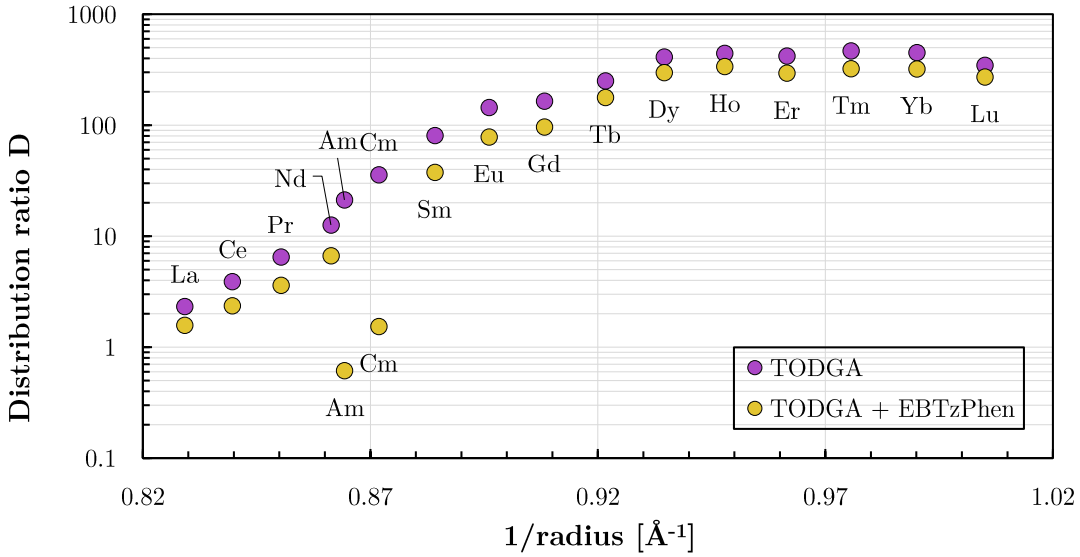

Figure 4.7: Comparison between a TODGA system and a TODGA + EBTzPhen (0.1 M) system; Org.: 0.2 M TODGA in 5% v/v 1-octanol/ISANE IP-175; Aq.: 0.3 M HNO_3; 10^{-5} M Ln(III) (w/o Pm, incl. Y); Am-241, Cm-244, Eu-152; 22°C; MT > 10 min.

From the obtained results, it is apparent that a satisfactory separation ($D_{Am} < 1$ and D_{Cm}, $D_{Ln} > 1$) is obtained for 0.1 M EBTzPhen in 0.3 M HNO_3. In such conditions, as it can be observed in figure 4.7, the distribution ratios of all the lanthanides follow the typical trend observed in a system containing only TODGA, in which D increases inversely with the ionic radius [49], but compared to the TODGA-only system the D values are slightly lower. On the other hand, D_{Am} and D_{Cm} are significantly lower: tetradentate phenanthroline based ligands are known for their high selectivity towards actinides [54]. Moreover, $SF_{Cm/Am}$ is close to 2.5, which points out the ligand's selectivity towards Am with respect to Cm. Finally, at this nitric acid concentration D_{La} is slightly larger than 2 when only TODGA is used, due to the low concentration of nitrates, which prevents an efficient lanthanides extraction. Due to the small decrease of D_{Ln} in presence of EBTzPhen, D_{La} decreases to a value similar to D_{Cm}. Hence, as expected, La represents a potentially problematic element for this system, which could be co-stripped with Am.

4.5. Temperature dependence

The temperature at which phase contacting is performed is an important factor for industrial implementation: in contacting devices the temperature of the phases can increase

due to friction effects, unless the device is thermostatically controlled. The extraction performance of the system can change quite significantly, hence it is important to monitor it.

4.5.1. TODGA system

TODGA is known to be an exothermic complexant [61]: the complexes tend to be less stable with increasing temperature, causing the distribution ratios to decrease. A first extraction series was performed using only TODGA as a complexant; the investigated temperatures were 22, 30 and 40°C, to simulate a realistic temperature increase that can occur in a contacting device.

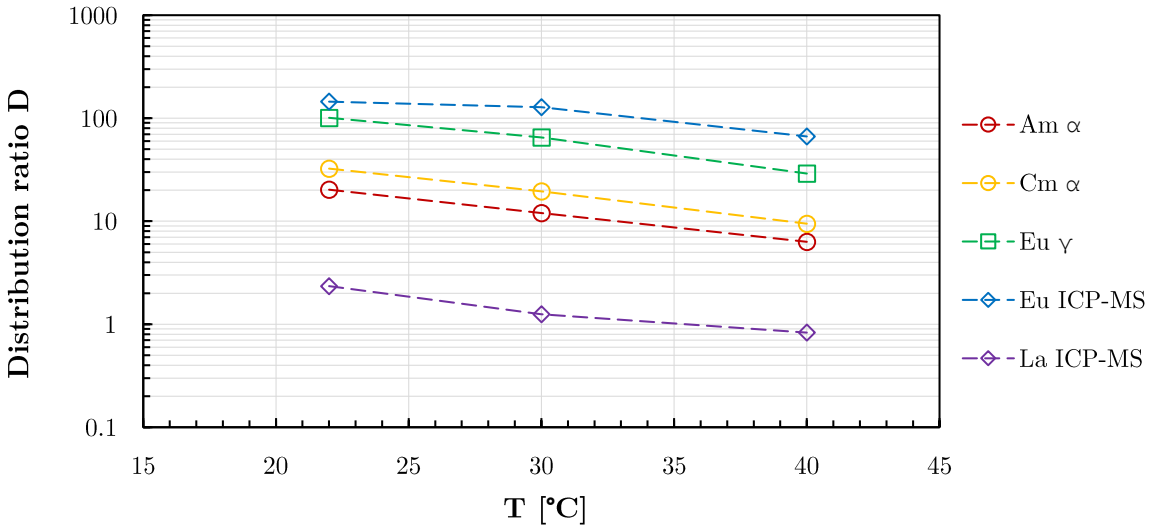

Figure 4.8: Org.: 0.2 M TODGA in 5% v/v 1-octanol/ISANE IP-175; Aq.: 0.3 M HNO_3; 10^{-5} M Ln(III) (w/o Pm, incl. Y); Am-241, Cm-244, Eu-152; 60 min.

As expected, the distribution ratios decrease with temperature (see figure 4.8), and $SF_{Cm/Am}$ is in agreement with values found in the literature, around 1.6 [44] (table 4.5). In figure 4.8 gamma measurements for Eu tend to be lower than ICP-MS: since the organic phase is particularly active in this experiment, the reason is probably phase contamination (see section 3.6).

Table 4.5: Distribution ratios for Am, Cm, Eu and La and separation factors as a function of temperature (in presence of TODGA). Eu data calculated with gamma measurements.

T [°C]	D_{Am}	D_{Cm}	D_{Eu}	D_{La}	$SF_{Cm/Am}$	$SF_{Eu/Am}$	$SF_{La/Am}$
22	20.2	32.4	101	2.34	1.60	4.98	0.116
30	12.0	19.5	65.0	1.25	1.63	5.42	0.104
40	6.31	9.47	29.0	0.829	1.50	4.60	0.131

By looking at the distribution ratios of all the lanthanides and actinides (figure 4.9), it appears that heavy Ln are less affected by temperature, probably due to the fact that TODGA is more affine towards them and their complexation is favoured. However, when temperature reaches 40°C, their D is visibly decreased, indicating that at this temperature the complexes stability is compromised even for the best extracted elements.

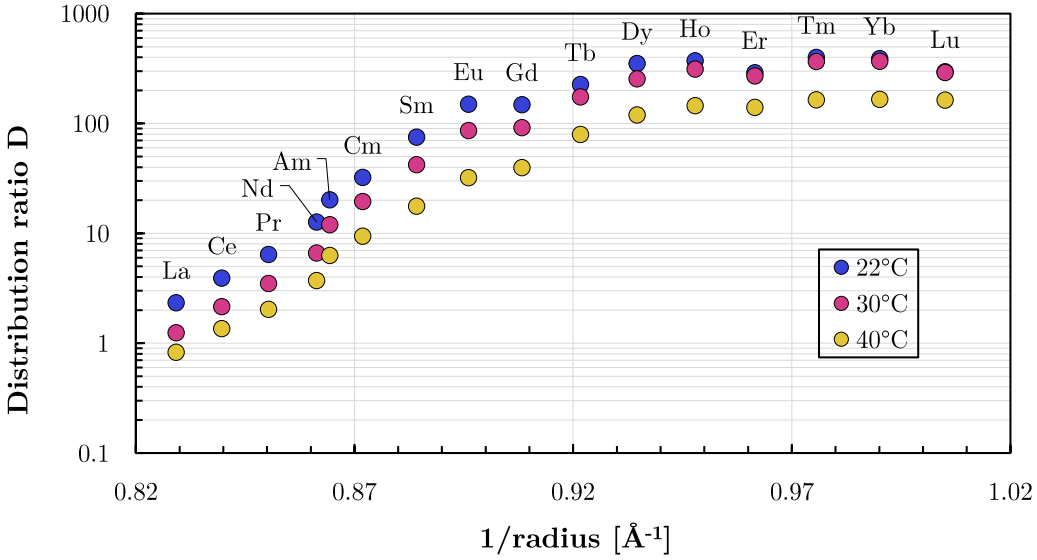

Figure 4.9: D as a function of the inverse ionic radius for 9-fold coordination; Org.: 0.2 M TODGA in 5% v/v 1-octanol/ISANE IP175; Aq.: 0.3 M HNO_3; 10^{-5} M Ln(III) (w/o Pm, incl. Y); Am-241, Cm-244, Eu-152; 60 min.

4.5.2. TODGA + EBTzPhen system

A second extraction series was performed on a system containing both TODGA and EBTzPhen. By observing the distribution ratios variation with temperature and confronting the results with the TODGA only system, it is possible to evaluate the EBTzPhen behaviour. The temperatures tested were 10, 22, 30, 40°C.

Overall, as it can be observed in figure 4.10, in this system the distribution ratios decrease with temperature in a more significant way than in a TODGA only system. This indicates that the complexation by the hydrophilic ligand improves with increasing temperature, suggesting an endothermic behaviour. This is in agreement with the results of Wan et al. [60].

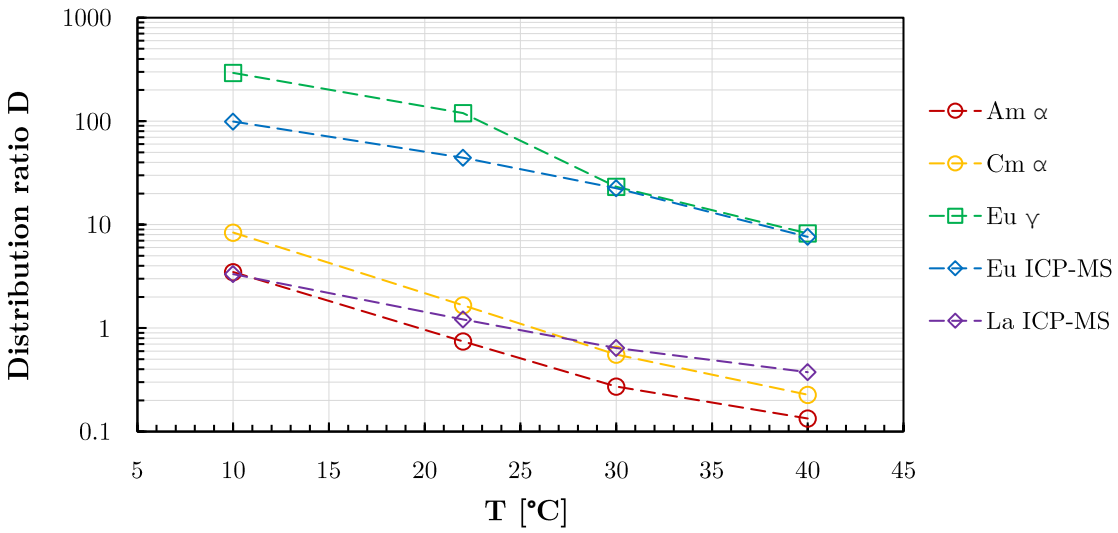

Figure 4.10: Org.: 0.2 M TODGA in 5% v/v 1-octanol/ISANE IP-175; Aq.: 0.1 M EBTzPhen (batch: GMA066) in 0.3 M HNO_3; 10^{-5} M Ln(III) (w/o Pm, incl. Y); Am-241, Cm-244, Eu-152; 10 min.

Table 4.6: Distribution ratios for Am, Cm, Eu and La and separation factors as a function of temperature (in presence of TODGA and EBTzPhen). Eu data calculated with gamma measurements.

T [°C]	D_{Am}	D_{Cm}	D_{Eu}	D_{La}	$SF_{Cm/Am}$	$SF_{Eu/Am}$	$SF_{La/Am}$
10	3.48	8.39	293	3.32	2.41	84.0	0.954
22	0.744	1.67	119	1.21	2.24	160.5	1.63
30	0.273	0.554	23.2	0.642	2.03	84.9	2.35
40	0.134	0.227	8.23	0.375	1.70	61.5	2.80

By looking at table 4.6, the $SF_{Cm/Am}$ is around 2 across the investigated range, but decreases with temperature, likely due to the combined effect on both the ligands. Regarding Eu, the gamma measurements at 10 and 22°C are clearly outliers: the D_{Eu} at 22°C is quite high compared to the previous tests. Since this is observed only for Eu, it is likely that

it is not related to the batch used, but to the measurement itself. The trend followed by Eu is more probably the one indicated by the ICP-MS measurements.

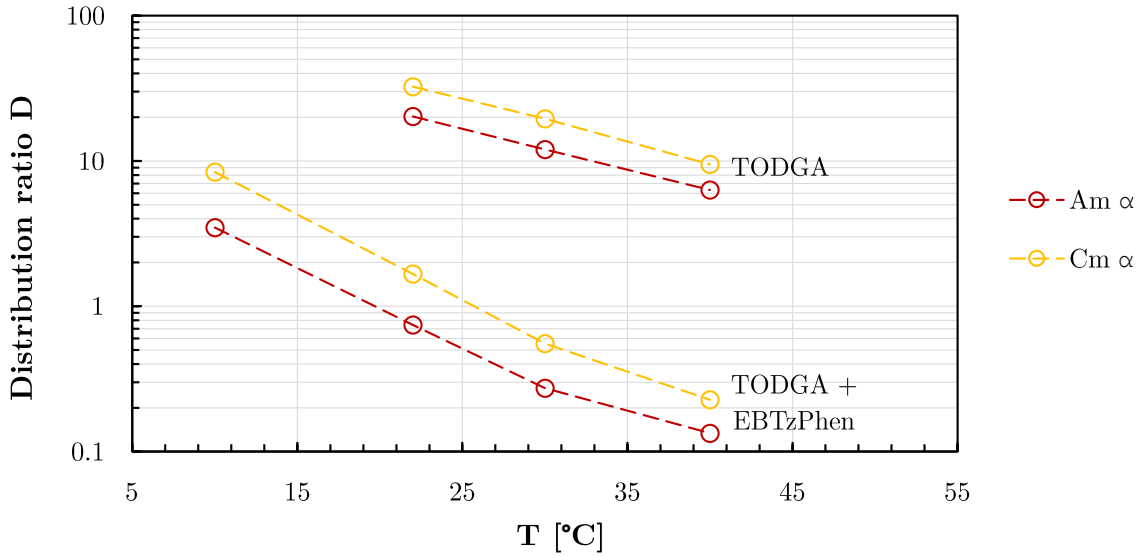

(a) D comparison for Am and Cm.

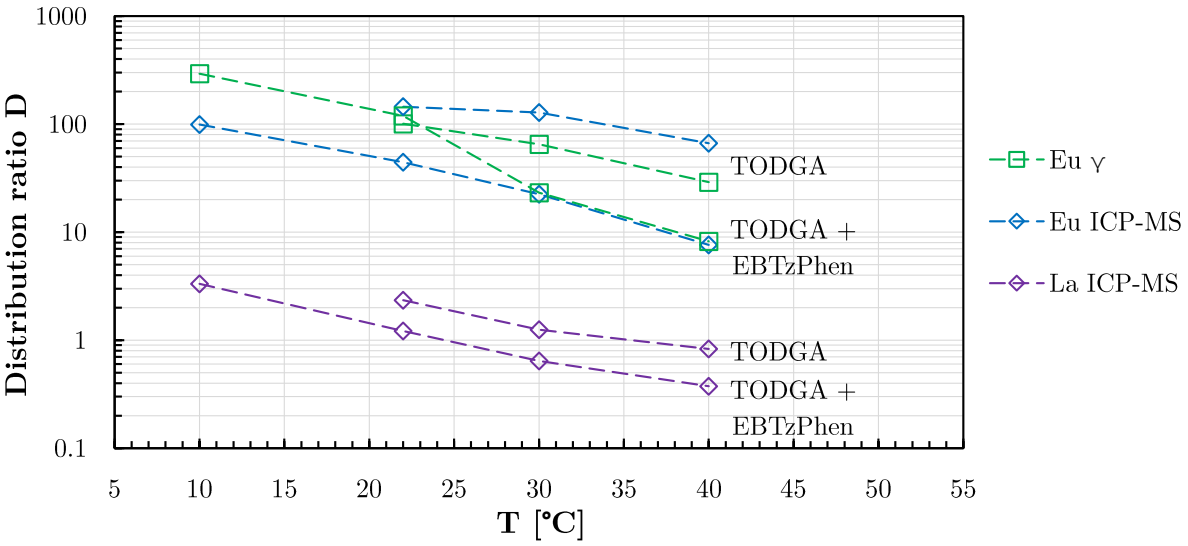

(b) D comparison for Eu and La.

Figure 4.11: Distribution ratios comparison between a TODGA system and a TODGA + EBTzPhen system, as a function of temperature.

Moreover, by comparing actinides and lanthanides behaviour in the two systems (figures 4.11a and 4.11b), Am and Cm seem to be more affected than Eu and La: this is an

additional proof of the larger affinity of the EBTzPhen towards actinides with respect to lanthanides.

By looking at the distribution ratios of all the lanthanides and actinides (figure 4.12), it is even more apparent that the temperature effect is significantly enhanced in presence of the hydrophilic ligand: at 40°C distribution ratios of all the metals have strongly decreased, and many remain in the aqueous phase. Moreover, as in the previous case, heavy Ln appear to be less affected by temperature up to 30°C, but their D is significantly lower at 40°C. This phenomenon could be related to a strong stabilization of heavy lanthanides complexes with EBTzPhen due to the high temperature, which hinders the decomplexation, combined to a destabilization of TODGA ones. Nevertheless, as previously stated, heavy Ln data are affected by high uncertainties (section 3.7), and to better investigate this trend it would be necessary to repeat this experiment and measure heavy Ln by back extraction. Moreover, as opposed to light lanthanides that remain in the aqueous phase, heavy lanthanides are still extracted, hence they do not affect the Am product.

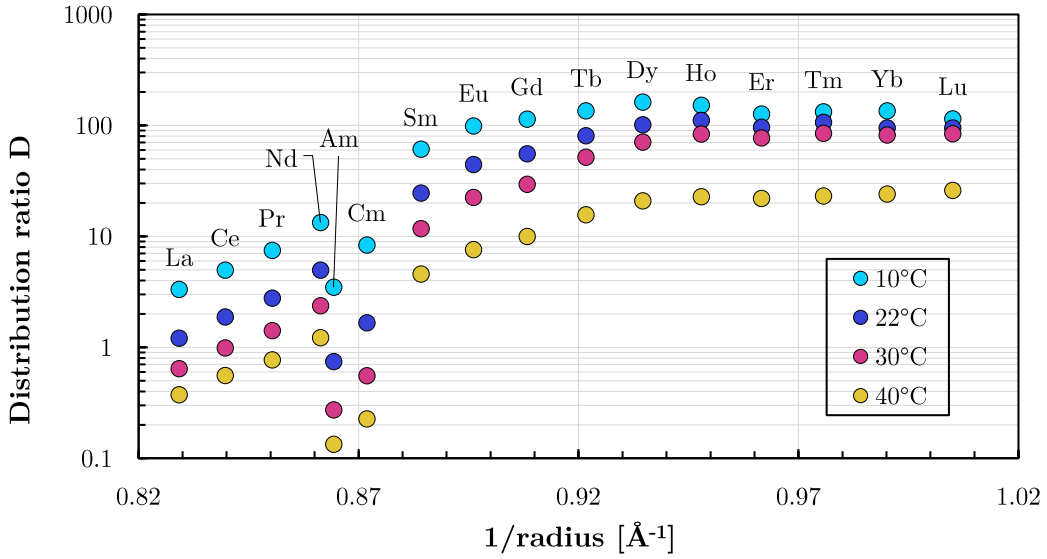

Figure 4.12: D as a function of the inverse ionic radius for 9-fold coordination; Org.: 0.2 M TODGA in 5% v/v 1-octanol/ISANE IP-175; Aq.: 0.1 M EBTzPhen (batch: GMA066) in 0.3 M HNO_3; 10^{-5} M Ln(III) (w/o Pm, incl. Y); Am-241, Cm-244, Eu-152; 10 min.

4.6. Extraction kinetics

With extraction experiments it is not possible to determine specific kinetics features of the EBTzPhen, because the time needed to reach equilibrium is a characteristic of the combined action of both the ligands. Moreover, also temperature and contacting device

have an important impact: temperature can improve the kinetics of the reaction, while an efficient phase mixing ensures equilibrium is reached faster. With an extperiment in which the mixing time is varied, the kinetics of the system in the specific contacting device is investigated.

A first extraction series was carried out with mixing times of 5, 10 and 20 minutes, and it is apparent that equilibrium is reached within 5 minutes (see figure 4.13 and table 4.7).

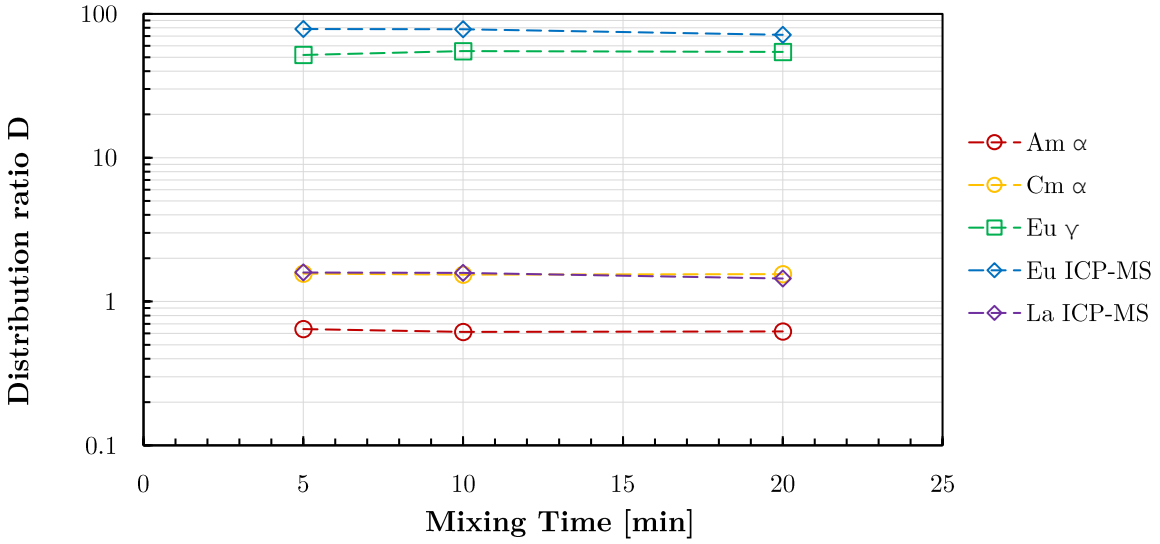

Figure 4.13: Org.: 0.2 M TODGA in 5% v/v 1-octanol/ISANE IP-175; Aq.: 0.1 M EBTzPhen (batch: GMA061) in 0.3 M HNO_3; 10^{-5} M Ln(III) (w/o Pm, incl. Y); Am-241, Cm-244, Eu-152; 22°C.

Table 4.7: Distribution ratios for Am, Cm, Eu and La and separation factors as a function of mixing time (MT). Eu data calculated with gamma measurements.

MT [min]	D_{Am}	D_{Cm}	D_{Eu}	D_{La}	$SF_{Cm/Am}$	$SF_{Eu/Am}$	$SF_{La/Am}$
5	0.644	1.56	51.8	1.59	2.43	80.5	2.47
10	0.615	1.54	55.1	1.58	2.50	89.7	2.57
20	0.621	1.55	54.5	1.45	2.50	87.8	2.33

For the purpose of a possible scale-up carried out in centrifugal contactors, devices characterized by significantly fast contacting, shorter mixing times were investigated: 1, 2, 5 and 10 minutes. Equilibrium appears to be reached within 5 minutes, but a satisfactory separation is achieved already after 2 minutes, as it can be seen from figure 4.14.

Fast kinetics is expected for a phenanthroline based ligand, due to the high degree of preorganization and low conformational variability [54, 71, 72].

However, it can be noted that Am, Cm and La distribution ratios and separation factor differ from the previous test. This difference in distribution ratios is likely due to the different batches of EBTzPhen used in the test, but it can also partially be related to the different mechanical shakers used in the two experiments (IKA VIBRAX VXR and IKA MATRIX Orbital Delta Plus respectively).

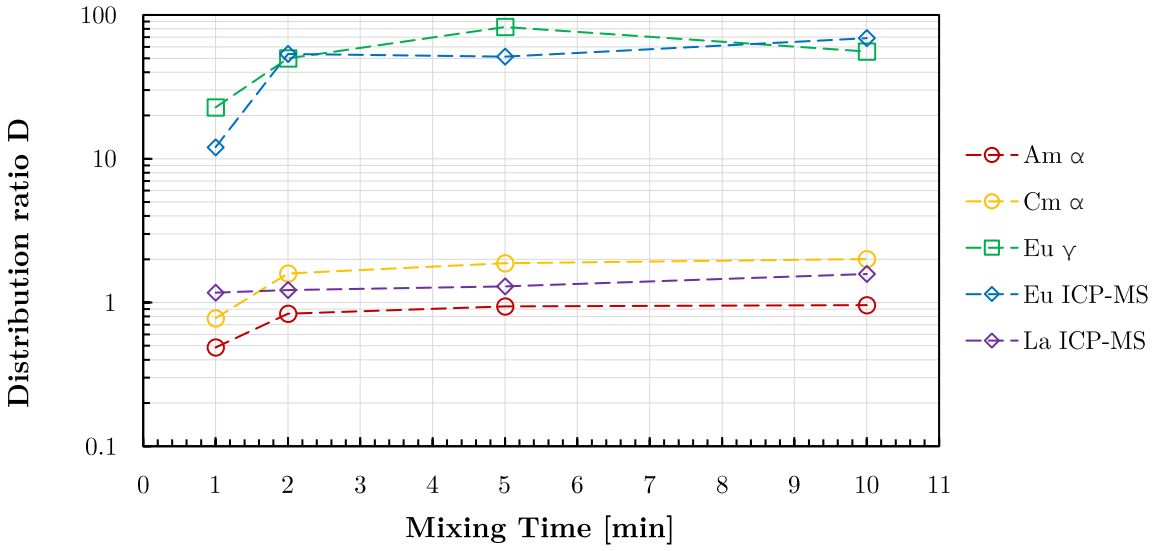

Figure 4.14: Org.: 0.2 M TODGA in 5% v/v 1-octanol/ISANE IP-175; Aq.: 0.1 M EBTzPhen (batch: GMA068) in 0.3 M HNO_3; 10^{-5} M Ln(III) (w/o Pm, incl. Y); Am-241, Cm-244, Eu-152; 22°C.

Table 4.8: Distribution ratios for Am, Cm, Eu and La and separation factors as a function of mixing time (MT). Eu data calculated with gamma measurements.

MT [min]	D_{Am}	D_{Cm}	D_{Eu}	D_{La}	$SF_{Cm/Am}$	$SF_{Eu/Am}$	$SF_{La/Am}$
1	0.486	0.777	22.8	1.17	1.60	46.8	2.41
2	0.834	1.59	50.0	1.22	1.91	59.9	1.46
5	0.940	1.87	82.5	1.29	1.99	87.7	1.37
10	0.959	2.00	55.6	1.58	2.09	58.0	1.65

From figure 4.15, it is interesting to notice that while for light Ln (La – Nd) equilibrium is reached almost immediately, for the heavy Ln it is reached after 2 minutes: this could

be related to a slower decomplexation of heavy Ln with EBTzPhen. The difference in decomplexation in between heavy and light Ln was observed also for SO_3−Ph−BTBP [69]: for the heavy Ln decomplexation was remarkably slower. Nevertheless, in the case of EBTzPhen, all the heavy Ln after 2 minutes are already extracted (D>50), hence they do not represent a problem for the AmSel process.

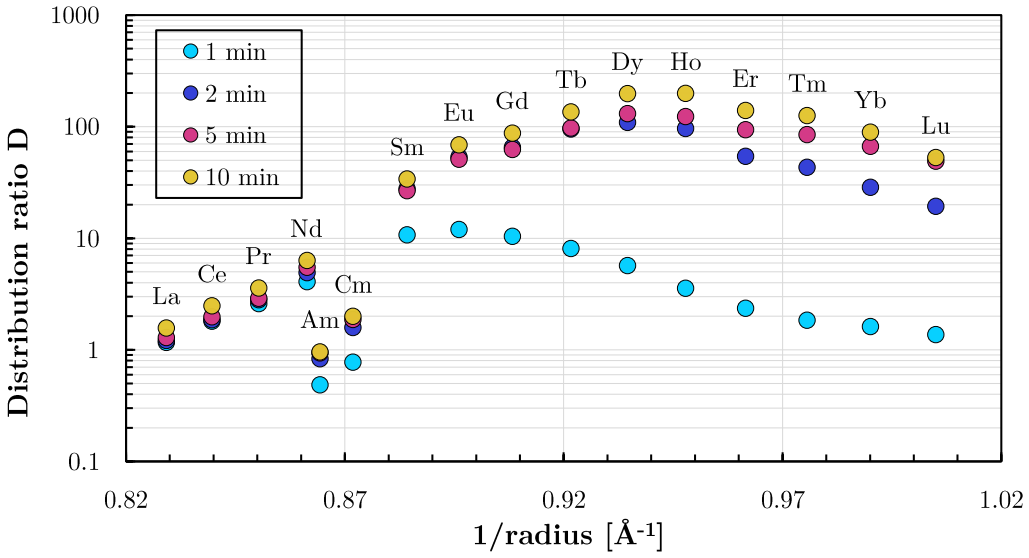

Figure 4.15: D as a function of the inverse ionic radius for 9-fold coordination; Org.: 0.2 M TODGA in 5% v/v 1-octanol/ISANE IP-175; Aq.: 0.1 M EBTzPhen (batch: GMA068) in 0.3 M HNO_3; 10^{-5} M Ln(III) (w/o Pm, incl. Y); Am-241, Cm-244, Eu-152; 22°C.

4.7. Stripping experiment

All the experiments carried out up to now are forward extractions, in which the EBTzPhen acts as a masking agent for TODGA. Since the AmSel process employs the hydrophilic ligand for a selective stripping of Am from a loaded organic phase, this experiment has been carried out in this condition.

The stripping experiment has been carried out in two main steps: loading and stripping. After every step, the distribution ratios of the different elements were evaluated, and the nitric acid concentration in the aqueous phase was measured via titration.

4.7.1. Loading

Besides actinides and lanthanides, also fission and corrosion products were added to the feed used for the loading, to simulate the PUREX raffinate. However, the metal concen-

tration (table A.1 in appendix A) was kept sub-stoichiometric with respect to the ligands, and no loading condition was tested. From the literature, it is expected that actinides and lanthanides are efficiently extracted by TODGA, but also co-extraction of problematic fission products is often observed. Generally, the most problematic are Sr(II), Pd(II), Zr(IV) and Ru; while Sr(II) can be scrubbed with lower HNO_3 concentration, for Zr(IV) and Pd(II) a masking agent (CDTA) is used [83]. On the other hand, Ru contamination is a known problem for TODGA based systems, but it is retained in the organic phase, hence it does not impact the Am(III) product [37].

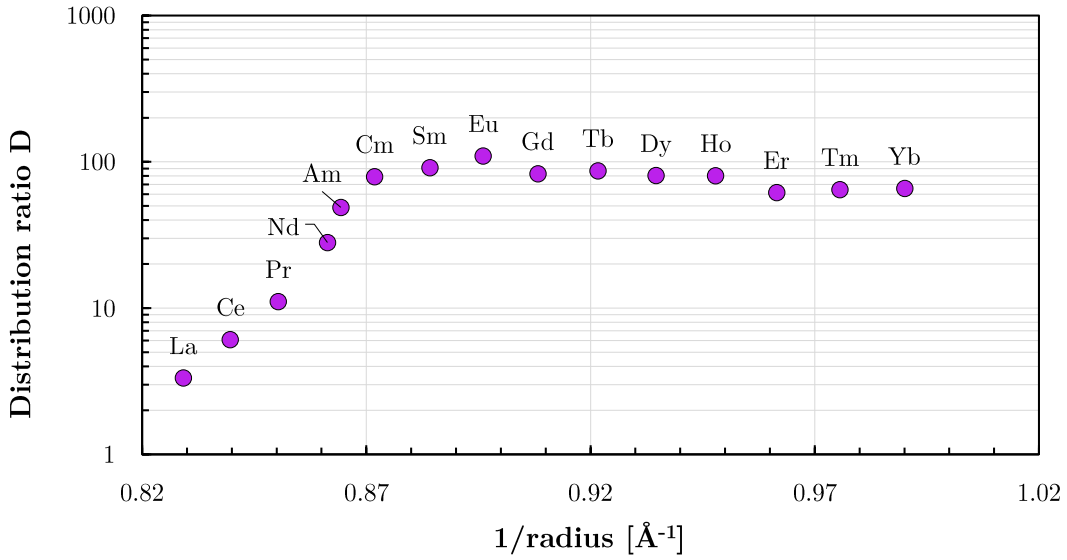

Figure 4.16: D as a function of the inverse ionic radius for 9-fold coordination; Org.: 0.2 M TODGA in 5% v/v 1-octanol/ISANE IP-175; Aq.: 0.5 M HNO_3; HAR dil. 1:400; 10^{-5} M Ln(III) (w/o Pm, incl. Y); Am-241, Cm-244, Eu-152; 22°C; 30 min.

Figure 4.16 reports the results of the loading; it appears that distribution ratios for lanthanides and actinides follow the typical curve of TODGA extraction [49] (no data available for Lu). However, distribution ratios seem to be lower with respect to other experiments performed at 0.3 M HNO_3. Since the nitric acid concentration used (0.5 M) is higher than this value, and nitrates promote TODGA extraction, it is expected that lanthanides and actinides are better extracted in this system. This could be due to the contacting device: TODGA is notoriously a fast ligand, but the shaking might have been less effective than in the other experiments, due to the large volume of phases contacted, the velocity setting and the type of shaking. Moreover, due to the high metal concentration used, the loading could have reduced the free TODGA concentration. Nevertheless, the extraction of actinides and lanthanides from the aqueous phase is satisfactory.

By looking at fission and activation products distribution ratios (figure 4.17, the only metals co-extracted are Y and Zr, while Pd and Ru are retained in the aqueous phase (no data available for Sr). The reason is likely the low acidity of the aqueous phase: when the organic phase is contacted with a PUREX raffinate simulate solution (HNO_3 concentration of 3.1 M), $D_{Zr} > 100$ and $D_{Pd} = 4.75$ [83]. At such high nitric acid concentration, Pd has a quite low distribution ratio, hence it is not surprising that it is not extracted at 0.5 M HNO_3.

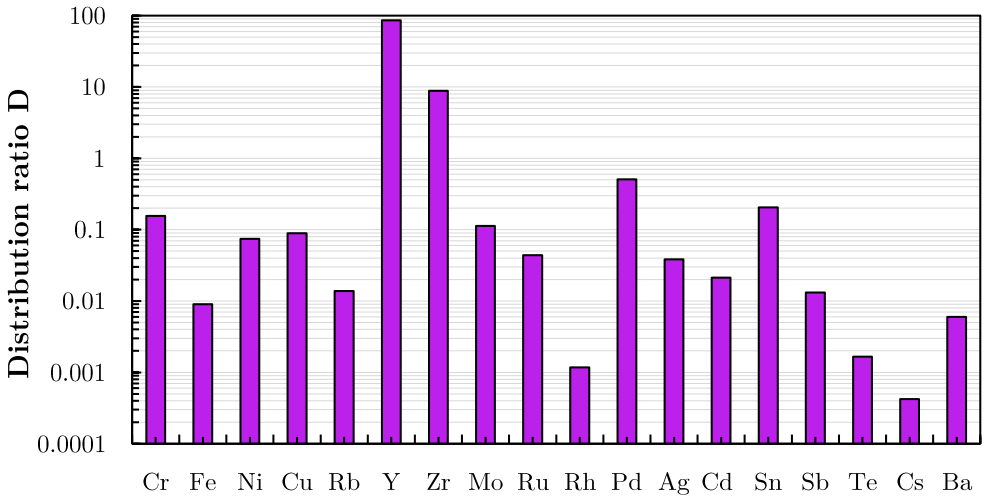

Figure 4.17: Distribution ratios of fission and activation products - Org.: 0.2 M TODGA in 5% v/v 1-octanol/ISANE IP-175; Aq.: 0.5 M HNO_3; HAR dil. 1:400; 10^{-5} M Ln(III) (w/o Pm, incl. Y); Am-241, Cm-244, Eu-152; 22°C; 30 min.

4.7.2. Stripping

Then, with the loaded organic phase, a stripping extraction series was performed, varying the mixing time. The investigated values were 1, 2, 5 and 10 minutes.

A test carried out in stripping conditions should lead to the same results obtained in forward extraction conditions. However, a change could be observed regarding the system's kinetics: decomplexation from a phase could be more hindered than from the other. Nevertheless, it can be seen from figure 4.18 that equilibrium is reached within 5 minutes also in stripping conditions. This value is significantly lower than the value observed by Wan et al. (15 minutes) [60], but the different experimental setup could have been the cause.

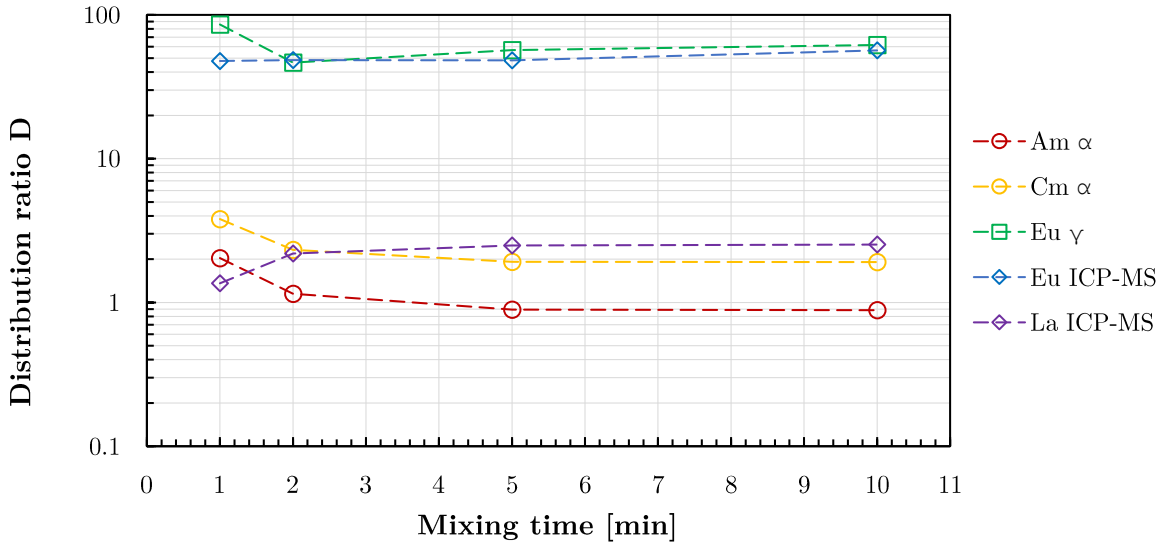

Figure 4.18: Org.: loaded 0.2 M TODGA in 5% v/v 1-octanol/ISANE IP-175; Aq.: 0.1 M EBTzPhen (batch GMA066) in 0.3 M HNO_3; 22°C.

By looking at Eu and La behaviour in figure 4.18, and comparing it with Am and Cm, it is likely that D_{Eu} at 1 minute is out of trend, and a new measurement should be performed. The actual trend is probably the one evaluated by ICP-MS. In fact, it appears that D_{Eu} after 1 minute is a very similar value of D_{Eu} after loading. The behaviour of the other metals is the opposite: after 1 minute, their D is significantly lower with respect to immediately after loading. Moreover, the trend observed in the gamma measurements indicates a release of Eu after 2 minutes. This is incompatible with the fast kinetics exhibited by TODGA [64].

Table 4.9: Distribution ratios of Am, Cm, Eu and La and separation factors as a function of mixing time (MT). Eu data calculated with gamma measurements.

MT [min]	D_{Am}	D_{Cm}	D_{Eu}	D_{La}	$SF_{Cm/Am}$	$SF_{Eu/Am}$	$SF_{La/Am}$
1	2.04	3.80	85.8	1.36	1.87	42.1	0.667
2	1.15	2.32	46.6	2.19	2.02	40.5	1.90
5	0.892	1.91	56.8	2.49	2.15	63.6	2.79
10	0.884	1.91	61.7	2.53	2.16	69.8	2.86

From the separation factors shown in table 4.9, a satisfactory separation is achieved in two minutes. Moreover, by observing the distribution ratios of the lanthanides (figure 4.19), it can be observed that they are not significantly affected by the mixing time: being in

the organic phase, they are already close to the final D value reached at equilibrium. Nevertheless, it appears that the organic phase partially releases the lanthanides immediately after mixing, and then they get progressively re-extracted. Since the organic phase, during the loading, has been contacted with an aqueous phase of higher HNO_3 concentration, the release could be related to an initial release of nitric acid. Moreover, The release is assumed to be immediate, because TODGA is characterized by a fast kinetics [64]. Since EBTzPhen displays a much higher affinity for actinides, they get progressively stripped while lanthanides are re-extracted. On the other hand, re-extraction is not immediate because de-complexation from EBTzPhen is slower, as observed in figure 4.15. However, to study better this different kinetics behaviour with heavy lanthanides, it could be interesting to study longer contacting times.

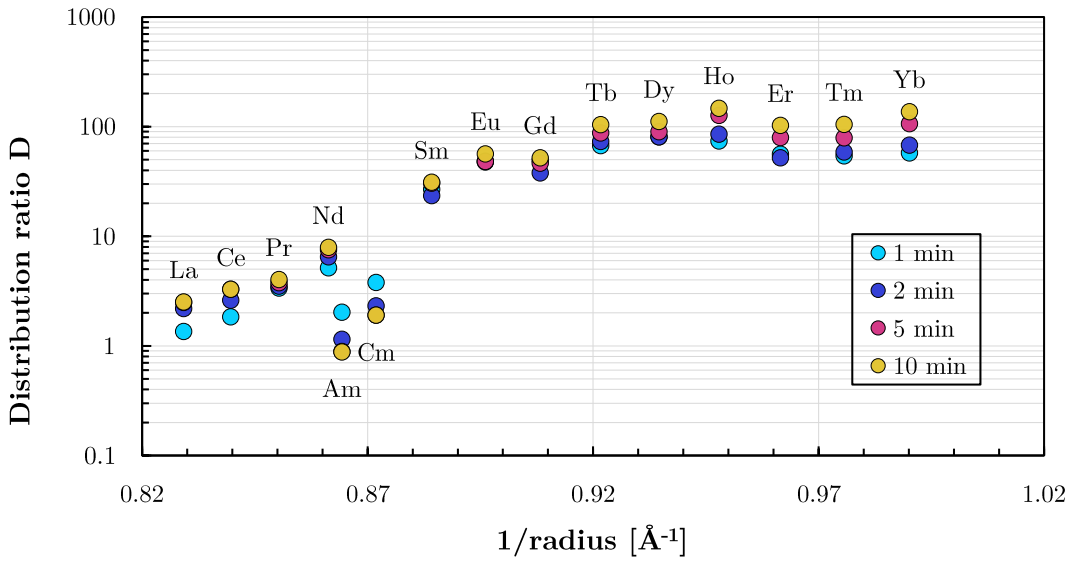

Figure 4.19: D as a function of the inverse ionic radius for 9-fold coordination; Org.: loaded 0.2 M TODGA in 5% v/v 1-octanol/ISANE IP-175; Aq.: 0.1 M EBTzPhen (batch GMA066) in 0.3 M HNO_3; 22°C.

Finally, only the distribution ratios of the co-extracted fission products Y and Zr are observed (table 4.10). The other metals, being mostly retained in the aqueous phase, presented a too low concentration in the organic phase for their measurements to be meaningful. Moreover, even though D_{Zr} and D_Y seem to change with mixing time, it appears to be more related to the uncertainty of the measurements, since no trend is observed. Nevertheless, both the metals are still retained in the organic phase during the stripping.

Table 4.10: Distribution ratios of Zr and Y after stripping.

MT [min]	D_{Zr}	D_Y
1	19.3	112
2	19.3	104
5	5.76	110
10	9.60	139

4.7.3. Nitric acid extraction

The nitric acid concentration was evaluated by titration in the aqueous phase before and after every step of the experiment. Naturally, since stripping and loading are performed at similar HNO_3 concentration, fluctuations in nitric acid are expected to be minimal. Before and after the loading, the aqueous phase was titrated: while initially the HNO_3 concentration was 0.509 M, after the loading it decreased to 0.483 M. Hence, D_{HNO_3} = 0.055, which is a value quite in alignment with the literature (for $[HNO_3]_{initial}$ = 0.490, D = 0.0463 [84]).

Table 4.11: $[HNO_3]$ in the aqueous phase during the stripping, and correspondent D_{HNO_3}.

MT [min]	1	2	5	10
$[HNO_3]$ [M]	0.303	0.301	0.291	0.289
D_{HNO_3}	0.065	0.072	0.111	0.117

Before the stripping, the nitric acid concentration of the aqueous phase was 0.296 M. From table 4.11, it appears that the organic phase immediately releases HNO_3 upon contacting, and then the HNO_3 concentration reaches an equilibrium value. This release and re-extraction has been observed also in ICP-MS measurements for the lanthanides. However, as it can be seen from the concentration values obtained by titration the variation of nitric acid is minimal. It has to be noted that the equilibrium distribution ratio is higher than expected from TODGA at this nitric acid concentration [84]. Nevertheless, the titration was carried out in the aqueous phase containing the ligand. If the latter is protonated, the pH measured in the aqueous phase is higher. Moreover, these measurements are affected by high uncertainty values, since the volume of aqueous phase available for titration was limited.

4.8. Batch comparison

To appreciate differences in ligand batches, a test in optimal extraction conditions was repeated for each batch, to compare them and evaluate differences in extraction behaviour. Specifically, the comparison is carried out through the distribution ratios and separation factors between Am and Cm, Eu and La.

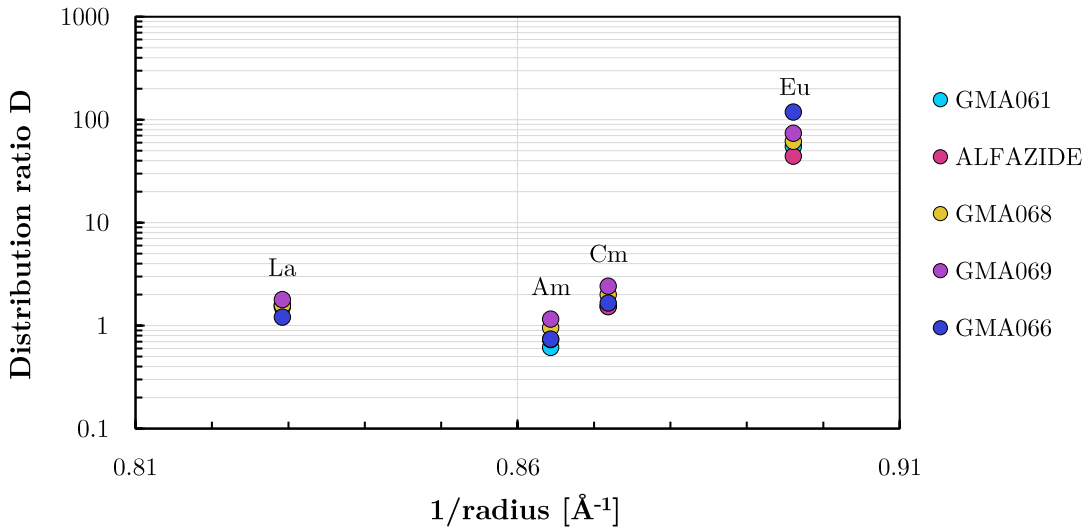

Figure 4.20: Org.: 0.2 M TODGA in 5% v/v 1-octanol/ISANE IP175 - IR [38] - Aq.: 0.1 M EBTzPhen in 0.3 M HNO_3; 10^{-5} M Ln(III) (w/o Pm, incl. Y); Am-241, Cm-244, Eu-152; 22°C; MT > 10 min.

Table 4.12: Distribution ratios for Am, Cm, Eu and La and separation factors evaluated in optimal extraction conditions for different batches.

Batch ID	D_{Am}	D_{Cm}	D_{Eu}	D_{La}	$SF_{Cm/Am}$	$SF_{Eu/Am}$	$SF_{La/Am}$
GMA061	0.615	1.54	55.1	1.58	2.50	89.7	2.57
ALFAZIDE	0.733	1.53	44.4	1.53	2.09	60.6	2.08
GMA068	0.959	2.00	61.7	1.58	2.09	64.3	1.65
GMA069	1.16	2.42	74.0	1.79	2.09	63.7	1.54
GMA066	0.744	1.67	119	1.21	2.24	160	1.63

From figure 4.20 and table 4.12, it is possible to observe that the distribution ratios values have a non negligible variability among the different batches. However, the dispersion of the D values is also due to statistical uncertainty, since they are results from different

experiments. Nevertheless, in case of Eu, the distribution ratio is for all batches significantly higher than D_{Am}, hence their separation is successful regardless. On the other hand, in the investigated system D_{Am} is close to D_{Cm} and D_{La}: their separation is based on a small difference, hence variability among the batches affects it in a more significant way.

By looking at table 4.12, it can be seen that the $SF_{Cm/Am}$ is quite constant in the range 2 - 2.5 ($SF_{Cm/Am,\ avg} = 2.2$, std. dev. = 8.2%). It is a parameter based on the distance between D_{Am} and D_{Cm}. It appears in table 4.12 that these values change quite significantly among the batches, but in the same way: when D_{Am} has a particularly high value, D_{Cm} also is higher, in such a way that their ratio remains around 2. Cm/Am selectivity is an intrinsic feature of the system: from the experimental results obtained in this work, $SF_{Cm/Am}$ is not affected by small fluctuations in ligand or nitric acid concentration. Therefore, the dispersion of this parameter is likely of statistical nature.

On the other hand, $SF_{Eu/Am}$ and $SF_{La/Am}$ have a much higher standard deviation (19% and 23% respectively) than $SF_{Cm/Am}$ (for $SF_{Eu/Am}$, the experimental point with batch GMA066 was not considered, since there was likely an error in the measurement, as showed in figure 4.10). Moreover, some trends can be observed. By looking at the distribution ratios, it can be observed that for certain batches the values are higher (for instance batch GMA069). Moreover, the distance between actinides and lanthanides seems to decrease (batches GMA068 and GMA069). This could be related to the undissolved particles found: the actual ligand concentration could be slightly lower than 0.1 M, which does not have a significant impact on $SF_{Cm/Am}$, but it strongly impacts separation from lanthanides, as it can be seen in the experiment in which EBTzPhen concentration is varied. This is not a concern for Eu, but it is for La separation, since it is based on a small difference in distribution ratios: $SF_{La/Am}$ decreases significantly.

In conclusion, the experimental results demonstrate that the behaviour of the system remains consistent across the different batches, with selectivity, kinetics, and temperature dependence left unaltered. The only observed discrepancies pertain to solubility. Nevertheless, since reproducibility is fundamental for large-scale applications, optimizing the synthetic route is fundamental to eliminate these solubility variations between batches.

4.9. Final remarks

$SF_{Cm/Am}$ is above 2: this is sufficient to achieve the Am separation in a multi-stage process [45]. Additionally, the separation from the lanthanides overall is satisfactory; $SF_{Eu/Am}$ is in agreement with the values found by Wan et al. [60]. Nevertheless, since La is hardly

retained in the organic phase, $SF_{La/Am}$ is comparable to $SF_{Cm/Am}$. Moreover, the kinetics of the system, both in forward extraction and in stripping conditions, is quite fast; this is a feature typical of phenanthrolines, due to their high degree of preorganization [54, 71, 72].

The system is visibly affected by temperature: in stripping conditions, a temperature increase will favour the release of metals from the organic phase. A possibility to counteract the cations release could be increasing the nitric acid concentration, pushing the equilibrium towards the complex formation. However, contacting devices can be thermostatically controlled with external cooling jackets and chillers.

Moreover, the $SF_{Cm/Am}$ is improved with respect to PrOH-BPTD [73] but not with respect to the old system [44]. Additionally, the achieved separation from light lanthanides is limited. However, the variables of the system cannot be changed significantly to further improve this aspect: the $SF_{Cm/Am}$ value is typical of BTrzPhen ligands used in combination with TODGA [76], and it cannot be increased. Moreover, the ligand requires 0.3 M HNO_3 to achieve a satisfactory separation ($D_{Am} < 1$ and $D_{Cm} > 1$), but at this nitric acid concentration TODGA extracts less efficiently, hence light lanthanides have low distribution ratios. A possibility to improve lanthanides separation, specifically La/Am, could be to increase the nitric acid concentration in order to improve TODGA extraction, and at the same time increase the ligand concentration (as was done in [73], [76]). Due to the increase in nitrates concentration, all the D will increase but, on the other hand, due to the higher ligand concentration, the increase in D_{Am} and D_{Cm} will be counteracted. In fact, as it can be seen from figure 4.7 and 4.4, EBTzPhen strongly retains actinides in the aqueous phase.

Furthermore, the ligand required high concentration to achieve separation. Aside from structural hindering of complexation, the molecule is affected by protonation: to understand its actual impact on the Am separation from Cm and La, it could be useful to repeat the test in which EBTzPhen concentration is varied at a significantly low nitric acid concentration, with the use of a nitrate salt (such as $NaNO_3$) to force the extraction by TODGA, as it was performed by Wan et al. for Am-Eu separation [60]. Nevertheless, this solution cannot be implemented in an industrial process: the addition of a nitrate salt adds a large amount of cations that remain in the aqueous phase and are not incinerable. Moreover, for an industrial process a higher nitric acid concentration would be preferred, since small pH variations are difficult to control. Additionally, if the loaded organic phase is contacted with an aqueous phase with very low HNO_3 concentration, the unwanted release of nitric acid and metal ions is significant.

Heavier lanthanides and other fission products are not particularly affecting the process:

they are mostly retained in the organic phase, and EBTzPhen did not display any selectivity towards these metals. Certainly, when the organic phase is contacted with real PUREX raffinate, which has a high nitric acid concentration (3 - 5 M), some metal ions are co-extracted with actinides and lanthanides [83]. However, this co-extraction can be partially overcome by means of a masking agent. The problematic fission products that are anyway co-extracted, such as Y or Ru, tend to remain in the organic phase even when the loaded organic phase is contacted with an aqueous phase with low HNO_3 concentration. This is surely a problem for solvent recycling, but it does not impact strongly the Am recovery.

In summary, while the investigated system presents several operational challenges, such as its thermal sensitivity or the high ligand concentration required due to competing phenomena, it exhibited many promising characteristics, among which robust separation factors and fast kinetics. These promising chemical and kinetic features, in addition to a CHON-compliant structure, render EBTzPhen a promising candidate for further development within the AmSel process.

5 | UV-VIS study

From previous complexation studies [50, 60, 82] and from the results of the extraction experiments, especially regarding the large amount of ligand required to achieve separation, it emerged that the investigated ligand has a low complexation efficiency. This feature is believed to be related both to protonation effect and to the molecular structure itself. To gain more insights regarding the complexation behaviour of the ligand, and specifically on these aspects, a UV-VIS titration with $Eu(NO_3)_3$ was performed.

5.1. Fundamentals

UV-VIS spectroscopy measures the light absorption of a sample, which receives a monochromatic beam in the ultraviolet and visible regions (λ = 200 - 800 nm). The absorption is related to the electrons of the sample: the range of 200-800 nm corresponds to the order of magnitude of the energy difference between electronic states [57]. If the beam wavelength excites the valence electrons from ground to excited state, the beam exiting the sample will have a lower intensity than its initial one. The absorption or extinction of the beam is called absorbance A and, for monochromatic light and dilute solutions ($<$ 0.01 M), it is described by the Boguer-Lambert-Beer law (equation 5.1) [85]:

$$A = \log\left(\frac{I_0}{I}\right) = \varepsilon \cdot C \cdot d \tag{5.1}$$

- A = absorbance
- I_0 = intensity of the beam entering the sample
- I = intensity of the beam exiting the sample
- $\varepsilon(\lambda)$ = molar absorption coefficient [M^{-1} cm^{-1}]. It is specific of each molecule, and it is function of the wavelength.
- C = concentration of the molecule in the sample solution [M]
- d = optical path [cm]. It is the thickness of the sample crossed by the beam.

In general, absorbance is an additive property: if in the sample different absorbing species are present, the total absorbance at a specific wavelength is the sum of the absorbances [85], [57]. Therefore, it is important to choose a solvent that does not interfere with the examined compound, and that is transparent within the wavelength range of interest. For instance, nitrates present a peak of absorbance around 220 nm.

With this technique, knowing the ε at a specific wavelength, it is possible to evaluate an unknown sample concentration. In addition, it is possible to investigate a range of wavelengths to determine the absorbance spectrum of the sample, which is usually plotted as $\varepsilon(\lambda)$. The different peaks observed in the spectrum correspond to different electronic transitions, while their intensity depends on the probability of the transition: the value of ε_{max} indicates whether the transition is forbidden or allowed [85]. Forbidden transitions (not allowed by selection rules) can still be observed due to different effects. The portion of the molecule able to absorb and subsequently emit electromagnetic radiation associated to certain electronic transitions is called chromophore. If the chromophore is included in a larger system, the position of the peaks is influenced by steric and resonance effects [85]. Moreover, the solvent in which the sample is dissolved can also influence the spectrum.

Usually, a UV-VIS titration is carried out adding metal aliquots to the ligand in solution: the reason is that, starting from the ligand's spectrum, it is possible to observe the changes indicating the complex formation. In fact, while metals do not have particular UV-VIS activity, ligands contain chromophoric groups: donor atoms with lone pairs, aromatic rings, alternated double bonds. UV-VIS titration studies with lanthanides have been already performed on BTrzPhen [58, 60, 75, 78] and, for all these molecules, the wavelength range of interest is 200 - 440 nm. Most lanthanides do not have absorption bands within this range [86], therefore titrations are carried out by adding metal aliquots to the ligand. The added species is not absorbing in the interest range, hence the changes in the spectrum are only related to complex formation.

The titration was carried out with $Eu(NO_3)_3$: to study the complexation behaviour of EBTzPhen with the lanthanides, europium was chosen as a representative element. The selected solvent was 0.01 M HNO_3, to mimic the acid conditions of the extraction experiments.

5.2. EBTzPhen spectrum

While the ethoxy-ethanol side chains are not chromophores and should not affect significantly the spectrum, EBTzPhen contains triazole rings and phenanthroline moieties: generally, aromatic rings are characterized by $\pi \rightarrow \pi^*$ electronic transitions, but if they

contain an atom with a lone pair, also $n \rightarrow \pi^*$ transitions can be observed [85]. These transitions correspond to peaks of absorbance in the spectrum. Moreover, transitions related the single chromophoric groups are affected by the molecule's structure. On one hand, since more atoms with lone pairs are present, they interact with each other affecting the $n \rightarrow \pi^*$ transitions. On the other hand, the triazole rings and the phenanthroline core constitute an extended aromatic system: a shift towards lower energies (bathochromic shift or redshift) is observed the more the aromatic system increases its size [87]. Finally, steric effect are also expected to be observed in the spectrum.

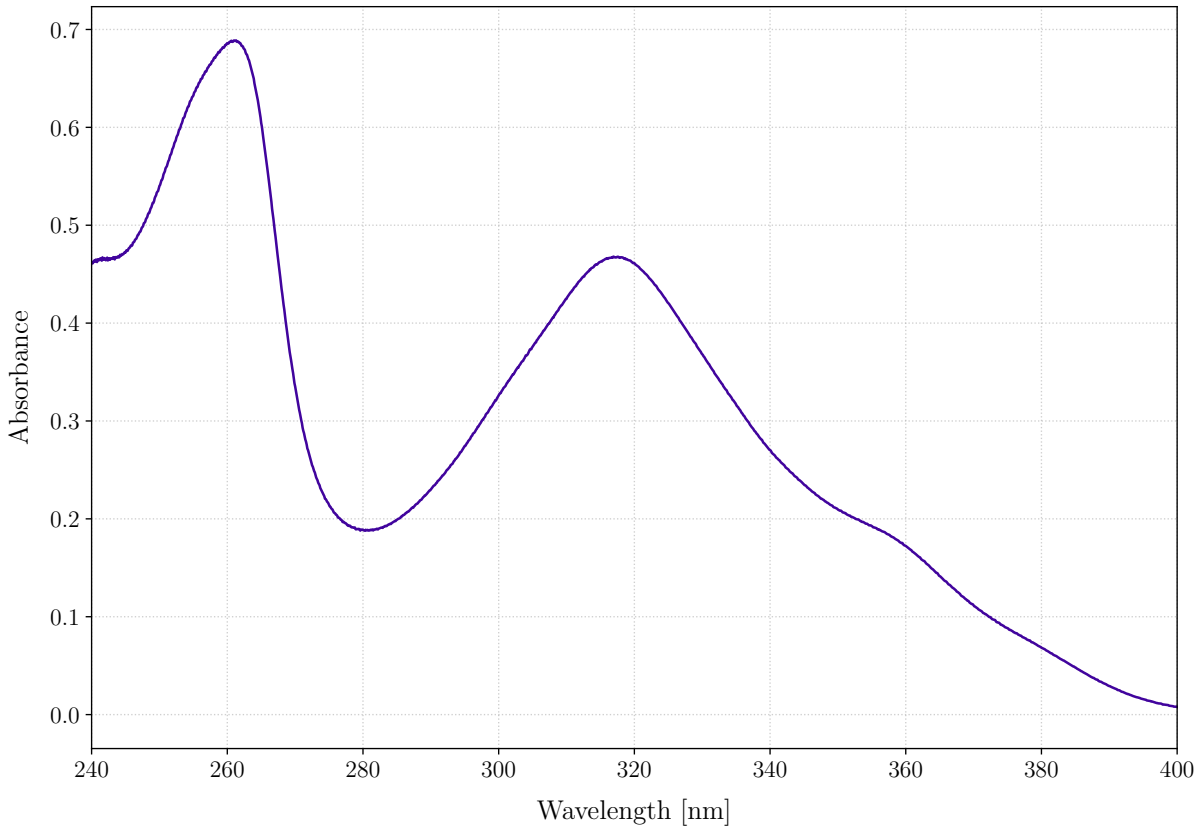

Figure 5.1: EBTzPhen spectrum measured with UV-VIS spectrophotometer; 2e-5 M EBTzPhen in 0.01 M HNO_3.

The recorded spectrum of the free ligand is similar to the ones of the BtrzPhen molecules in the literature [58, 60, 75]. As it can be observed from figure 5.1, there is a sharp peak close to 260 nm (in this case 261 nm), and a broad peak in the region of 315-320 nm. Moreover, there is a small shoulder at 360 nm.

The peak at 261 nm is related to the phenanthroline. In fact, the phenanthroline UV-VIS spectrum displays the same peak, which is attributed to $\pi \rightarrow \pi^*$ transitions [88]. Instead, the broad peak in the region of 315-325 nm is probably related to the addition

of triazole rings. The triazole moiety has its own absorption peak around 215 nm, which is outside the investigated range, but the broad peak observed could be produced by the extended aromatic system. In such system, the energy required for a $\pi \rightarrow \pi^*$ transition is reduced, causing a redshift of the absorbance peak. Moreover, vibrational and rotational levels introduced by the triazole rings are probably responsible for the broadening of the peak [57]. The shoulder at 360 nm could be related to the N atoms, specifically to their lone pairs. Their orbital is orthogonal to the plane of the molecule, while the π^* orbital is parallel and develops above and below the aromatic ring. These two orbitals, n and π^*, do not overlap, hence the $n \rightarrow \pi^*$ transition is forbidden due to overlap exclusion [57, 85, 89]. For this reason, it is observed as a low intensity peak, typically a shoulder, at low energies. Moreover, when there are neighbouring N atoms, their lone pairs interact, causing a bathochromic shift of the $n \rightarrow \pi^*$ transition peak [85].

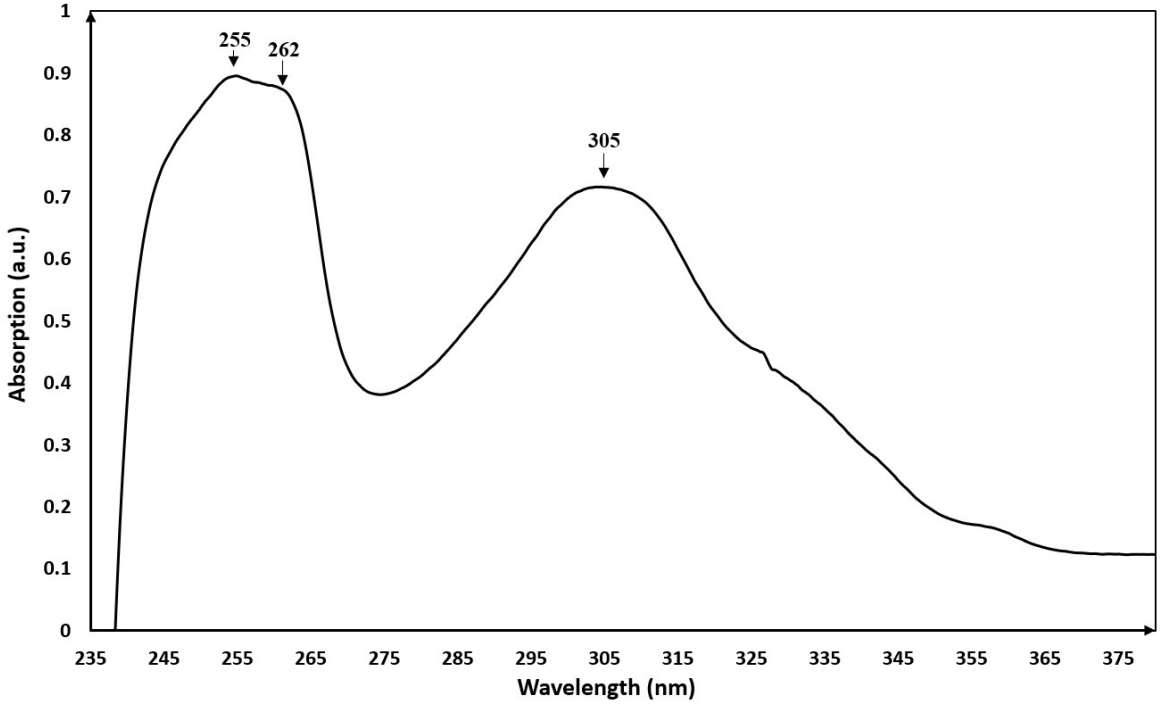

Figure 5.2: EBTzPhen spectrum measured with UV-VIS spectrophotometer; 2e-5 M EBTzPhen in water [60].

The EBTzPhen spectrum recorded by Wan et al. [60] (figure 5.2) is quite similar to the one measured in this work (figure 5.1), even though the authors used neutral water with a nitrate salt instead of an acidic solution. The different environment is likely the cause of the small differences observed. As an example, the peak observed in this work at 261 nm is the overlap of two close peaks. However, these transitions are not distinguishable in acidic conditions.

5.2.1. Molar absorption coefficient

The EBTzPhen molar absorption coefficient (or molar extinction coefficient) ε at 261 nm was evaluated at 22°C in 0.01 M HNO_3, by means of a calibration (figure 5.3 and table 5.1).

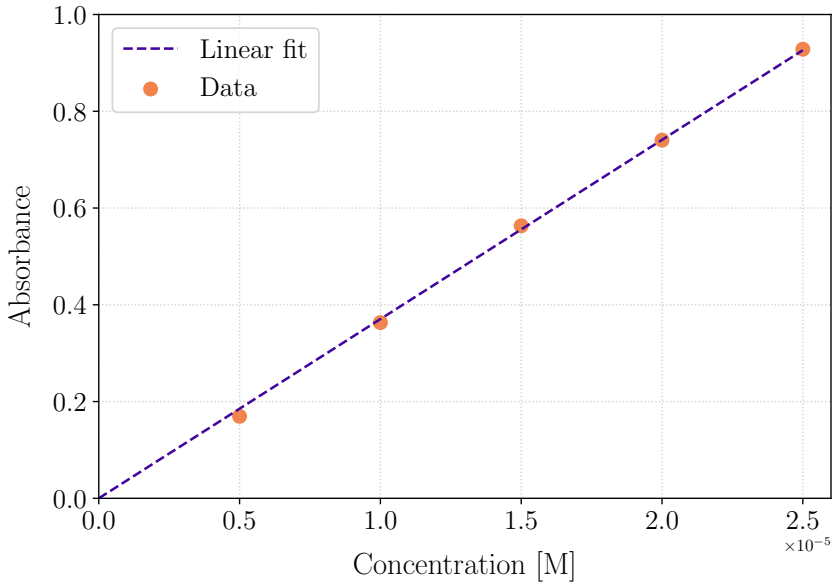

Figure 5.3: Calibration through standards of different EBTzPhen concentration values at 261 nm, 22°C, 0.01 M HNO_3.

Table 5.1: Absorbance values at 261 nm, 22°C, 0.01 M HNO_3 of the standards of different EBTzPhen concentration values, plotted in figure 5.3

[EBTzPhen] [M]	A	Err(A)
0.5e-5	0.170	-0.016
1.0e-5	0.363	-0.007
1.5e-5	0.563	0.008
2.0e-5	0.740	-0.001
2.5e-5	0.928	0.002

The calibration method is 'linear through zero': the slope of the interpolation line is the molar absorption coefficient at 261 nm. The value obtained is ε @ 261 nm = 37047.71 M^{-1} cm^{-1} (error = 0.0095). As expected, this peak is due to an allowed $\pi \rightarrow \pi^*$ transition: for allowed transitions, $10^3 < \varepsilon < 10^5$ M^{-1} cm^{-1}[85].

5.3. Titration with EU$(NO_3)_3$

5.3.1. Titration experiment

A metal titration with europium nitrate was carried out at 22°C, in 0.01 M HNO_3, on a 2e-5 M EBTzPhen solution. The titrating solution used contained 4e-4 M Eu$(NO_3)_3$, according to the procedure described in 3.9.4.

The complexation time can vary from seconds to hours: it is essential to measure the spectrum only when equilibrium is reached. Therefore, before the titration, a kinetics test was carried out: 10 µL of titrating solution were added to 2 mL of 2e-5 M EBTzPhen solution, and spectra were recorded at regular time intervals over a 20 minutes time. Additionally, a spectrum was recorded after 1 and 3 hours. Since no change was observed, it has been assumed the equilibrium is achieved immediately, and 10 minutes of waiting time after stirring was chosen as a conservative value.

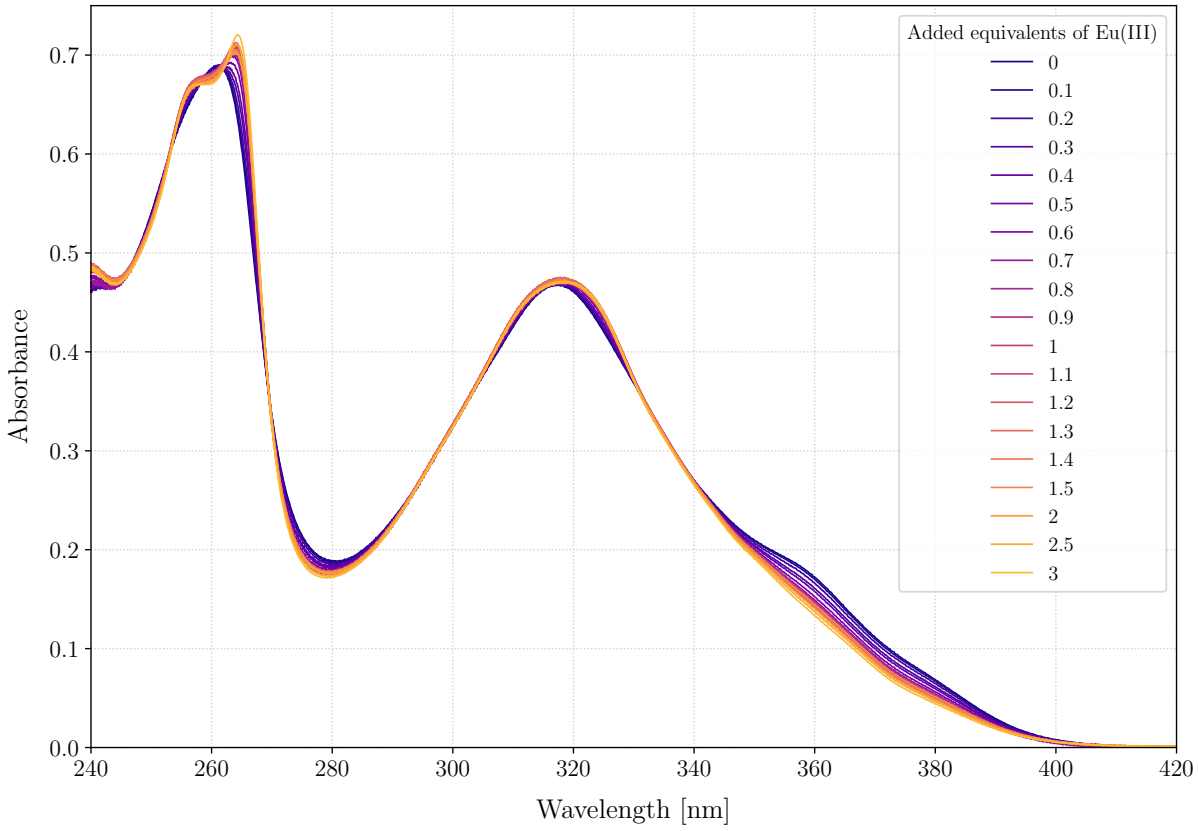

Figure 5.4: Titration of EBTzPhen with Eu$(NO_3)_3$ in 0.01 M HNO_3; Initial conditions: [EBTzPhen] = 2e-5 M, Volume = 2 mL; Titrant: [Eu$(NO_3)_3$] = 4e-4 M.

The spectral changes observed were small, but visible up to the addition of 1 equivalent.

After, no significant change was observed. For comparison, Wan et al. performed a titration with $Eu(NO_3)_3$ in neutral water (figure 5.5): what stands out the most is that the spectrum of complex exhibits a bathochromic shift (redshift: at lower energies) and splitting of the two close peaks already visible in the free ligand spectrum.

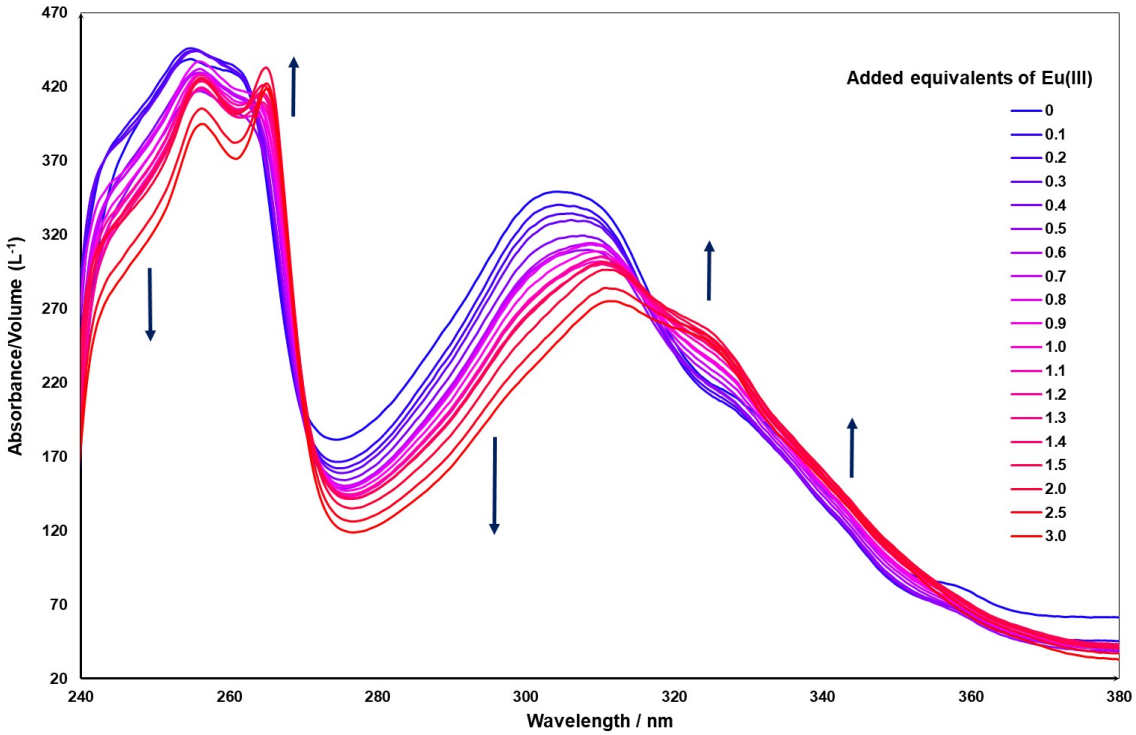

Figure 5.5: Titration of EBTzPhen with $Eu(NO_3)_3$ in neutral water (0.01 M Me_4NNO_3); Initial conditions: [EBTzPhen] = 2e-5 M, Volume = 2.0 mL; Titrant: $[Eu(NO_3)_3]$ = 1e-3 M) [60].

By comparing figure 5.4 and figure 5.5, it is apparent that for the titration performed in acidic conditions spectral changes are significantly lower, and no bathochromic shift is recorded. However, as the titrant is added, small but visible changes can still be observed in the spectrum: the peak at 261 nm splits in two components (also observed in [60]), the shoulder at 360 nm disappears, the peak 315-325 nm is slightly broader and shifted towards lower energies. Nevertheless, the fact that spectral changes in acid are significantly lower than in water is a clear indication of protonation of the ligand. It has to be noted that the spectral changes are significantly lower also when compared to a titration of BTrzPhen-tetraol in 0.01 M HNO_3 [75].

5.3.2. Titration data fitting

To evaluate the stoichiometry and the stability constants of the complexes there are several methods [57], but they all present some limitations. Today, to study systems in which several equilibria are present, and the stoichiometry of the complexes is unknown, computational methods are preferred. Among the different softwares, HypSpec2014 was used for this study.

Solver

HypSpec is part of the HyperQuad suite of programs [90]. It has been developed to evaluate stability constants from spectrophotometric data. It takes as input the titration data, which can be in different formats, depending on the procedure. It requires the absorbance spectra and the concentration of the two reagents for every titration step. Additionally, it is possible to load the spectrum of the two reagents. To model the system, it is necessary to indicate the species in solution: the free ligand L, the free metal M, the complexes formed and, if the system is subject to protonation, also H^+ ions and the pK_a.

The software performs a non-linear refinement of the stability constants $\log\beta_i$ from initial estimates. During this process, for each species i, the mass balance equations are always satisfied, and the molar absorbance values are evaluated using the Lambert-Beer equation (5.1) by linear least-squares fitting. During the refinement, at every iteration, the new stability constants and parameters are evaluated: specifically, a shift-vector is calculated, which contains the amount by which every $\log\beta_i$ should be changed. The objective function is the sum of squared residuals between the experimental spectra and the spectra calculated with the new set of parameters. A weighting scheme is applied to evaluate the sum of squared residuals. The solver minimizes the objective function, and it prevents the divergence by imposing some constraints on the shift-vector [91].

Stability constants determination

A first simple model was used for this system: only EBTzPhen and europium were considered as reagents, while no protonation equilibrium was evaluated (the protonation constant of the ligand is unknown). From the literature, BTrzPhen molecules appear to form 1:1 and 1:2 complexes [58, 60, 75, 78], but for a first estimation the model was built considering only 1:1 complexes. The wavelength range considered was selected accurately, removing parts of the spectrum in which the absorbance is close to the baseline, where data points are affected by considerable noise. The selected weighting scheme was 'unit weights', in which every wavelength have the same importance: no region of the spectrum

was affected by particularly high noise or high absorbance values (>1). After, the 1:2 complexes have been added among the species in solution, and the fitting process has been performed again.

Table 5.2: Stability constants for $[Eu(EBTzPhen)]^{3+}$ and $[Eu(EBTzPhen)_2]^{3+}$ complexes evaluated with HypSpec.

M:L	logβ	SD
1:1	6.46	0.03
1:2	-	-

The stability constant for the 1:1 complexes was evaluated, but it was not possible to obtain a value for $\log\beta_{1:2}$ (table 5.2): the refinement terminated prematurely due to shift-cutting (divergence of the shift-vector) [91]. The cause could be that no 1:2 complexes are formed in solution. However, this error can occur for different reasons, including noise, low concentration of one of the chemical species, spectra very similar to each other. Essentially, the experimental data do not contain sufficient information to determine the stability constants [91]. The small changes observed in the spectrum probably do not allow to determine the presence of 1:2 complexes, or these are not formed in this specific titration environment.

The obtained value for the 1:1 stability constant (table 5.2) is similar to the one obtained by Edwards et al. [75] ($\log\beta_{1:1} = 6.6$) for the titration of BTrzPhen-tetraol in 0.01 M HNO_3, but also of many other BTrzPhen ligands titrated in different media. Nevertheless, Wan et al. calculated a lower stability constant ($\log\beta_{1:1} = 5.5$) for EBTzPhen in neutral water. The authors obtained also a stability constant for 1:2 complexes [60].

The value of stability constant obtained in this study is evaluated with a simplified model, which does not include protonation equilibria. A more accurate evaluation of $\log\beta_{1:1}$ in acidic conditions should be performed including the contribution of H^+ ions and the pK_a of the ligand.

Moreover fluorescence studies indicated the presence of both 1:1 and 1:2 complexes in solution, with a prevalence of the first species [60]. It is possible that the low spectral changes, combined with the low concentration of 1:2 complexes, do not allow the software to detect them. Another possibility is that since most of the ligand is protonated, and the small fraction of free molecules forms only 1:1 complexes.

The software produced also a speciation plot (figure 5.6) with the evaluated concentrations of all the species in solution.

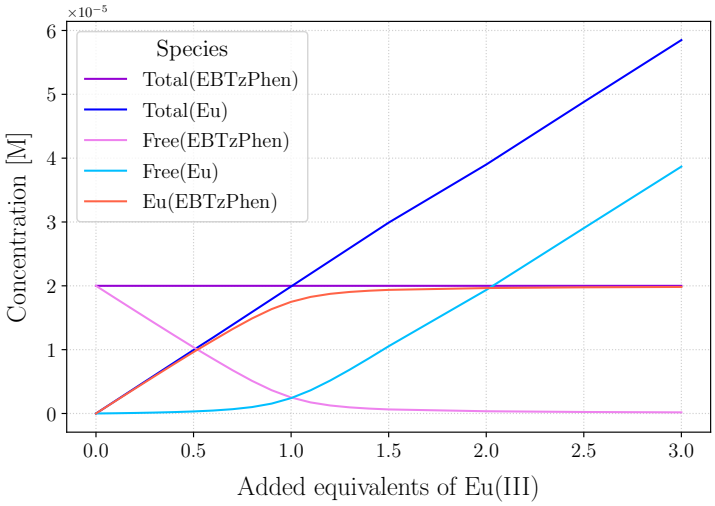

Figure 5.6: Speciation plot produced by HypSpec, according to the stability constants displayed in table 5.2.

[Eu(EBTzPhen)]$^{3+}$ spectrum

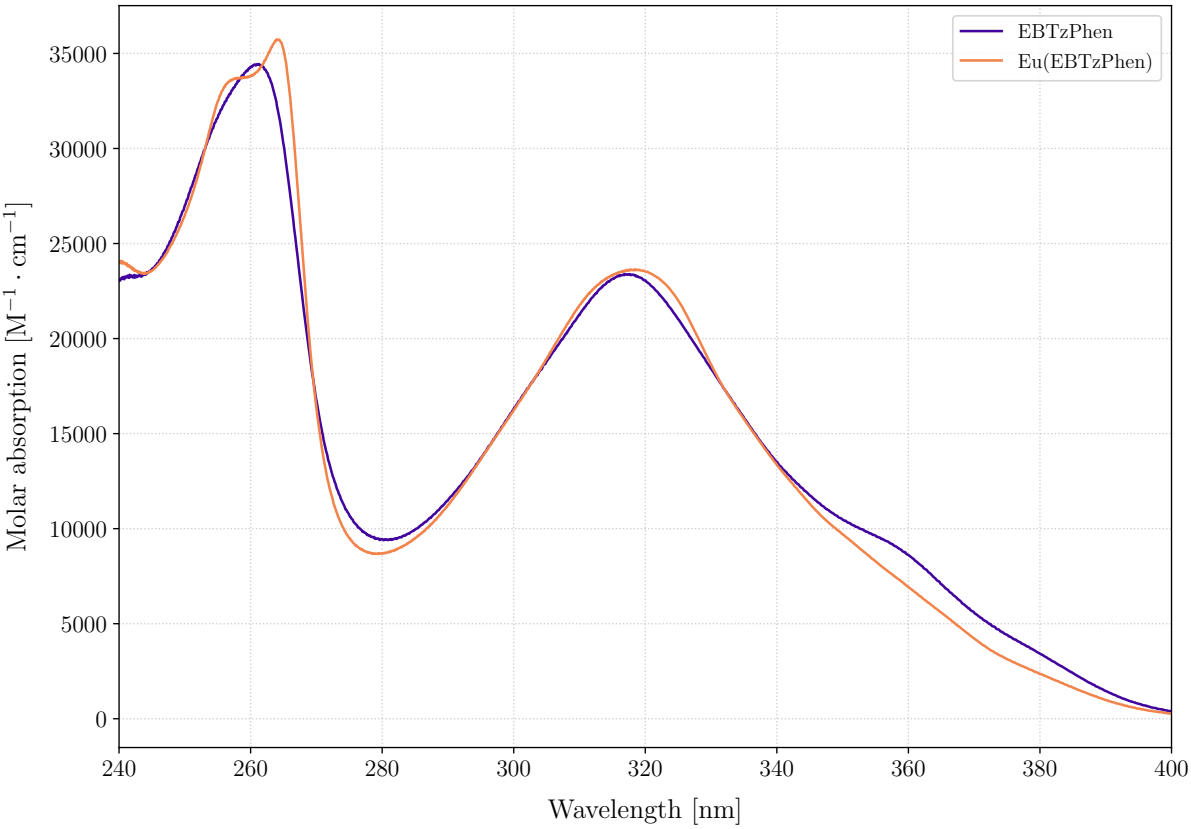

Figure 5.7: [Eu(EBTzPhen)]$^{3+}$ spectrum evaluated with HypSpec compared with the EBTzPhen spectrum (figure 5.1).

The software produces the spectrum, in molar absorption [M^{-1} cm^{-1}], for both the free ligand and the 1:1 complex (figure 5.7). For the latter, the spectrum is evaluated starting from the stability constant obtained and the titration data, while for the former is simply evaluated from the recorded spectrum taken as input for the calculation.

The shoulder at 360 nm completely disappears: it is probably subject to a blueshift, hence it is hidden by higher absorption bands. By looking at the free EBTzPhen spectrum, it has to be noted that the molar absorbance of the shoulder is not particularly low: ε_{max} is around 8500, and for allowed transitions $10^3 < \varepsilon < 10^5$. This could be related to the fact that triazole rings can rotate, and the $n \rightarrow \pi^*$ transition becomes allowed (n and π^* orbitals can overlap). In the complex spectrum the shoulder disappears, pointing that it is actually related to the lone pairs of the donor atoms. In fact, the electrons are not free like in the EBTzPhen spectrum, but they are coordinating the metal. Therefore, the energy necessary to be excited from their orbital to π^* orbitals is way larger [85].

The peak at 261 nm splits in two, and undergoes to a slight bathochromic shift. By looking at the literature [58, 60, 75, 78], it is interesting to notice that this double peak is a common characteristic to all the BTrzPhen; it is already present in the spectrum of the free ligand, and the distinction between the two peaks is intensified during the titration. This feature can only be observed when the titration is carried out in acetonitrile (CH_3CN) or water. When the titration is performed in nitric acid no double peak is observed [75]. For the specific case of EBTzPhen, the two peaks, even though close, can be observed in neutral water [60], but not in acid.

The double peak could be related to the vibrational and rotational states of the molecule. The 1,10-phenanthroline moiety has vibrational levels, which normally are not resolved in a UV-VIS spectrum [88]. However, it has to be noted that a polar solvent (acetonitrile) is used. On the other hand, in apolar solvents (such as hexane) it is possible to resolve the vibronic structure [92]. The reason is that in polar solvents, hydrogen bonds or dipole-dipole interactions are formed with the N atoms of the 1,10-phenanthroline. These interactions are not rigid, and have a broadening effect which smears out the vibronic structure.

On the other hand, BTrzPhen ligands seem to display better the vibronic structure in water or acetonitrile. In these molecules the system is extended due to the addition of triazole rings, which can also rotate: in principle this should cause an additional decrease of the vibrational spacing between the electronic levels. However, some steric effects might play a fundamental role. First, the triazole rings and the side chains are bulky substituents which can hinder the interaction between the solvent and the nitrogen atoms on

the phenanthroline core. Second, the aromatic system is extended to the triazole rings: the molecule tends to stay in a planar configuration. By looking at DFT calculations performed on EBTzPhen in a previous work [50], the possible conformations are all planar. Due to this effect, the phenanthroline moiety could be stabilized even in a polar solvent, allowing the resolution of the vibronic structure. An additional cause could be exciton splitting due to the coupling between the two triazole rings, since the molecule is symmetric [93].

When the ligand is complexed with europium, its structure is fixed in a plane and the conformational variability is significantly reduced. The symmetry is also increased, increasing the coupling between the triazole rings. This explains why the splitting of the peak is increased during the complex formation, as it can be observed in the literature [58, 75, 78].

Finally, when the ligand is dissolved in 0.01 M HNO_3, it is likely protonated: both in this work and in Edwards et al. [75] experiment, the ligand concentration is much lower than the nitric acid one ([L] = 2e-5 M $<$ 0.01 - 0.1 M HNO_3). Protonation is known to cause a bathochromic shift and to have a smearing effect on vibronic bands [93]. In fact, it can occur on a single nitrogen atom in the ligand, causing asymmetry in the π^* orbital and electrostatic repulsion. This process disrupts the planarity of the molecule.

5.4. Final remarks

The model used to obtain the stability constant and the complexes stoichiometry is not accurate, because it does not include protonation effect. The final spectrum of the complex was evaluated with the underlying hypothesis that all the ligand was involved in complexes at the end of the titration (see free(EBTzPhen) curve in figure 5.6). However, it is likely that a significant part of the ligand remains protonated in solution: the final spectrum at the end of the titration is the overlap of the spectrum of the complex (in a small concentration) and the spectrum of the protonated ligand. This would explain the small changes in the spectra during the titration. Nevertheless, part of the ligand complexed europium, as demonstrated by the splitting of the peak at 261 nm. By comparison with the UV-VIS titration of BTrzPhen-tetraol in 0.01 M nitric acid, the spectral changes are also lower for EBTzPhen. It should be noted that BTrzPhen-tetraol achieve equal extraction performance at similar pH with ligand concentrations in the order of tens of mM [76], while for EBTzPhen a 100 mM concentration is required (see section 4.2.2). Since the complexing core is unchanged, this different behaviour in the two molecules suggests that, besides protonation, the complexation efficiency of EBTzPhen is hindered

by an intrinsic phenomenon related to the structure. The ligand's complexation ability is likely compromised by the hydrophilizing side chains, causing steric hindrance effect. As it was indicated by previous complexation and crystallographic studies, they might interfere directly with the complexation. Moreover, the adopted *anti-anti* ligand conformation might partially hinder the complexation [60].

To evaluate better the stability constant, if the titration is performed in acid environment, it is fundamental to perform the fitting including the protonation equilibrium, but this would require the evaluation of the pK_a of the ligand. Finally, other spectroscopic techniques such as TRLFS could be used, to get a better estimation of the stability constants and more information on protonation and nitrates influence. Instead, to investigate the different affinity with respect to other metals, the titration should be repeated with light and heavy lanthanides, and actinides.

6 | Conclusions and future developments

EBTzPhen, a novel CHON-compliant hydrophilic ligand, was investigated as a more sustainable candidate than $SO_3-Ph-BTBP$ for an improved AmSel process. Its selectivity towards Am(III) was systematically tested in multiple conditions through extraction experiments, in combination with TODGA and in presence of Cm(III) and all the Ln(III).

The investigated hydrophilic ligand resulted to be a promising candidate for the AmSel process. Indeed, it is currently among the hydrophilic ligands under study in the Horizon 2020 TRANSPARANT project for the selective Am separation. It exhibited sufficiently good solubility in diluted aqueous acidic solutions to work with the required TODGA concentration in the organic phase. Furthermore, it demonstrated a good extraction efficiency, high enough to be implemented in a multi-stage process, and a strong affinity towards actinides, visibly decreasing D_{Am} and D_{Cm} with respect to a TODGA system with no hydrophilic complexant, while only slightly impacting lanthanides. Its selectivity towards Am with respect to Cm was satisfactory, even though not improved with respect to the current hydrophilic ligands under consideration. Finally, it showed fast kinetics, suitable for industrial contacting devices.

Specifically, under optimal extraction conditions (0.1 M EBTzPhen, 0.3 M HNO_3, 22°C), the system yielded the following separation factors:

- $SF_{Cm/Am}$ = 2 - 2.5
- $SF_{Eu/Am}$ = 60 - 90
- $SF_{La/Am}$ = 1.6 - 2.5

The achieved $SF_{Cm/Am}$ value is an intrinsic characteristic of BTrzPhen molecules used in combination with TODGA, and it showed to be resilient to fluctuations in ligand and nitric acid concentrations. Moreover, Am separation from all the lanthanides, even light ones, is carried out successfully. The actinide-lanthanide separation is strictly related to the nitric acid concentration adopted: most of proposed CHON-compliant molecules

require a low pH to function, but the low nitrate concentration renders TODGA extraction inefficient, causing the light lanthanides to be less extracted in the organic phase. Often, the combination of these two factors can lead to a co-stripping of the light lanthanides. However, EBTzPhen is able to separate Am also from all the light lanthanides, with a $SF_{La/Am}$ (the lowest across the lanthanides series) comparable to $SF_{Cm/Am}$.

Nevertheless, the investigated system presents also some challenges. Since temperature increase promotes the release of the metal ions in the aqueous phase, the process requires thermostatically controlled contacting devices. Additionally, according to the results obtained by extraction experiments and UV-VIS titration, protonation, steric hindrance and unfavourable conformational effects seem to significantly impact complexation efficiency, thereby requiring a larger ligand concentration to achieve separation. Finally, the ligand batches showed different solubility characteristics but, since $SF_{Cm/Am}$ is quite stable to fluctuations in ligand concentration, the Am-Cm separation was not compromised. Moreover, differences among the batches can be solved by optimizing the synthesis process.

In general, the main drawback of this ligand, which is common to many other CHON-compliant candidates for the AmSel process, is the narrow operational window of temperature, ligand and nitric acid concentration required to achieve separation conditions ($D_{Am}<1$ and D_{Cm}, $D_{Ln}>1$). Especially with respect to Cm and La, this window is constrained by a narrow selectivity margin. If the system was able to achieve higher separation factors, the range in which a separation conditions can be obtained would be significantly larger, and the process would be far more robust to fluctuations.

Through an extensive study of the extraction properties of EBTzPhen, this work highlights its promising features as substitute hydrophilic ligand for the AmSel process. However, the experimental results also put in evidence some inherent flaws, such as side chains interference or ligand protonation. With further complexation and structural studies, the role of the side chains could be further understood, with the objective of refining the molecular design. Additionally, it could be possible to determine the stoichiometry of the complexes, the different affinity of the molecule to actinides and lanthanides, the covalent character of the bonds, and the potential formation of molecular aggregates in the aqueous phase. Finally, other fundamental properties for a scale-up experiment should be investigated, such as resistance to hydrolysis and radiolysis, impact of degradation compounds, loading capacity, behaviour in different contacting devices.

Bibliography

[1] Ch Poinssot, S Bourg, N Ouvrier, N Combernoux, C Rostaing, M Vargas-Gonzalez, and J Bruno. Assessment of the environmental footprint of nuclear energy systems. Comparison between closed and open fuel cycles. *Energy*, 69:199–211, 2014. ISSN 0360-5442. doi: 10.1016/j.energy.2014.02.069. URL http://www.sciencedirect.com/science/article/pii/S0360544214002035http://dx.doi.org/10.1016/j.energy.2014.02.069.

[2] C Poinssot, S Bourg, and B Boullis. Improving the nuclear energy sustainability by decreasing its environmental footprint. Guidelines from life cycle assessment simulations. *Prog. Nucl. Energy*, 92:234–241, 2016. ISSN 0149-1970. doi: 10.1016/j.pnucene.2015.10.012. URL <GotoISI>://WOS:000384786400027.

[3] OECD Nuclear Energy Agency. *Unlocking the Hidden Value of Nuclear Fuel: The Societal Benefits of Diverse Material Recycling*. OECD Publishing, 2025.

[4] Gregory Choppin, Jan-Olov Liljenzin, Jan Rydberg, and Christian Ekberg. The Nuclear Fuel Cycle. In *Radiochemistry and Nuclear Chemistry*, chapter 21, pages 685–751. Elsevier, fourth edition, 2013. doi: 10.1016/B978-0-12-405897-2.00021-5.

[5] OECD Nuclear Energy Agency. *Management of recyclable fissile and fertile materials*. OECD Publishing, 2007. ISBN 9789264032552.

[6] Patrice Bruneton and Michel Cuney. Geology of uranium deposits. In *Uranium for Nuclear Power: Resources, Mining and Transformation to Fuel*, chapter 2, pages 11–52. Elsevier Inc., 3 2016. ISBN 9780081003077. doi: 10.1016/B978-0-08-100307-7.00002-8.

[7] International Atomic Energy Agency (IAEA). Methods of exploitation of different types of uranium deposits. Technical report, 2000.

[8] D. C. Seidel. Extracting uranium from its ores, 2007.

[9] Gregory Choppin, Jan-Olov Liljenzin, Jan Rydberg, and Christian Ekberg. The

Actinide and Transactinide Elements. In *Radiochemistry and Nuclear Chemistry*, chapter 14, pages 405–444. Elsevier, 2013. doi: 10.1016/b978-0-12-405897-2.00014-8.

[10] World Nuclear Association. Supply of Uranium, . URL `https://world-nuclear.org/information-library/nuclear-fuel-cycle/uranium-resources/supply-of-uranium`.

[11] IAEA International Atomic Energy Agency. Impact of extended burnup on the nuclear fuel cycle, 1993.

[12] OECD Nuclear Energy Agency. *Strategies and Considerations for the Back End of the Fuel Cycle*. OECD Publishing, 2021.

[13] OECD-NEA. *Homogeneous versus Heterogeneous Recycling of Transuranics in Fast Nuclear Reactors*, volume NEA No. 7077. OECD Nuclear Energy Agency, Issy-les-Moulineaux, France, 2012. ISBN 978-92-64-99177-4.

[14] International Atomic Energy Agency (IAEA). Classification of Radioactive Waste, . URL `http://www-ns.iaea.org/standards/`.

[15] Ogugua P. Unokiwedi, Jiachen Gao, Tristan Bethune, and Adedapo N. Awolayo. Deep geological repositories — A review of design concepts, near-field evolution, and their implications for nuclear waste containment, 10 2025. ISSN 18791700.

[16] World Nuclear Association. Storage and Disposal of Radioactive Waste, . URL `https://world-nuclear.org/information-library/nuclear-fuel-cycle/nuclear-waste/storage-and-disposal-of-radioactive-waste`.

[17] International Atomic Energy Agency (IAEA). Country Nuclear Power Profiles, . URL `https://www-pub.iaea.org/MTCD/Publications/PDF/CNPP-2021/pages/index.htm`.

[18] W B Lanham, T C Runion, and Oak Ridge National Laboratory. PUREX Process for Plutonium and Uranium Recovery. Technical Report ORNL-479, Oak Ridge, TN, USA, 1949.

[19] World Nuclear Association. Processing of Used Nuclear Fuel, . URL `https://world-nuclear.org/information-library/nuclear-fuel-cycle/fuel-recycling/processing-of-used-nuclear-fuel#reprocessing-today-ndash-purex`.

[20] Orano la Hague: the world leader in recycling nuclear materials. URL `https://`

www.orano.group/en/nuclear-expertise/orano-s-sites-around-the-world/recycling-spent-fuel/la-hague.

[21] World Nuclear Association. Mixed Oxide (MOX) Fuel, . URL https://world-nuclear.org/information-library/nuclear-fuel-cycle/fuel-recycling/mixed-oxide-fuel-mox.

[22] Christophe Poinssot, Christine Rostaing, Stéphane Greandjean, and Bernard Boullis. Recycling the Actinides, The Cornerstone of Any Sustainable Nuclear Fuel Cycles. *Procedia Chemistry*, 7:349–357, 2012. doi: 10.1016/j.proche.2012.10.055.

[23] OECD-NEA. *Minor Actinide Burning in Thermal Reactors*, volume NEA no. 6997. OECD Nuclear Energy Agency, Issy-les-Moulineaux, France, 2013. URL www.oecd.org/publishing/corrigenda.

[24] Andrei Fokau, Youpeng Zhang, Shinya Ishida, and Janne Wallenius. A source efficient ADS for minor actinides burning. *Annals of Nuclear Energy*, 37(4):540–545, 2010. doi: 10.1016/j.anucene.2009.12.025.

[25] Jinrui Wang, Pei Wu, Wentao Zhou, Yong Chen, Liudong Hou, and Jing Ma. Research progress in pyrochemical reprocessing of spent nuclear fuel, 10 2025. ISSN 1572901X.

[26] Thea Lyseid Authen, Jean-Marc Adnet, Stéphane Bourg, Michael Carrott, Christian Ekberg, Hitos Galán, Andreas Geist, Philippe Guilbaud, Manuel Miguirditchian, Giuseppe Modolo, Chris Rhodes, Andreas Wilden, and Robin Taylor. An Overview of Solvent Extraction Processes Developed in Europe for Advanced Nuclear Fuel Recycling, Part 2 - Homogeneous Recycling. *Sep. Sci. Technol.*, 57(11): 1724–1744, 2022. ISSN Print ISSN: 0149-6395 Online ISSN: 1520-5754. doi: 10.1080/01496395.2021.2001531. URL https://www.tandfonline.com/doi/full/10.1080/01496395.2021.2001531https://juser.fz-juelich.de/record/902511https://twitter.com/WildenAndreas/status/1461678518589394950.

[27] OECD Nuclear Energy Agency. State-of-the-art Report on Innovative Fuels for Advanced Nuclear Systems. Technical report, 2014. URL www.oecd.org/publishing/corrigenda.

[28] R J Taylor, C R Gregson, M J Carrott, C Mason, and M J Sarsfield. Progress towards the Full Recovery of Neptunium in an Advanced PUREX Process. *Solvent Extr. Ion Exch.*, 31(4):442–462, 2013. ISSN 0736-6299. doi: 10.1080/07366299.2013.800438. URL http://dx.doi.org/10.1080/07366299.2013.800438.

[29] Gregory R Choppin, Jan Rydberg, and Jan-Olov Liljenzin. *Radiochemistry and Nuclear Chemistry*. Butterworth-Heinemann Ltd, Oxford, England, 2nd edition, 1995. ISBN 0-7506-2300-4.

[30] D Serrano-Purroy, P Baron, B Christiansen, R Malmbeck, C Sorel, and J P Glatz. Recovery of minor actinides from HLLW using the DIAMEX process. *Radiochim. Acta*, 93(6):351–355, 2005. ISSN 0033-8230. doi: 10.1524/ract.93.6.351.65642. URL <GotoISI>://000230200300006.

[31] Giuseppe Modolo, Hanna Asp, Hendrik Vijgen, Rikard Malmbeck, Daniel Magnusson, and Christian Sorel. Demonstration of a TODGA-Based Continuous Counter-Current Extraction Process for the Partitioning of Actinides from a Simulated PUREX Raffinate, Part II: Centrifugal Contactor Runs. *Solvent Extr. Ion Exch.*, 26(1):62–76, 2008. ISSN 0736-6299. doi: 10.1080/07366290701784175. URL http://www.tandfonline.com/doi/abs/10.1080/07366290701784175.

[32] Andreas Geist, Jean-Marc Adnet, Stéphane Bourg, Christian Ekberg, Hitos Galán, Philippe Guilbaud, Manuel Miguirditchian, Giuseppe Modolo, Chris Rhodes, and Robin Taylor. An Overview of Solvent Extraction Processes Developed in Europe for Advanced Nuclear Fuel Recycling, Part 1 - Heterogeneous Recycling. *Sep. Sci. Technol.*, 56(11):1866–1881, 2021. ISSN 0149-6395. doi: 10.1080/01496395.2020.1795680. URL https://www.tandfonline.com/doi/abs/10.1080/01496395.2020.1795680.

[33] Giuseppe Modolo, Andreas Wilden, Henrik Daniels, Andreas Geist, Daniel Magnusson, and Rikard Malmbeck. Development and Demonstration of a new SANEX Partitioning Process for Selective Actinide(III)/Lanthanide(III) Separation using a mixture of CyMe4BTBP and TODGA. *Radiochim. Acta*, 101(3):155–162, 2013. doi: 10.1524/ract.2013.2016. URL http://www.oldenbourg-link.com/doi/abs/10.1524/ract.2013.2016?af=R.

[34] Daniel Magnusson, Andreas Geist, Andreas Wilden, and Giuseppe Modolo. Direct Selective Extraction of Actinides (III) from PUREX Raffinate using a Mixture of CyMe4-BTBP and TODGA as 1-cycle SANEX Solvent Part II: Flow-sheet Design for a Counter-Current Centrifugal Contactor Demonstration Process. *Solvent Extr. Ion Exch.*, 31(1):1–11, 2013. doi: 10.1080/07366299.2012.700596. URL http://www.tandfonline.com/doi/abs/10.1080/07366299.2012.700596.

[35] Andreas Wilden, Giuseppe Modolo, Peter Kaufholz, Fabian Sadowski, Steve Lange, Michal Sypula, Daniel Magnusson, Udo Müllich, Andreas Geist, and Dirk Bos-

bach. Laboratory-Scale Counter-Current Centrifugal Contactor Demonstration of an Innovative-SANEX Process Using a Water Soluble BTP. *Solvent Extr. Ion Exch.*, 33(2):91–108, 2015. ISSN 0736-6299. doi: 10.1080/07366299.2014.952532. URL http://dx.doi.org/10.1080/07366299.2014.952532.

[36] Elena Macerata, Eros Mossini, Stefano Scaravaggi, Mario Mariani, Andrea Mele, Walter Panzeri, Nathalie Boubals, Laurence Berthon, Marie-Christine Charbonnel, Francesco Sansone, Arturo Arduini, and Alessandro Casnati. Hydrophilic Clicked 2,6-Bis-triazolyl-pyridines Endowed with High Actinide Selectivity and Radiochemical Stability: Toward a Closed Nuclear Fuel Cycle. *J. Am. Chem. Soc.*, 138(23):7232–7235, 2016. ISSN 0002-7863. doi: 10.1021/jacs.6b03106. URL http://dx.doi.org/10.1021/jacs.6b03106.

[37] Andreas Wilden, Dimitri Schneider, Zaina Paparigas, Maximilian Henkes, Fabian Kreft, Andreas Geist, Eros Mossini, Elena Macerata, Mario Mariani, Maria Chiara Gullo, Alessandro Casnati, and Giuseppe Modolo. Selective actinide(III) separation using 2,6-bis[1-(propan-1-ol)-1,2,3-triazol-4-yl]pyridine (PyTri-Diol) in the innovative-SANEX process: laboratory scale counter current centrifugal contactor demonstration. *Radiochim. Acta*, 110(6-9):515–525, 2022. doi: 10.1515/ract-2022-0014. URL http://dx.doi.org/10.1515/ract-2022-0014https://juser.fz-juelich.de/record/906294https://twitter.com/WildenAndreas/status/1517395835985743873.

[38] Daniel Lundberg and Ingmar Persson. The size of actinoid(III) ions – structural analysis vs. common misinterpretations. *Coord. Chem. Rev.*, 318:131–134, 2016. ISSN 0010-8545. doi: https://doi.org/10.1016/j.ccr.2016.04.003. URL http://www.sciencedirect.com/science/article/pii/S0010854515300862.

[39] Peter Zsabka, Andreas Wilden, Karen Van Hecke, Giuseppe Modolo, Marc Verwerft, and Thomas Cardinaels. Beyond U/Pu separation: separation of americium from the highly active PUREX raffinate. *J. Nucl. Mater.*, 581(1 August 2023):154445, 2023. doi: 10.1016/j.jnucmat.2023.154445. URL https://www.sciencedirect.com/science/article/abs/pii/S0022311523002131https://juser.fz-juelich.de/record/1006770https://twitter.com/WildenAndreas/status/1646833458054832131.

[40] Giuseppe Modolo, Paul Kluxen, and Andreas Geist. Selective Separation of Americium(III) from Curium(III), Californium(III), and Lanthanides(III) by the LUCA Process, 2009.

[41] Marie-Jordane Bollesteros, Jean-Noël Calor, Sylvain Costenoble, Marc Montuir, Vincent Pacary, Christian Sorel, Fabien Burdet, Denis Espinoux, Xavier Hérès, and Catherine Eysseric. Implementation of Americium Separation from a PUREX Raffinate. *Proc. Chem.*, 7:178–183, 2012. ISSN 1876-6196. doi: http://dx.doi.org/10.1016/j.proche.2012.10.030. URL `http://www.sciencedirect.com/science/article/pii/S1876619612001040`.

[42] S Chapron, C Marie, G Arrachart, M Miguirditchian, and S Pellet-Rostaing. New Insight into the Americium/Curium Separation by Solvent Extraction Using Diglycolamides. *Solvent Extr. Ion Exch.*, 33(3):236–248, 2015. ISSN 0736-6299. doi: 10.1080/07366299.2014.1000792. URL `http://dx.doi.org/10.1080/07366299.2014.1000792`.

[43] Steve Lange, U W Scherer, and Andreas Wilden. *Selective extraction of trivalent Americium from PUREX raffinate by the use of CyMe4BTPhen and TEDGA (1-cycle SAmEX)*. PhD thesis, 2014.

[44] Christoph Wagner, Udo Müllich, Andreas Geist, and Petra J Panak. Selective Extraction of Am(III) from PUREX Raffinate: The AmSel System. *Solvent Extr. Ion Exch.*, 34(2):103–113, 2016. ISSN 0736-6299. doi: 10.1080/07366299.2015.1129192. URL `http://dx.doi.org/10.1080/07366299.2015.1129192`.

[45] Vincent Vanel, Andreas Wilden, Giuseppe Modolo, Andreas Geist, and Marc Montuir. Flowsheets for the Validation of the Reference AmSEL System. *EPJ Web Conf.*, 317(6th International ATALANTE Conference on Nuclear Chemistry for Sustainable Fuel Cycles (ATALANTE-2024)):1013, 2025. ISSN 2100-014X. doi: 10.1051/epjconf/202531701013. URL `https://doi.org/10.1051/epjconf/202531701013https://juser.fz-juelich.de/record/1038897https://x.com/WildenAndreas/status/1887442276638482679`.

[46] J Bisson, B Dinh, P Huron, and C Huel. PAREX, A Numerical Code in the Service of La Hague Plant Operations. *Procedia Chem.*, 21:117–124, 2016. ISSN 1876-6196. doi: 10.1016/j.proche.2016.10.017. URL `http://www.sciencedirect.com/science/article/pii/S1876619616300596`.

[47] Birgit Weber. *Coordination Chemistry: Basics and Current Trends*. Springer Berlin Heidelberg, 1 2023. ISBN 9783662664414. doi: 10.1007/978-3-662-66441-4.

[48] C Wagner, U Mullich, A Geist, and P J Panak. TRLFS Study on the Complexation of Cm(III) and Eu(III) with SO3-Ph-BTBP. *Dalton Trans.*, 44(39):17143–

17151, 2015. ISSN 1477-9226. doi: 10.1039/c5dt02923f. URL <GotoISI>://WOS:000362353100016.

[49] Yuji Sasaki, Yumi Sugo, Shinichi Suzuki, and Shoichi Tachimori. The Novel Extractants, Diglycolamides, for the Extraction of Lanthanides and Actinides in HNO3-n-dodecane System. *Solvent Extr. Ion Exch.*, 19(1):91–103, 2001. ISSN 0736-6299. doi: 10.1081/SEI-100001376. URL http://www.informaworld.com/10.1081/SEI-100001376.

[50] Fabrizio Piromalli. Synyhesis of new bipyridine and phenantroline based ligands for the separation of americium from the active PUREX raffinate, 2023.

[51] Daniel Whittaker, Andreas Geist, Giuseppe Modolo, Robin Taylor, Mark Sarsfield, and Andreas Wilden. Applications of Diglycolamide Based Solvent Extraction Processes in Spent Nuclear Fuel Reprocessing, Part 1: TODGA. *Solvent Extr. Ion Exch.*, 36(3):223–256, 2018. doi: 10.1080/07366299.2018.1464269. URL https://www.tandfonline.com/doi/full/10.1080/07366299.2018.1464269.

[52] Andreas Geist and Giuseppe Modolo. TODGA Process Development: an Improved Solvent Formulation. In *GLOBAL (The Nuclear Fuel Cycle: Sustainable Options & Industrial Perspectives)*, pages 1022–1026, Paris, 2009.

[53] Ralph A Leonard, Arup K SenGupta, and Bruce A Moyer. Design Principles and Applications of Centrifugal Contactors for Solvent Extraction. In Bruce A Moyer, editor, *Ion Exchange and Solvent Extraction, A Series of Advances*, volume 19, chapter 10, pages 563–616. CRC Taylor and Francis, Boca Raton, FL, USA, 2009. doi: 10.1201/9781420059700-c10. URL http://www.taylorandfrancis.com/books/details/9781420059694/http://www.crcnetbase.com/doi/pdfplus/10.1201/9781420059700-c10.

[54] Frank W Lewis, Laurence M Harwood, Michael J Hudson, Michael G B Drew, Jean F Desreux, Geoffrey Vidick, Nouri Bouslimani, Giuseppe Modolo, Andreas Wilden, Michal Sypula, Trong-Hung Vu, and Jean-Pierre Simonin. Highly Efficient Separation of Actinides from Lanthanides by a Phenanthroline-Derived Bis-triazine Ligand. *J. Am. Chem. Soc.*, 133(33):13093–13102, 2011. ISSN 0002-7863. doi: 10.1021/ja203378m. URL http://pubs.acs.org/doi/abs/10.1021/ja203378m.

[55] Jan Rydberg, Michael Cox, Claude Musikas, and Gregory R. Choppin. *Solvent Extraction Principles and Practice*. CRC Press, 3 2004. ISBN 9780203021460. doi: 10.1201/9780203021460. URL https://www.taylorfrancis.com/books/9780203021460.

[56] V D Athawale and Vidyagauri Lele. Stability Constants and Thermodynamic Parameters of Complexes of Lanthanide Ions and (()-Norvaline. Technical report, 1996. URL `https://pubs.acs.org/sharingguidelines`.

[57] Heinz-Helmut Perkampus. *UV-VIS Spectroscopy and Its Applications*. Springer - Verlag, Heidelberg, 1992. ISBN 978-3-642-77479-9. doi: 10.1007/978-3-642-77477-5.

[58] Yong Qiang Wan, Huaixin Hao, Lu Yu, Zhi Peng Wang, and Pavle Mocilac. Novel hydrophilic bistriazolyl-phenanthroline ligands with improved solubility and performance in An/Ln separations. *RSC Advances*, 13(32):21982–21990, 7 2023. ISSN 20462069. doi: 10.1039/d3ra02707d.

[59] Ashley N. Carolan, Gregory M. Cockrell, Neil J. Williams, Gang Zhang, Donald G. Vanderveer, Hee Seung Lee, Randolph P. Thummel, and Robert D. Hancock. Selectivity of the highly preorganized tetradentate ligand 2,9-Di(pyrid-2-yl)-1,10-phenanthroline for metal ions in aqueous solution, including lanthanide(III) ions and the uranyl(VI) cation. *Inorganic Chemistry*, 52(1):15–27, 1 2013. ISSN 00201669. doi: 10.1021/ic3002509.

[60] Yong Qiang Wan, Yang Yang Zhang, Shi Lin Zhang, Huai Xin Hao, Ji Yao Bai, Zhi Jun Ma, Long Geng, Zhi Peng Wang, John F. Gallagher, Jun Li, and Pavle Mocilac. Development and comparative study of a hydrophilic bis-triazolyl-phenanthroline ligand and two bis-triazolyl-pyridine ligands. *Dalton Transactions*, 2026. ISSN 14779234. doi: 10.1039/d6dt00312e.

[61] S A Ansari, P N Pathak, M Husain, A K Prasad, V S Parmar, and V K Manchanda. Extraction of Actinides Using N, N, N, N-Tetraoctyl diglycolamide (TODGA): a Thermodynamic Study. *Radiochim. Acta*, 94(6-7):307–312, 2006. ISSN 2193-3405. doi: 10.1524/ract.2006.94.6.307. URL `http://dx.doi.org/10.1524/ract.2006.94.6.307`.

[62] S A Ansari, P Pathak, P K Mohapatra, and V K Manchanda. Chemistry of Diglycolamides: Promising Extractants for Actinide Partitioning. *Chem. Rev.*, 112(3): 1751–1772, 2012. ISSN 0009-2665. doi: 10.1021/cr200002f. URL `<GotoISI>://WOS:000301988700013`.

[63] W S Nobley and M P Jensen. The impact of phase modification on the equilibrium and kinetics of lanthanide(III) extraction from nitric acid media by TODGA. *RSC Adv.*, 15(51):43941–43954, 2025. doi: 10.1039/d5ra06417a. URL `https://pubs.rsc.org/en/content/articlelanding/2025/ra/d5ra06417a`.

[64] A Wilden, G Modolo, S Lange, F Sadowski, B B Beele, A Skerencak-Frech, P J Panak,

A Geist, M Iqbal, W Verboom, and D Bosbach. Modified Diglycolamides for Actinide Separation: Solvent Extraction and Time Resolved Laser Fluorescence Spectroscopy Complexation Studies. In *GLOBAL 2013 "Nuclear Energy at a Crossroad"*, pages 907–911, Salt Lake City, UT, USA, 2013.

[65] Ana Gil-Martin, Frederic Lepretre, Florian Meze, Lionel Moisan, Nicolas Vigier, Bénédicte Arab-Chapelet, Anne Lelias, Justine Cambe-Issaadi, Hervé Roussel, and S Legand. Diversification of Suppliers on Diluent (TPH) at La Hague Plant. In *Atalante 2024*, Avignon, 9 2024. URL `https://hal.science/hal-04737252v1`.

[66] Frank Lewis, L Harwood, Michael J Hudson, Andreas Geist, Valery Nikolaevich Kozhevnikov, Petr Distler, and Jan John. Hydrophilic Sulfonated Bis-1,2,4-Triazine Ligands Are Highly Effective Reagents for Separating Actinides(III) from Lanthanides(III) via Selective Formation of Aqueous Actinide Complexes. *Chem. Sci.*, 6(8):4812–4821, 2015. ISSN 2041-6520. doi: 10.1039/C5SC01328C. URL `http://dx.doi.org/10.1039/C5SC01328C`.

[67] Andreas Geist, Clement Hill, Giuseppe Modolo, Mark R St J Foreman, Michael Weigl, Klaus Gompper, Michael J Hudson, and Charles Madic. 6,6'-Bis(5,5,8,8-tetramethyl-5,6,7,8-tetrahydro-benzo[1,2,4]triazin-3-yl)[2,2']bipyridine, an effective extracting agent for the separation of americium(III) and curium(III) from the lanthanides. *Solvent Extr. Ion Exch.*, 24(4):463–483, 2006. doi: 10.1080/07366290600761936.

[68] Irena Herdzik-Koniecko, Christoph Wagner, Michael Trumm, Udo Müllich, Bernd Schimmelpfennig, Jerzy Narbutt, Andreas Geist, and Petra J Panak. Do An(III) and Ln(III) ions form heteroleptic complexes with diglycolamide and hydrophilic BT(B)P ligands in solvent extraction systems? A spectroscopic and DFT study. *New J. Chem.*, 43(16):6314–6322, 2019. ISSN 1144-0546. doi: 10.1039/c9nj00651f. URL `<GotoISI>://WOS:000465091000026`.

[69] Fynn S Sauerwein, Thomas Sittel, Andreas Geist, Petra J Panak, Andreas Wilden, and Giuseppe Modolo. Selective Americium Separation: New Insights into the Complexation of Trivalent f-Elements with SO3-Ph-BTBP. *EPJ Web Conf.*, 317(6th International ATALANTE Conference on Nuclear Chemistry for Sustainable Fuel Cycles (ATALANTE-2024)):1012, 2025. ISSN 2100-014X. doi: 10.1051/epjconf/202531701012. URL `https://doi.org/10.1051/epjconf/202531701012https://juser.fz-juelich.de/record/1038896https://x.com/WildenAndreas/status/1887438741993578496`.

[70] Andreas Geist, Udo Müllich, Daniel Magnusson, Peter Kaden, Giuseppe Modolo, Andreas Wilden, and Thomas Zevaco. Actinide(III)/lanthanide(III) Separation Via Selective Aqueous Complexation of Actinides(III) Using a Hydrophilic 2,6-Bis(1,2,4-Triazin-3-yl)-Pyridine in Nitric Acid. *Solvent Extr. Ion Exch.*, 30(5):433–444, 2012. doi: 10.1080/07366299.2012.671111. URL http://www.tandfonline.com/doi/abs/10.1080/07366299.2012.671111.

[71] A Bremer, D M Whittaker, C A Sharrad, A Geist, and P J Panak. Complexation of Cm(III) and Eu(III) with CyMe4-BTPhen and CyMe4-BTBP studied by time resolved laser fluorescence spectroscopy. *Dalton Trans.*, 43(6):2684–2694, 2014. ISSN 1477-9226. doi: 10.1039/c3dt52204k. URL <GotoISI>://WOS:000329928700040.

[72] F W Lewis, L M Harwood, M J Hudson, M G B Drew, V Hubscher-Bruder, V Videva, F Arnaud-Neu, K Stamberg, and S Vyas. BTBPs versus BTPhens: Some Reasons for Their Differences in Properties Concerning the Partitioning of Minor Actinides and the Advantages of BTPhens. *Inorg. Chem.*, 52(9):4993–5005, 2013. ISSN 0020-1669. doi: 10.1021/ic3026842. URL <GotoISI>://WOS:000318669400037.

[73] Patrik Weßling, Melina Maag, Giana Baruth, Thomas Sittel, Fynn S Sauerwein, Andreas Wilden, Giuseppe Modolo, Andreas Geist, and Petra J Panak. Complexation and Extraction Studies of Trivalent Actinides and Lanthanides with Water-Soluble and CHON Compatible Ligands for the Selective Extraction of Americium. *Inorg. Chem.*, 61(44):17719–17729, 2022. doi: 10.1021/acs.inorgchem.2c02871. URL https://pubs.acs.org/doi/10.1021/acs.inorgchem.2c02871https://juser.fz-juelich.de/record/910340https://twitter.com/WildenAndreas/status/1584509664347443203.

[74] Peter Kaufholz, Giuseppe Modolo, Andreas Wilden, Fabian Sadowski, Dirk Bosbach, Christoph Wagner, Andreas Geist, Petra J Panak, Frank W Lewis, and Laurence M Harwood. Solvent extraction and fluorescence spectroscopic investigation of the selective Am(III) complexation with TS-BTPhen. *Solvent Extr. Ion Exch.*, 34(2):126–140, 2016. ISSN 0736-6299. doi: 10.1080/07366299.2016.1151308. URL http://dx.doi.org/10.1080/07366299.2016.1151308.

[75] A C Edwards, P Mocilac, A Geist, L M Harwood, C A Sharrad, N A Burton, R C Whitehead, and M A Denecke. Hydrophilic 2,9-bis-triazolyl-1,10-phenanthroline ligands enable selective Am(III) separation: a step further towards sustainable nuclear energy. *Chem. Commun.*, 53(36):5001–5004, 2017. ISSN 1359-7345. doi: 10.1039/c7cc01855j. URL <GotoISI>://WOS:000400579100028.

[76] P. Troosters, T. Opsomer, K. Van Hecke, K. Verguts, F. Reniers, K. Van Hoecke, P. Zsabka, T. Cardinaels, and W. Dehaen. New synthetic pathway towards BTrzPhen-tetraol: a hydrophilic 2,9-bis-triazolyl-1,10-phenanthroline ligand for selective americium stripping. *Dalton Transactions*, 54(11):4697–4705, 2 2025. ISSN 14779234. doi: 10.1039/d4dt03399j.

[77] Xuan Fu, Yang Liu, Heng Yi Zhou, Cong Zhi Wang, Tao Yuan Xiu, Zhe Xiao, Hong Bin Tang, Zhi Wei Huang, Zhi Heng Zhou, Li Yong Yuan, Ze Yi Yan, and Wei Qun Shi. New clicked hydrophobic 2,9-bis-triazolyl-1,10-phenanthroline ligands used as extractants for actinide/lanthanide separation: Towards deep purification. *Journal of Hazardous Materials*, 495, 9 2025. ISSN 18733336. doi: 10.1016/j.jhazmat.2025.139085.

[78] Fengxin Gao, Xiaocheng Xu, Xiaofan Yang, Dong Fang, and Chengliang Xiao. Effect of Incremental Preorganization in Bis-triazole-substituted Phenanthroline Ligands on Eu(III) Coordination: Spectroscopy, X-ray Crystallography, and DFT Studies. *Inorganic Chemistry*, 64(38):19338–19347, 9 2025. ISSN 1520510X. doi: 10.1021/acs.inorgchem.5c03099.

[79] Yong Qiang Wan, Huai Xin Hao, Yang Yang Zhang, Yu Xiao Guo, Zhi Jun Ma, Zhi Peng Wang, Jun Li, and Pavle Mocilac. Efficient Trivalent Actinide-Lanthanide Separations Using Hydrophilic CHON-Compliant Phenanthroline-Dicarboxamide Ligands. *Industrial and Engineering Chemistry Research*, 64(24):12185–12199, 6 2025. ISSN 15205045. doi: 10.1021/acs.iecr.5c00795.

[80] P D'Angelo, A Zitolo, V Migliorati, G Chillemi, M Duvail, P Vitorge, S Abadie, and R Spezia. Revised Ionic Radii of Lanthanoid(III) Ions in Aqueous Solution. *Inorg. Chem.*, 50(10):4572–4579, 2011. ISSN 0020-1669. doi: 10.1021/ic200260r. URL `<GotoISI>://WOS:000290246600049`.

[81] P D'Angelo, F Martelli, R Spezia, A Filipponi, and M A Denecke. Hydration Properties and Ionic Radii of Actinide(III) Ions in Aqueous Solution. *Inorg. Chem.*, 52(18):10318–10324, 2013. ISSN 0020-1669. doi: 10.1021/ic400678u. URL `https://pubs.acs.org/doi/10.1021/ic400678u`.

[82] Letizia Di Matteo. Innovative hydrophilic ligands for the selective recovery of Am(III) from spent nuclear fuel, 2024.

[83] Michal Sypula, Andreas Wilden, Christian Schreinemachers, Rikard Malmbeck, Andreas Geist, Robin Taylor, and Giuseppe Modolo. Use of polyaminocarboxylic acids as hydrophilic masking agents for fission products in actinide partitioning processes.

Solvent Extr. Ion Exch., 30(7):748–764, 2012. doi: 10.1080/07366299.2012.700591. URL `http://www.tandfonline.com/doi/abs/10.1080/07366299.2012.700591`.

[84] David Woodhead, Fiona McLachlan, Robin Taylor, Udo Müllich, Andreas Geist, Andreas Wilden, and Giuseppe Modolo. Nitric Acid Extraction into a TODGA Solvent Modified with Octanol. *Solvent Extr. Ion Exch.*, 37(2):173–190, 2019. doi: 10.1080/07366299.2019.1625201. URL `https://www.tandfonline.com/doi/full/10.1080/07366299.2019.1625201`.

[85] Herbert; Zeeh Bernd Hesse, Manfred; Meier. Spectroscopic Methods in Organic Chemistry. chapter UV/VIS spectroscopy. Georg Thieme Verlag, Stuttgart, 3rd edition edition, 2021. doi: DOI:10.1055/b000000049.

[86] C. Binnemans, K.; Görller-Walrand. On the color of the trivalent lanthanide ions. *Chemical Physics Letters*, 235:163–174, 1995.

[87] M. L.M. Rocco, M. Häming, C. E.V. De Moura, M. Barbatti, A. B. Rocha, A. Schöll, and E. Umbach. High-Resolution Near-Edge X-ray Absorption Fine Structure Study of Condensed Polyacenes. *Journal of Physical Chemistry C*, 122(50):28692–28701, 12 2018. ISSN 19327455. doi: 10.1021/acs.jpcc.8b08945.

[88] Jaana Tammiku, Peeter Burk, and Ants Tuulmets. UV-VIS spectrum of the 1,10 -phenanthroline - ethylmagnesium bromide complex. An experimental and computational study. *Main Group Metal Chemistry*, 23(5):301–305, 5 2000.

[89] Nathalie Proos Vedin, Josene M. Toldo, Sílvia Escayola, Slavko Radenković, Miquel Solà, and Henrik Ottosson. Toward a Systematics for the Lowest Excited States of Heteroaromatics Enabled via Cyclic π-Conjugated Carbenes and Heteroelement Analogues. *Journal of Organic Chemistry*, 2025. ISSN 15206904. doi: 10.1021/acs.joc.5c00578.

[90] Peter Gans, Antonio Sabatini, and Alberto Vacca. Investigation of equilibria in solution. Determination of equilibrium constants with the HYPERQUAD suite of programs. *Talanta*, 43:1739–1753, 1996.

[91] Peter Gans, Antonio Sabatini, and Alberto Vacca. HypSpec help documentation, 2014.

[92] Barbara Boldrini, Enrico Cavalli, Anna Painelli, and Francesca Terenziani. Polar dyes in solution: A joint experimental and theoretical study of absorption and emission band shapes. *Journal of Physical Chemistry A*, 106(26):6286–6294, 7 2002. ISSN 10895639. doi: 10.1021/jp020031b.

[93] S. Eriksson, B. Källebring, S. Larsson, J. Mårtensson, and O. Wennerström. Exciton splitting in the spectra of covalently linked porphyrins. *Chemical Physics*, 146(1-2): 165–177, 9 1990. ISSN 0301-0104. doi: 10.1016/0301-0104(90)90015-2. URL `https://www.sciencedirect.com/science/article/abs/pii/0301010490900152`.

A | Appendix A

Table A.1: Metal concentrations in the aqueous phase used for the organic phase loading: HAR diluted 400 times with a 0.5 M HNO_3 10^{-5} M Ln all solution; concentration [mg/L] measured with ICP-MS (no data available for Lu, Se lower than the detection limit); concentration [mM] derived with molar masses.

Metal	**Concentration**		**Metal**	**Concentration**	
-	**[mg/L]**	**[mM]**	**-**	**[mg/L]**	**[mM]**
Sc	0.0145	0.0003	**Sb**	0.0254	0.0002
Cr	0.490	0.009	**Te**	0.657	0.005
Fe	11.8	0.2	**Cs**	2.89	0.02
Ni	0.280	0.005	**Ba**	1.65	0.01
Cu	0.128	0.002	**La**	2.85	0.02
Se	-	-	**Ce**	4.89	0.03
Rb	0.398	0.005	**Pr**	2.81	0.02
Y	1.55	0.02	**Nd**	5.26	0.04
Zr	4.60	0.05	**Sm**	2.85	0.02
Mo	4.11	0.04	**Eu**	2.02	0.01
Ru	2.14	0.02	**Gd**	2.06	0.01
Rh	0.445	0.004	**Tb**	1.38	0.01
Pd	0.521	0.005	**Dy**	1.89	0.01
Ag	0.0251	0.0002	**Ho**	1.87	0.01
Cd	0.106	0.001	**Er**	1.67	0.01
Sn	0.0763	0.0006	**Tm**	1.22	0.01
Sb	0.0254	0.0002	**Yb**	1.70	0.01

List of Figures

List of Tables

Acknowledgements

This work is funded by the European Union through the EURATOM research and training programme, project TRANSPARANT (Technological Research Action Necessary for Safe PARtitioning and Nuclear Transmutation), Grant Agreement: 101166386. Funding for this research was partially provided by the German Federal Ministry of Research, Technology and Space through the COORDEX project, grant number 02NUK103B. Additional funding was provided by Politecnico di Milano through the scolarship 'Tesi all'estero' a.a. 2024/2025 - Bando 4377, for the academic year 2025/2026. The author gratefully acknowledges A. Sacchetti and G. Marcolli for the ligand synthesis, Z. Paparigas and K. Peters for laboratory assistance and guidance, M. Henkes and D. Schneider for ICP-MS measurements, and M. F. S. Tentorio for reviewing the manuscript.